

# Halo and Bunch Purity Monitoring

= Very High Dynamic Beam Profile Measurements;  
Transversal (and Longitudinal)

Kay Wittenburg, DESY, Hamburg



# Outline

- Halo diagnostic:
  - What is Halo?
  - Halo Quantification
- Transversal Halo Measurements with:
  - Wire Scanners etc. (slow)
  - Optical Methods (fast)
- Longitudinal Halo
  - Bunch Purity
  - "Beam in Gap"
  - Coasting Beam



- Halo diagnostic:
  - **What is Halo?**
  - Halo Quantification
- Transversal Halo Measurements with:
  - Wire Scanners etc. (slow)
  - Optical Methods (fast)
- Longitudinal Halo
  - Bunch Purity,
  - "Beam in Gap"
  - Coasting Beam

# What's Halo?

... because of the beam distribution's phase-space rotations, the observed halo in 1D oscillates, so that halo at different locations along the beam line is observable in differing degrees. For example, at some locations the halo may project strongly along the spatial coordinate and only weakly along the momentum coordinate, while at others the reverse is true, and the halo can be hidden in the spatial projection. In most circumstances, the beam halo from simulation appears as an irreversible effect, when observed in the 2D phase-space distributions. Therefore, it is also important to search for another definition of halo in the 2D phase-space distributions....

---

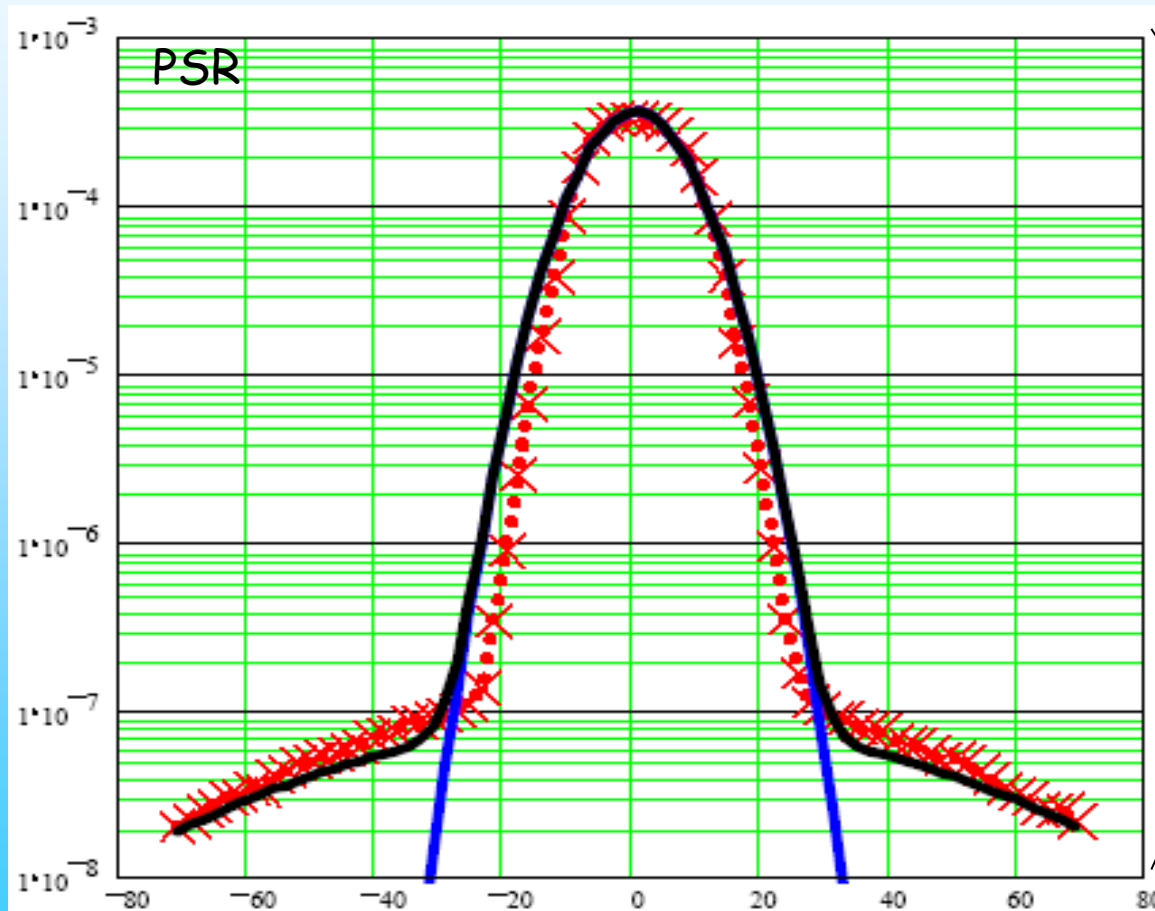
...it became clear that even at this workshop (HALO 03) a **general definition of "Beam Halo" could not be given**, because of the **very different requirements** in different machines, and because of the **differing perspectives** of instrumentation specialists and accelerator physicists.

**From the diagnostics point of view, one thing is certainly clear - by definition halo is low density and therefore difficult to measure...**



# What is Halo?

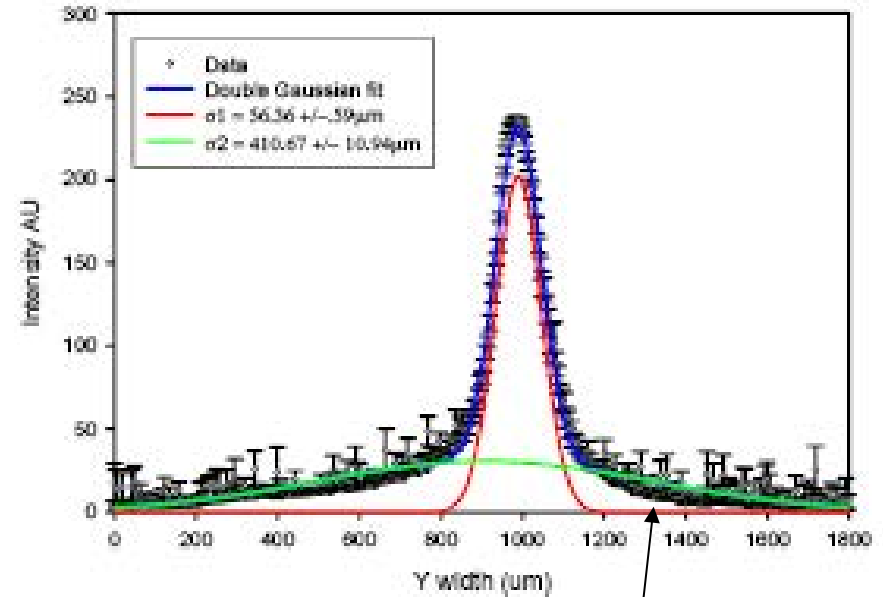
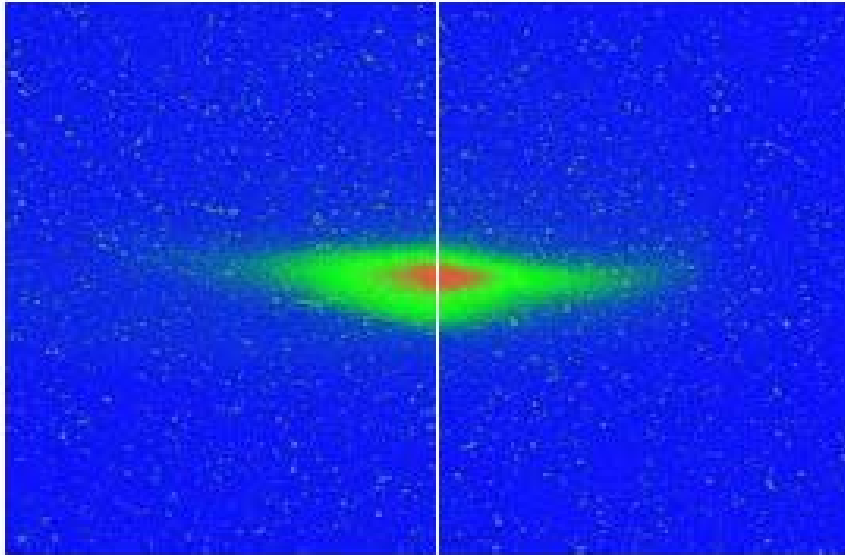
From the diagnostics point of view, one thing is certainly clear - by definition halo is low density and therefore difficult to measure...



Halo measurements require **high dynamic range instruments and methods**

Dynamic range  $> 10^5$

# What is Halo?



That's not a halo,  
that's a tail!  
Dynamic range  $<10^3$

# What is Halo?

## *Halo Definition*

We will use the definition of halo recently agreed upon by a representative group of beam instrumentation experts. In short, **the beam charge distribution inside the vacuum chamber can be separated to three parts: the beam core, the beam halo and the transition (the transition is often called “shoulders”, “tails” etc.).** These parts are characterized by the charge density relative to the peak density. The boundaries are not defined exactly but for the majority of the cases the beam core boundary is at about  $10^{-2}$  level, **the beam halo is at  $10^{-4}$  -  $10^{-6}$  level and below.**

The low boundary of the halo region is decreasing with higher intensity beams, obviously, but the  $10^{-4}$  -  $10^{-6}$  range represents a good reference number for a large range of today's accelerators and is the current state-of-the art in beam measurements. In the context of this paper we add to the halo definition a notion that the halo extends far from the beam core, it has a negative effect on an accelerator operation, and this effect has to be measured and mitigated.

Path to Beam Loss Reduction in the SNS Linac Using Measurements, Simulation and Collimation

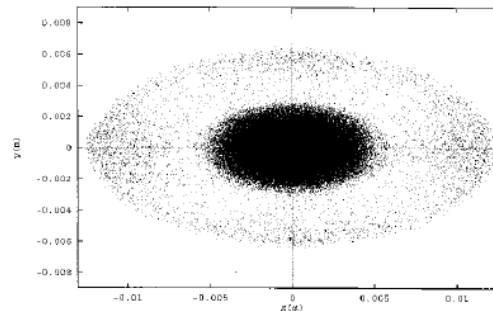
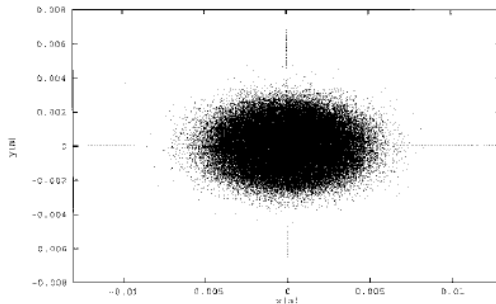
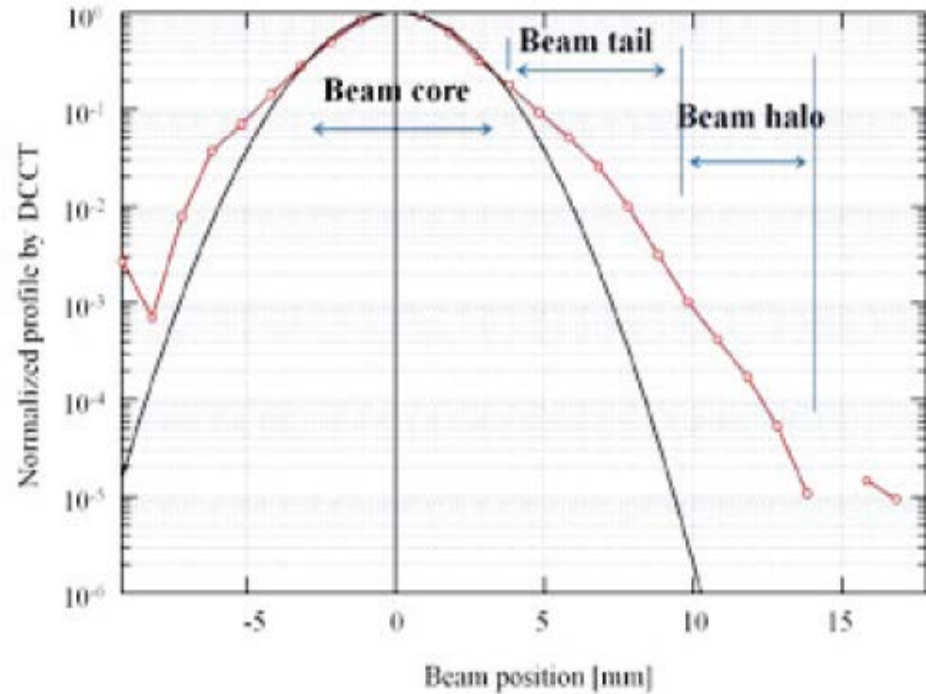
A.V. Aleksandrov, A.P. Shishlo, Proceedings of the 57th ICFA Advanced Beam Dynamics Workshop on High-Intensity, High Brightness and High Power Hadron Beams, Malmö, Sweden, 2016

# What is Halo?

## • Sources of halo are:

- space charge forces of the beam
- Mismatch of beam with accel. optics
- beam beam forces
- instabilities and resonances
- RF noise
- Scattering (inside beam, residual gas, macroparticles, photons, obstacles (stripping foil, screens etc.)
- nonlinear forces, e.g. aberrations and nonlinearities of focusing elements
- Misalignments of accel. components
- electron clouds
- Beam energy tails from uncaptured particles
- Transverse-longitudinal coupling in the RF field
- etc.

transversal



DEVELOPMENT OF THE BEAM HALO MONITOR IN THE J-PARC 3-GeV RCS, M. Yoshimoto, IPAC12

Techniques for Intense-Proton-Beam Profile Measurements; J. D. Gilpatrick, BIW98

**FIGURE 4.** This figure shows a typical representation of the extent to which mismatches can cause halo growth. The figure on the right shows the transverse profile of a beam well-matched to a transverse periodic lattice. The figure on the right shows that a 50% mismatch can cause halo growth.

- Halo diagnostic:
  - What is Halo?
  - Halo Quantification
- Transversal Halo Measurements with:
  - Wire Scanners etc. (slow)
  - Optical Methods (fast)
- Longitudinal Halo
  - Bunch Purity,
  - "Beam in Gap"
  - Coasting Beam

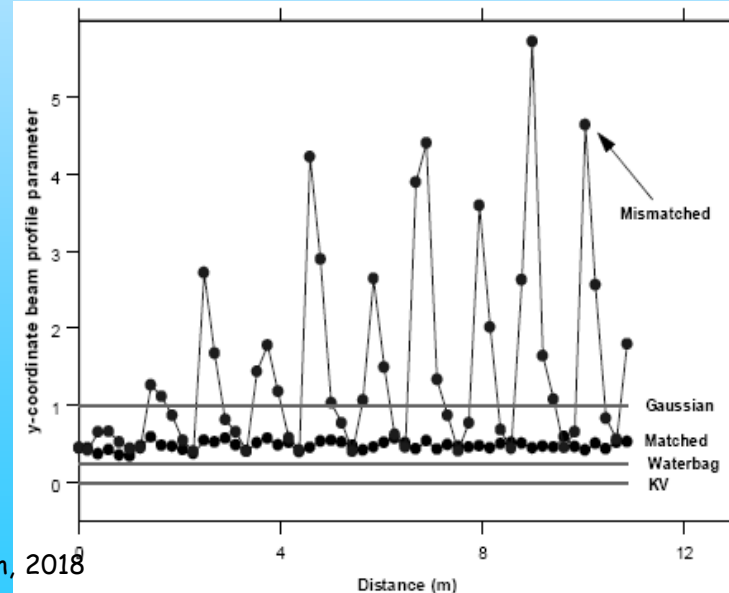
# HALO QUANTIFICATION

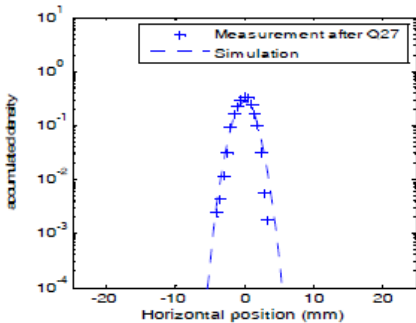
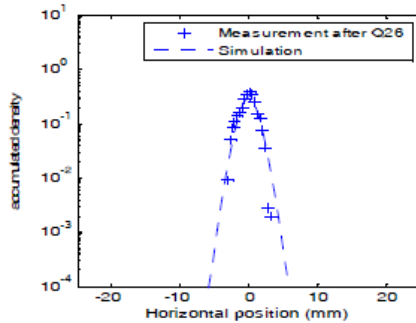
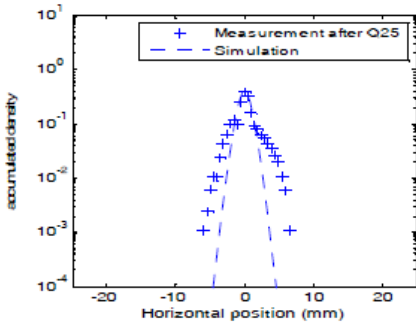
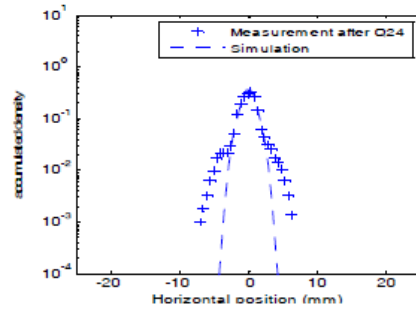
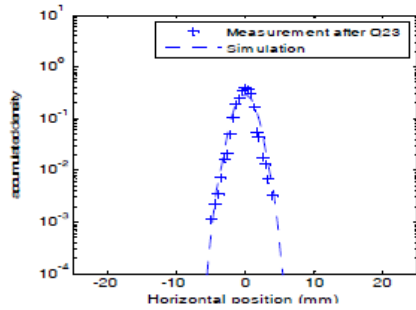
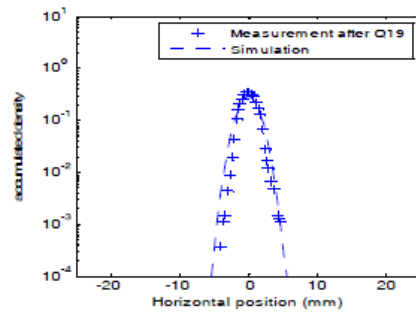
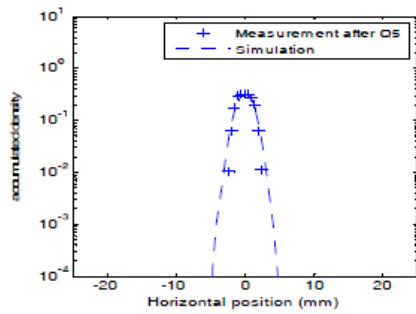
It is important to have a definition of halo in 1D spatial projections for which experimental measurements are relatively easy to obtain.

However, because of the beam's phase-space rotations, the observed halo in 1D projections oscillates. For example, at some locations the halo may project strongly along the **spatial coordinate** and only weakly along the **momentum coordinate**, while at others the reverse is true, and the halo can be hidden from the spatial projection. Therefore one should extend the 1D work to obtain a halo parameter suitable for description of beam halo in **whole phase space**. This lead naturally to the *kinematic invariants* and are the consequence of the linear forces and symplectic structure imposed by Hamilton's equations.

## Used mainly in simulations

The excursions above the Gaussian level indicate a large halo.





Simulation and (wire-Scanner) measurements at the beam transport line at the end of the IHEP RFQ.

Hongping Jiang et al, IPAC14

From the Figure 2 we can see in the most locations the simulations can properly reproduce the beam profiles, and there are a little halo particles in two locations. That means the beam in the phase space is not elliptic symmetry.

# HALO QUANTIFICATION

- There is **no clearly defined separation** between the halo and the main core of the beam. Consequently, there has been some difficulty identifying a suitable quantitative measure of the halo content of a beam in a model-independent way.
  - A general characteristic of beam halo is the increased population of the outer part of the beam.
  - Methods have been developed, and computationally studied, to characterize and quantify beam halo.
- 1) Kurtosis
  - 2) The Gaussian area ratio method
  - 3) Ratio of beam core to offset
  - 4) Ratio of halo to core

## Note that

1. A measurement always contains instrumental effects!!!!
2. Powerful simulations are useless if significant physical mechanisms are missing or if the beam input distribution is unrealistic.

# HALO QUANTIFICATION

## 1) Kurtosis

This method is based on analyzing the **fourth moment of the beam profile**. The kurtosis is a measure of **whether a data set is peaked or flat relative to a normal (Gaussian) distribution**.

$$k \equiv \frac{\langle (x - x_0)^4 \rangle}{\langle (x - x_0)^2 \rangle^2} - 2$$

Distributions with high kurtosis have sharp peaks near the mean that come down rapidly to heavy tails. An important feature of such quantifiers is that they are **model independent** and rely only on the characteristics of the beam distribution itself.

**Might be not so well suited for us instrumental specialists.**

**Beam Halo in Proton Linac Beams**

BEAM HALO IN PROTON LINAC BEAMS T. P. Wangler, et al., Linac 2000

# HALO QUANTIFICATION

## 1) Kurtosis

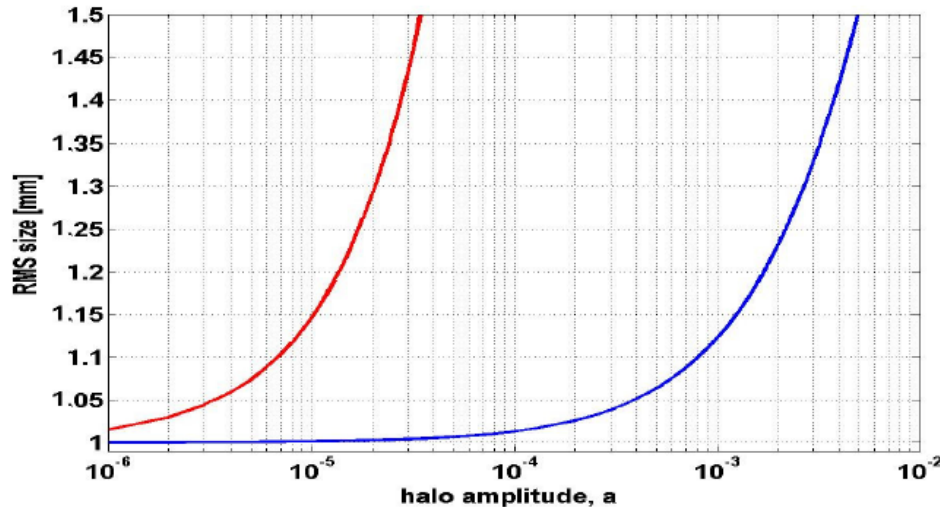
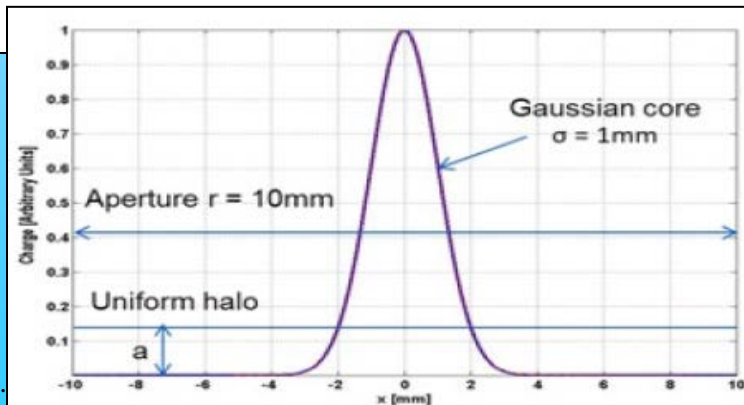


Figure 3: Dependence of the RMS size (blue line) and of the kurtosis (red line) on the halo amplitude for the profile of Fig. 2.



The kurtosis is more sensitive to the halo amplitude.

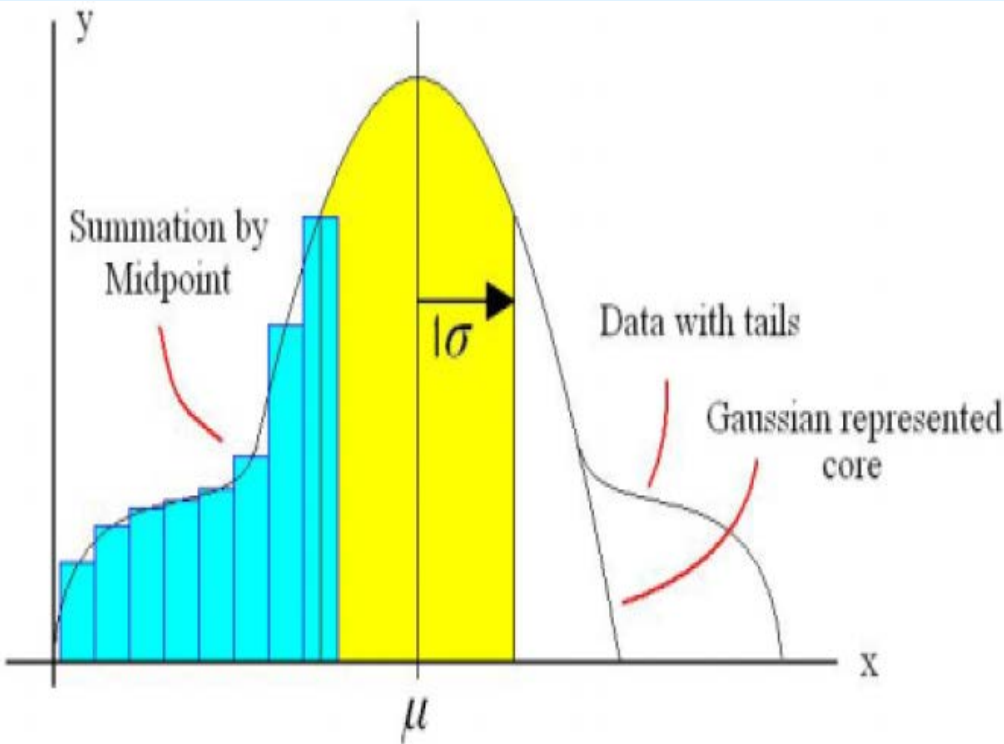
Unfortunately, statistical quantities using high order moments, including kurtosis, are very sensitive to small variations of the beam density in the transition zone (:tails), which makes them impractical to use for real life measurements. And, more important, there is not an equation, similar to the RMS envelope equation, to calculate the kurtosis everywhere in the beam line using a limited number of profile measurements.

Beam Halo Characterization and Mitigation  
A.V. Aleksandrov, IPAC16, BEXCO, Busan Korea

# HALO QUANTIFICATION

## 2) The Gaussian area ratio method:

Unlike the Kurtosis method, this method is not as sensitive to outlying particles but was found to be more useful for experimental data. The Gaussian area ratio method attempts to quantify the "non-Gaussian" component of the beam profile. After the data is filtered, it is fitted to a Gaussian of the form:

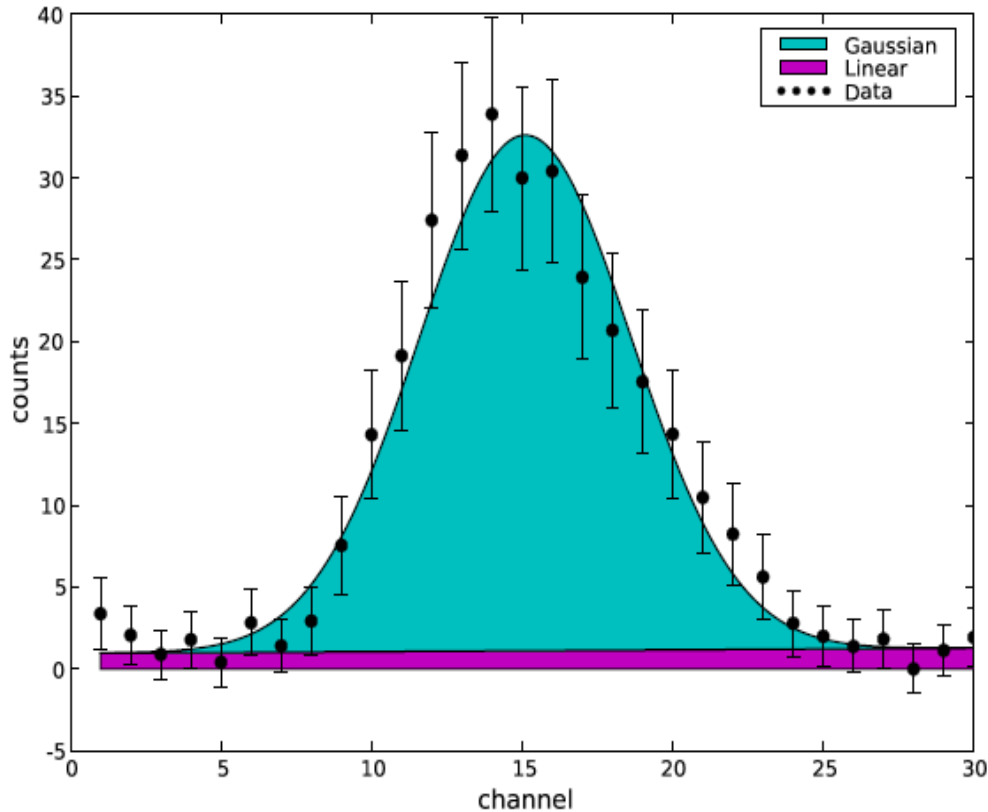


$$f(x) = A \exp(-(x-x_0)^2/(2\sigma^2))$$

In order to represent the core, a Gaussian fit is performed on the top (90 percent) of the profile since most profiles greatly resemble Gaussian's in this region of the beam core. Dividing the total area by the area under the Gaussian outside 1  $\sigma$  gives a ratio of the tails to the core and, therefore, a quantitative measure of the halo present.

# HALO QUANTIFICATION

## 3) Ratio of beam core to offset:



An experimentally robust technique for halo measurement using the IPM at the Fermilab Booster ; AMUNDSON J. ; et al, NIM A, Vol. 570, no1

Fit the raw data to the function:

$$f(x) = g(x) + l(x);$$

where

$$g(x) = N \exp -(x -x_0)^2/(2\sigma^2)$$

and

$$l(x) = c_0 + c_1x$$

The two components of  $f(x)$  can be thought of as the Gaussian core  $g(x)$  and non-Gaussian tails  $l(x)$  of the beam distribution. Defining

$$L = \int_{\text{detector}} l(x)dx$$

and

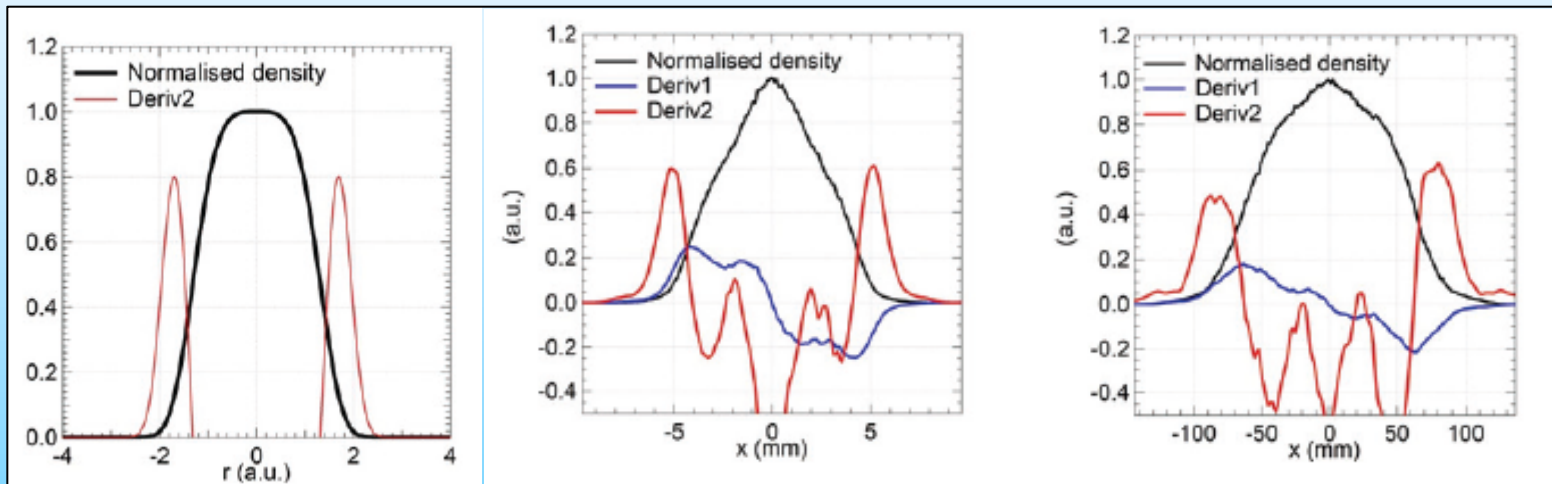
$$G = \int_{\text{detector}} g(x)dx$$

we can now characterize the beam shape by the ratio  $L/G$ . A perfectly Gaussian beam will have  $L/G = 0$ , whereas a beam with halo will have  $L/G > 0$ .

# HALO QUANTIFICATION

## 4. Ratio of halo to core:

a) Define core-halo limit: The core-halo limit can be equivalently defined as the location **where there is the largest slope variation in the density profile**, i.e. where the density second derivative is maximum. A pure Gaussian profile with  $\sigma$  RMS has a halo starting from  $\sqrt{3} \cdot \sigma$ , containing thus 8.3% particles of the beam.



b) Halo characterization: By two quantities, PHS and PHP which are respectively the percentage of halo size and of halo particles:

$$PHS = 100 \frac{\text{Halo size}}{\text{Total beam size}}$$

$$PHP = 100 \frac{\text{Nb of Particles in the Halo}}{\text{Total Nb of particles}}$$

PHS and PHP offer concrete numbers for characterizing the relative importance of the halo.  
P.A.P. Nghiem et al, IPAC14

- Halo diagnostic:
  - What is Halo?
  - Halo Quantification
- Transversal Halo Measurements with:
  - **Wire Scanners etc.**
  - Optical Methods (fast)
- Longitudinal Halo
  - Bunch Purity,
  - "Beam in Gap"
  - Coasting Beam

# Halo Measurements

- The focus of the accelerator physicists is on designing and operating their machines to minimize this halo.
- The focus of the collimation experts is on cleanly and efficiently disposing of this halo as it appears, a consequence of the clean and efficient disposal being that useful diagnostic information is often lost, buried in the collimators.
- The focus of the instrumentation specialists is twofold;
  - ✓ to provide information useful to the accelerator physicists in their machine tuning efforts to avoid halo formation, and
  - ✓ to provide direct measurement of halo.

Definition of halo diagnostics: Classification into three categories.

1. Devices that directly measure halo and halo evolution. An example is the wire scanner.
2. Devices that contribute to the diagnosis of machine conditions that cause halo formation. An example would be a tune measurement system.
3. Devices that measure the effects of halo development. An example would be the loss monitor system.

# Transversal Halo Measurements

Profile monitors like Wire, IPM, LPM, Laser Wire, ... are typically not designed for halo measurements. Their dynamic range is limited to about  $10^3$  (**to be discussed!!!**)! These monitors need some extras to increase their high dynamic range. Therefore, if we talk about halo monitors we discuss mainly about the extras of a beam profile monitor (or a scraper).

Some Ideas of Extras are folloing:

- **Invasive and non-invasive Techniques**
  - IPM
  - Wire Scanners
  - Scrapers
  - Diamonds
- **Optical Methods (fast)**
  - Screens
  - CID camera
  - Micro-Mirror Array
  - Coronagraph for Halo Measurements

# IPM

- J-Parc RCS: Idea to use additional MCP arrangement with lower resolution but high gain for halo observations.
- Upgrade in 2012, H. Harada, IPAC12

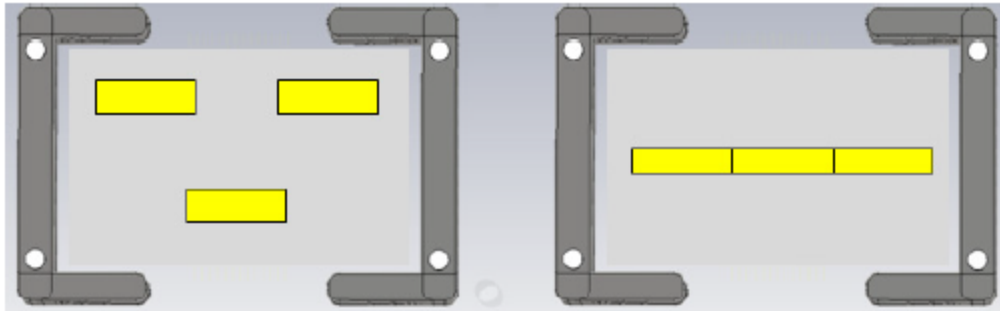
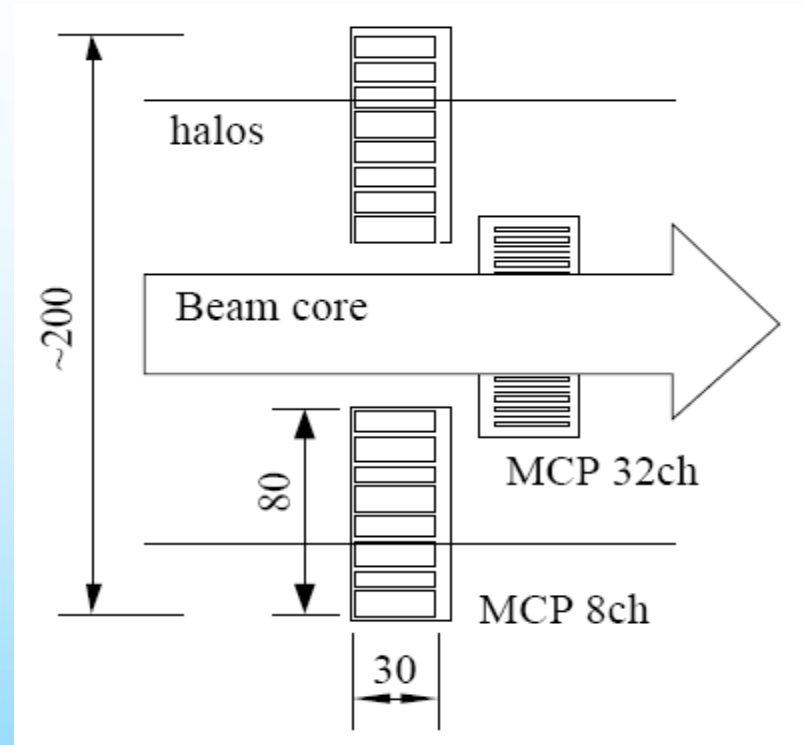
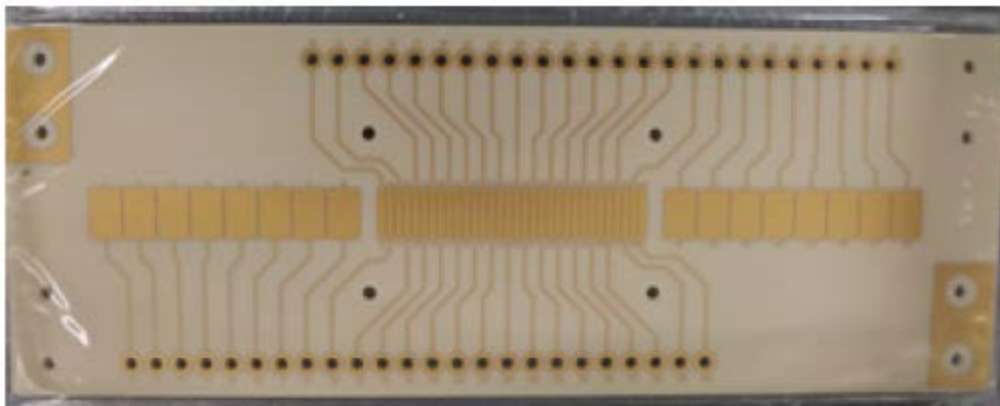


Figure 3: Old (left) and new (right) MCP structure and location. Yellow rectangles are MCPs.

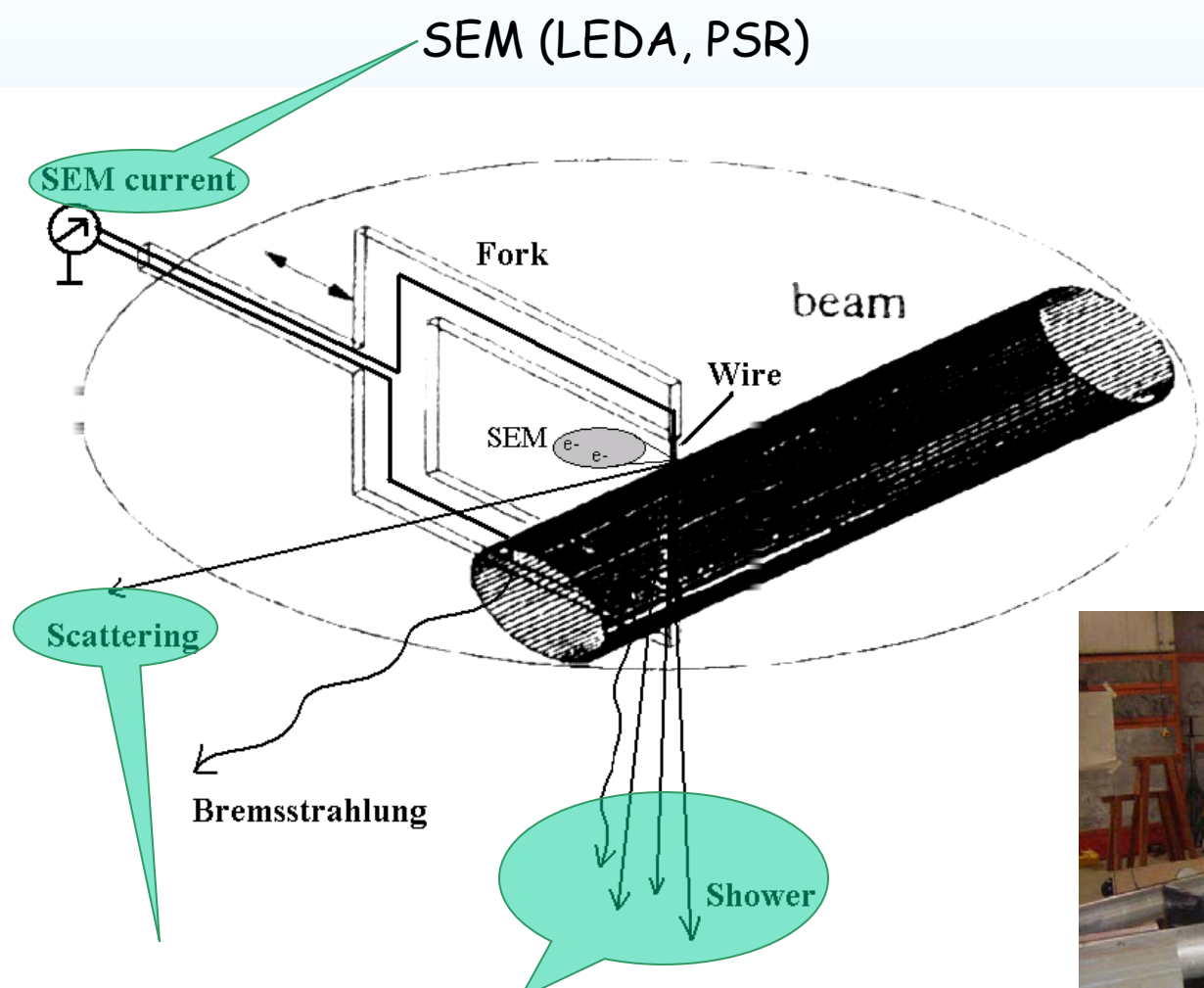


S.Lee et al.  
The 14th Symposium on Accelerator Science and Technology, Tsukuba, Japan, November 2003

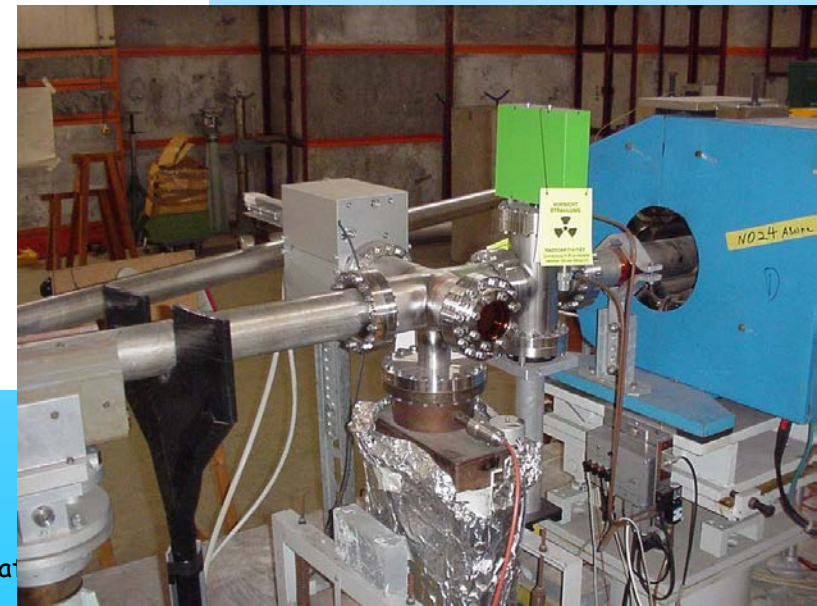
# Wire Scanners and Scrapers

- Used around the world, focus here:  
Dynamic range and sensitivity
- Problems are well known:  
Emittance blow up, wire heating.
- Readout by Scintillators and/or SEM
- Huge dynamic range by:
  - Log-amplifier (PSR)
  - Varying the PMT voltage (ATF)
  - Wire + Scrapers (LEDA)
  - scanning + counting (J-Lab, DESY, AGS)
  - Scraping with collimators (LEP)
  - Other methods
- **Real Halo Measurements**

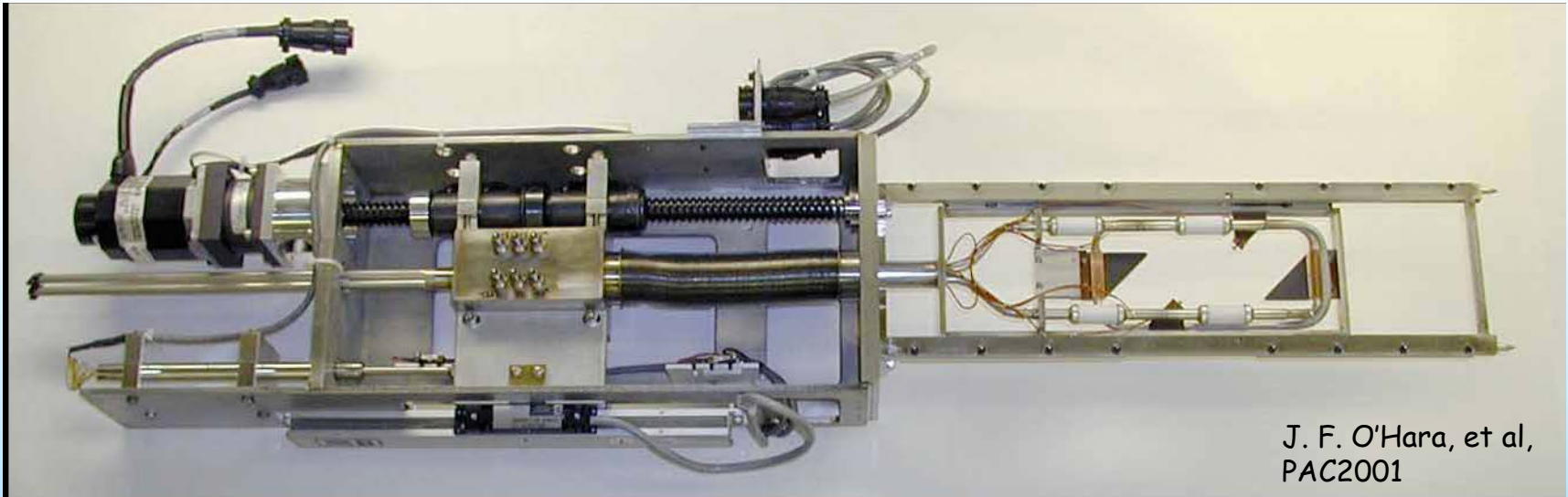
# Wire Scanners



PMT, Counting mode, bunch by bunch



# Wire Scanners at LEDA (Proton LINAC, SEM readout)

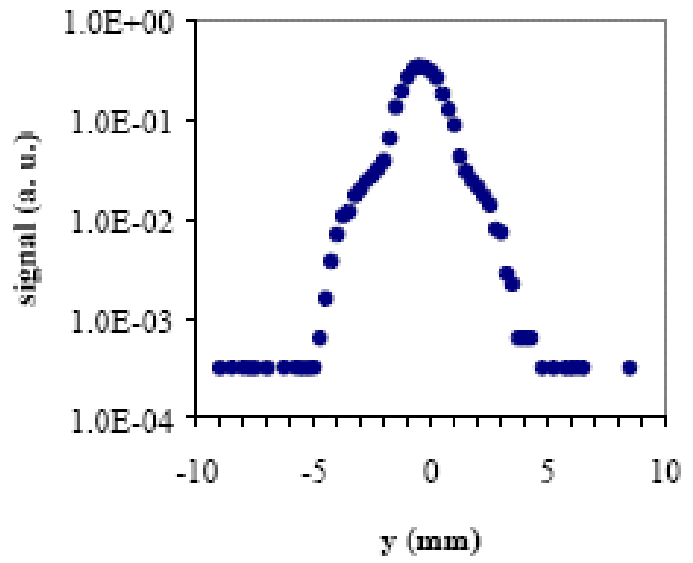


To plot the complete beam distribution for each axis, the **wire scanner and two scraper data sets must be joined**. To accomplish this joining, several analysis tasks are performed on the wire and scraper data including:

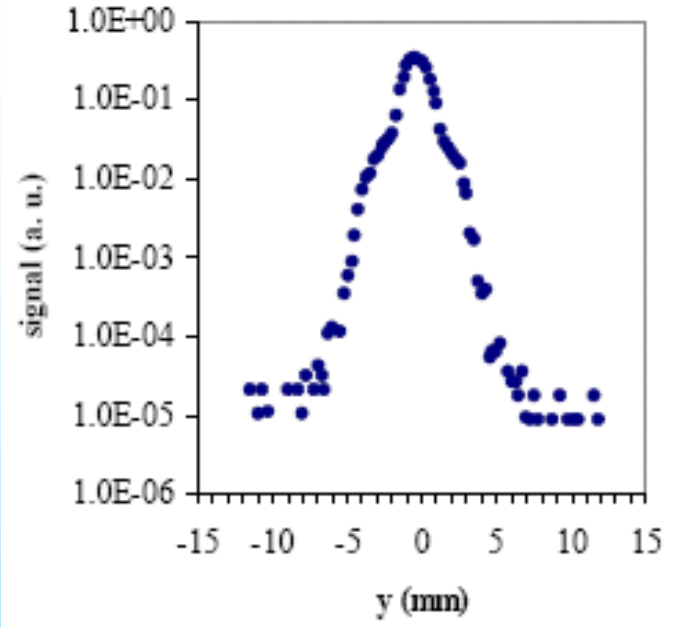
1. Scraper data are spatially differentiated and averaged,
2. Wire and scraper data are acquired with sufficient spatial overlap (where the wire scanner signal rises above the noise),
3. Differentiated scraper data are normalized to the wire beam core data,
4. Normalize data to axis
5. Normalize data to beam current and beam position (true for all kind of halo measurements)!!!!

Procedure explained in: J. H. Kamperschroer, et al., PAC2001  
**ANALYSIS OF DATA FROM THE LEDA WIRE SCANNER/HALO SCRAPER**

### Y-axis wire scan

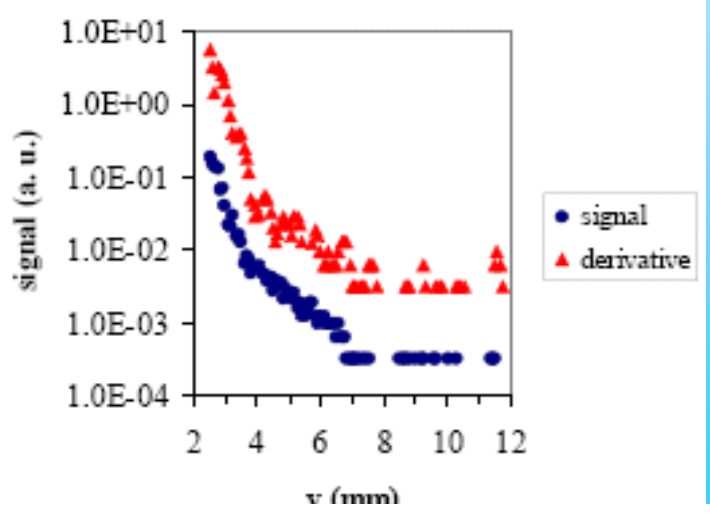
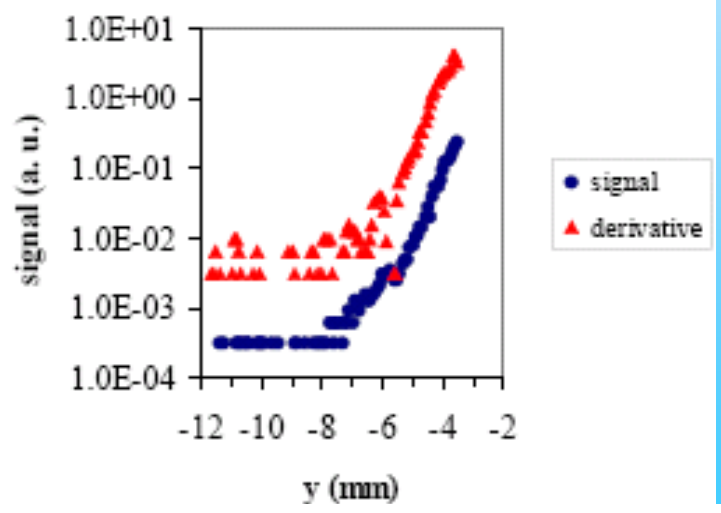


### Combined distribution in y.



+

+



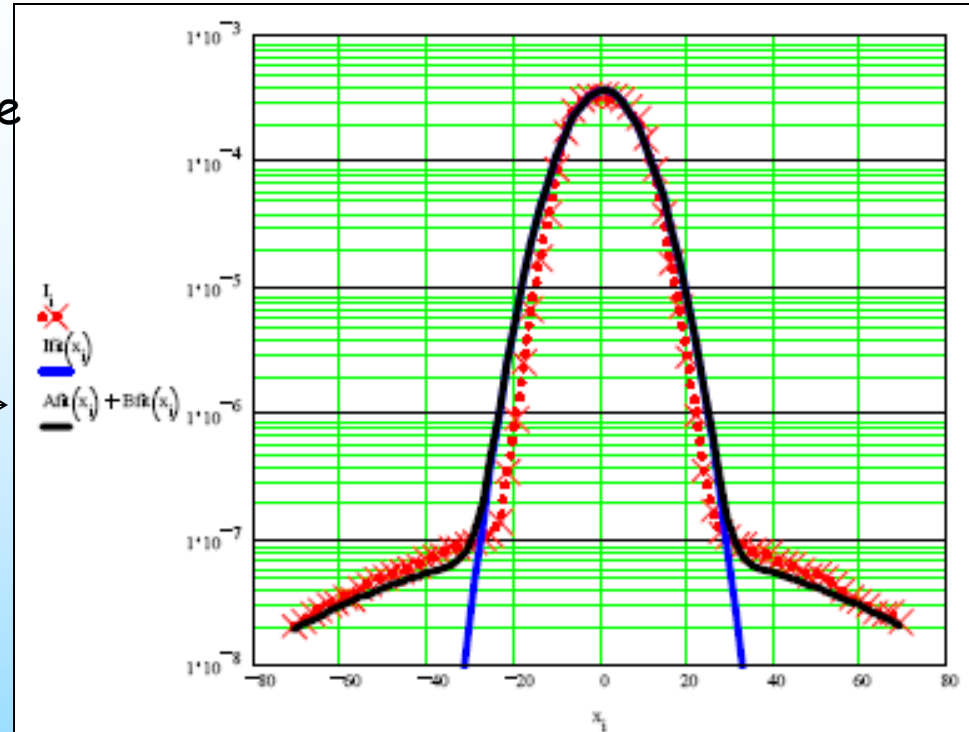
-Y and +Y scrape signal and derivative. The derivative has been multiplied by ten.

# Wire Scanners at PSR

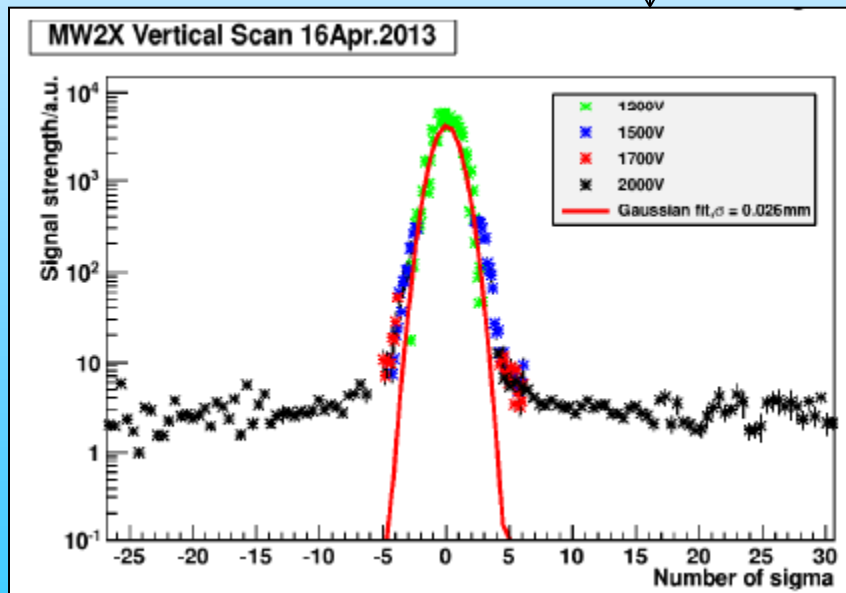
linear amplification and  $10^5$  dynamic range  
 $\Rightarrow$  16-bit A/D converter

As an alternative solution is to process the integrated signal using a logarithmic amplifier.

Or to use different PMT voltages.



A normal function shown in solid blue has been fit to the data (red x's). A sum of two normal functions is shown in solid black. The x-axis is scaled as scanner position in mm's and the y-axis is log-amp input current in Amps.

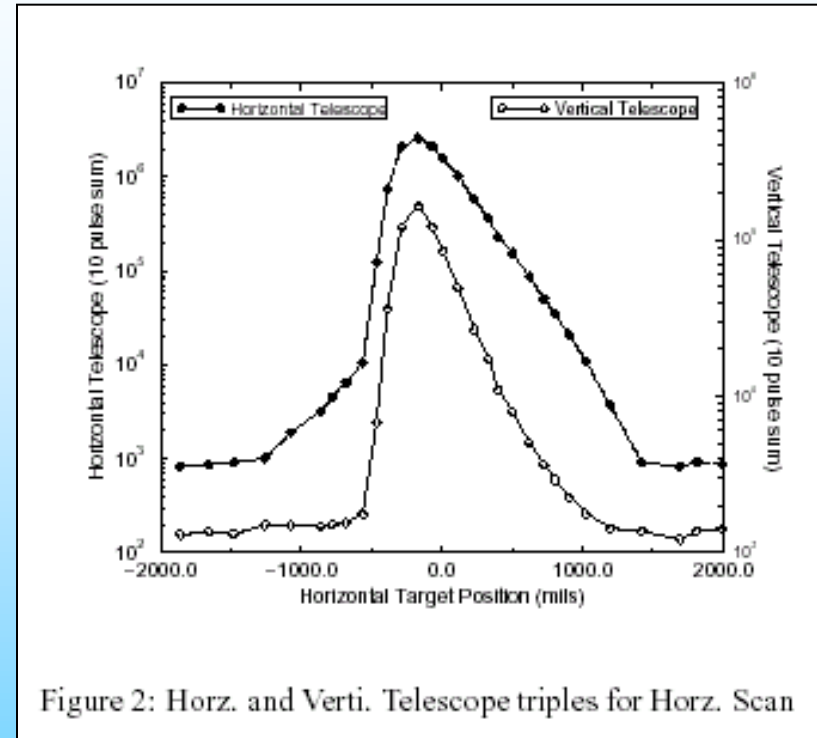
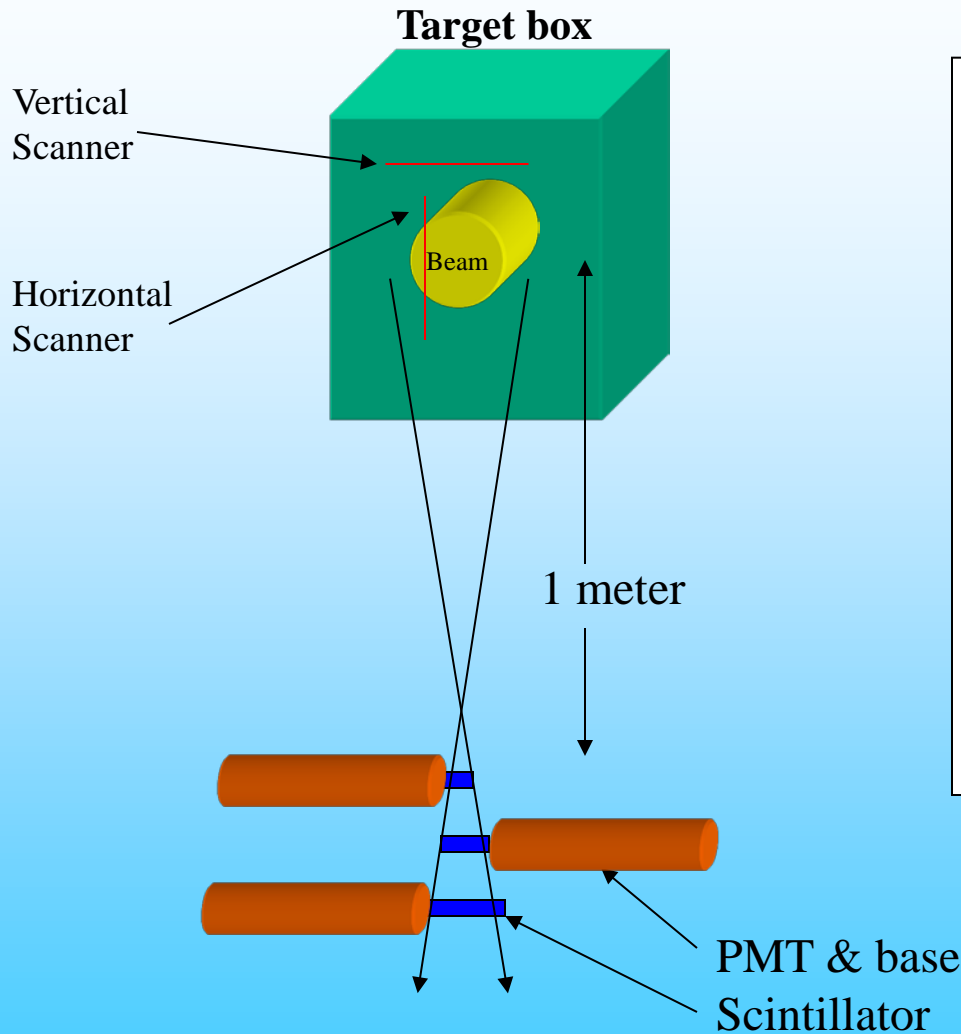


ATF2, L.Lui et al., IPAC14

Halo Measurements of the Extracted Beam at the Los Alamos Proton Storage Ring; A. Browman, et al., PAC03

# Wire Scanners

## Telescope Operation at the extracted beams (AGS)

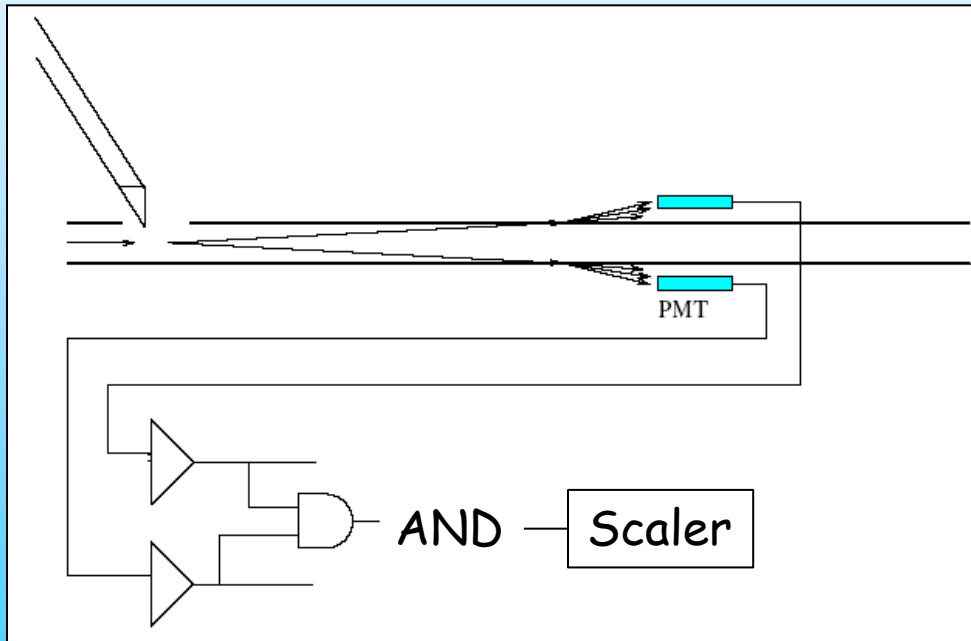


Solid angle remains the same through scan  
 Narrow acceptance, reduces noise.  
 Telescope acceptance about  $10^{-4}$  steradian.

Scintillator Telescope in the AGS Extracted Beamline; D. Gassner, Ket al.; 29th ICFA Advanced Beam Dynamics Workshop on Beam Halo Dynamics, 2003 Workshop, Long Island, New York.

# Wire Scanners at Jefferson Lab

Huge dynamic range ( $10^8$ ) by different wire diameters and coincident counting:



Large Dynamic Range Beam Profile Measurements  
T. Freyberger, DIPAC05

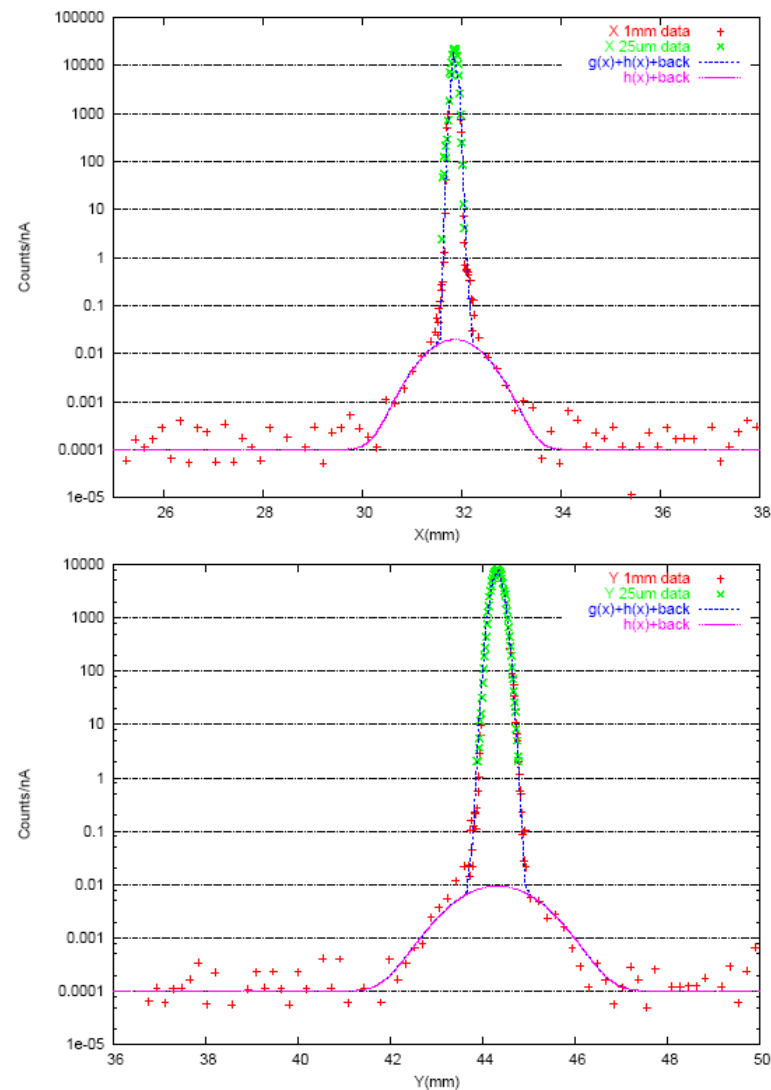


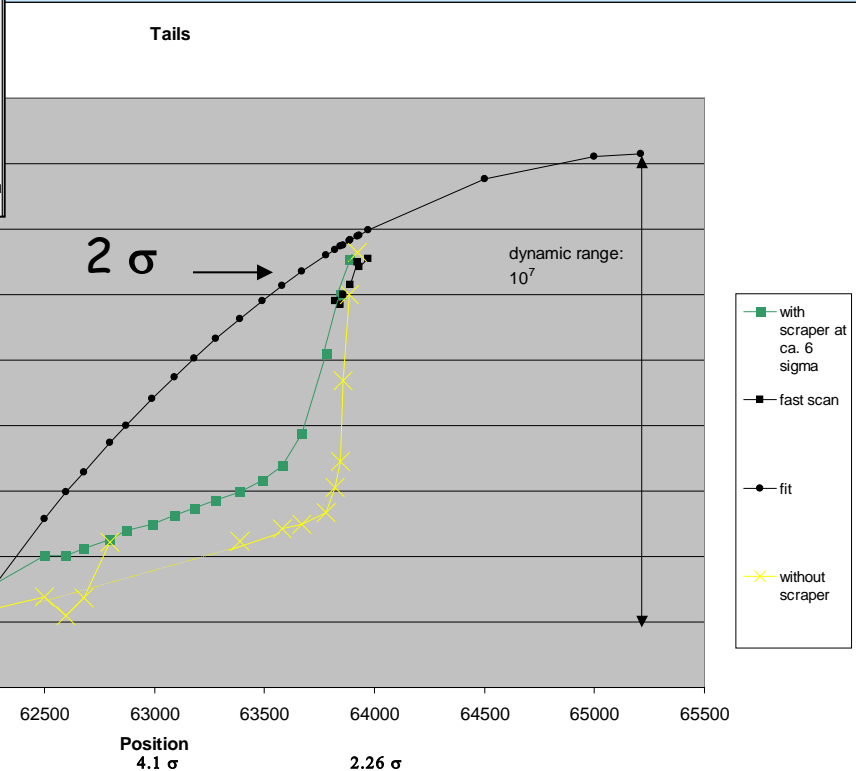
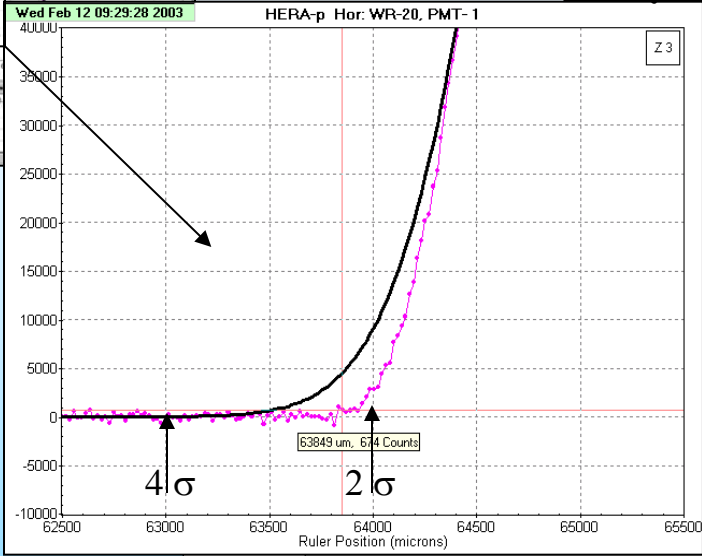
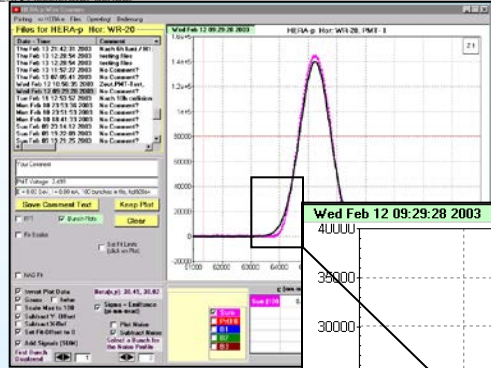
Figure 4: Beam Profile combining the  $25\mu\text{m}$  and  $1\text{mm}$  Fe wire data. The top(bottom) plot shows the X(Y) data and results of the fit to the data. The red points represent the  $1\text{mm}$  wire data, the green points the  $25\mu\text{m}$  wire data, the blue curve is the overall fit to the data and the red curve is the halo portion of the fit. The ordinate is plotted with a log-scale and the count rate is normalized to the beam current.

# Wire Scanners at HERA

Fast scan  
 $E=920 \text{ GeV}/c$   
 $p\text{-}e^+$  collisions

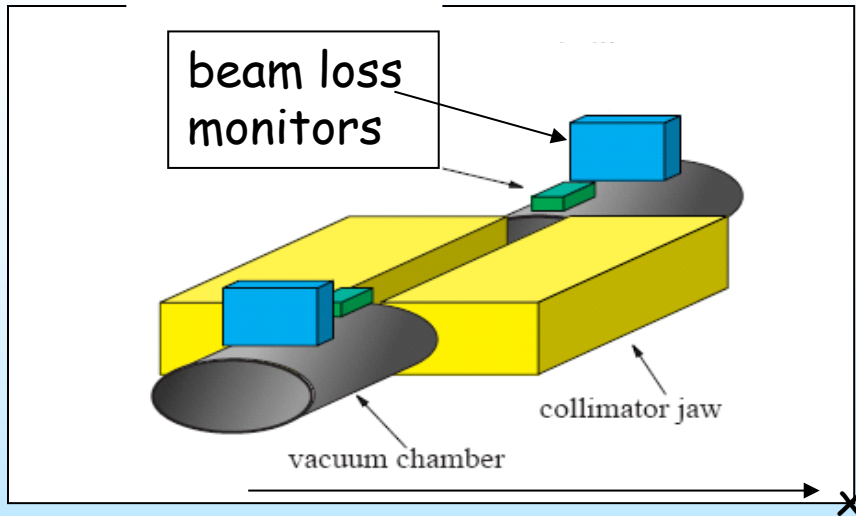
Huge dynamic range by scanning + counting  
 No scraping, single scintillator! (HERA):  
**Very clean beam conditions (no losses)**

No halo,  
 even smaller than gaussian.



Beam Tail Measurements using Wire Scanners at DESY  
 S. Arutunian, M. Werner, and K. Wittenburg  
 29th ICFA Advanced Beam Dynamics Workshop on Beam Halo Dynamics,  
 2003 Workshop, Long Island, New York.

# Halo scraping by collimators



In a synchrotron one jaw will scrape both sides of the beam distribution ( $\beta$ -oscillation)  
 $\Rightarrow$  meas. symmetric halo  
 Such a tail scan yields information about particles which oscillate with an amplitude larger than the position of the collimator = Halo Scraping

TRANSVERSE BEAM TAILS DUE TO INELASTIC SCATTERING  
 H. Burkhardt, I. Reichel, G. Roy  
 CERN-SL-99-068 (OP)

TRANSVERSE H-BEAM HALO SCRAPER SYSTEM IN THE J-PARC L3BT  
 K. Okabe et al.,  
 IPAC14



Figure 2: Picture of the new scraper head with the thin carbon foil. The carbon foil is mounted by the metal foil folder.

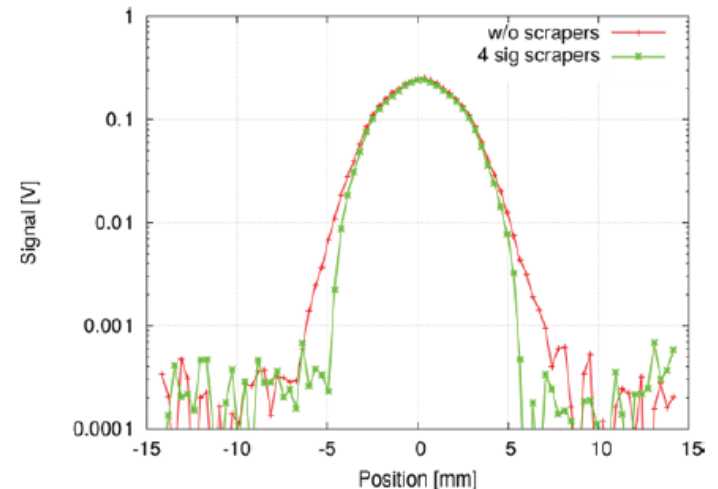
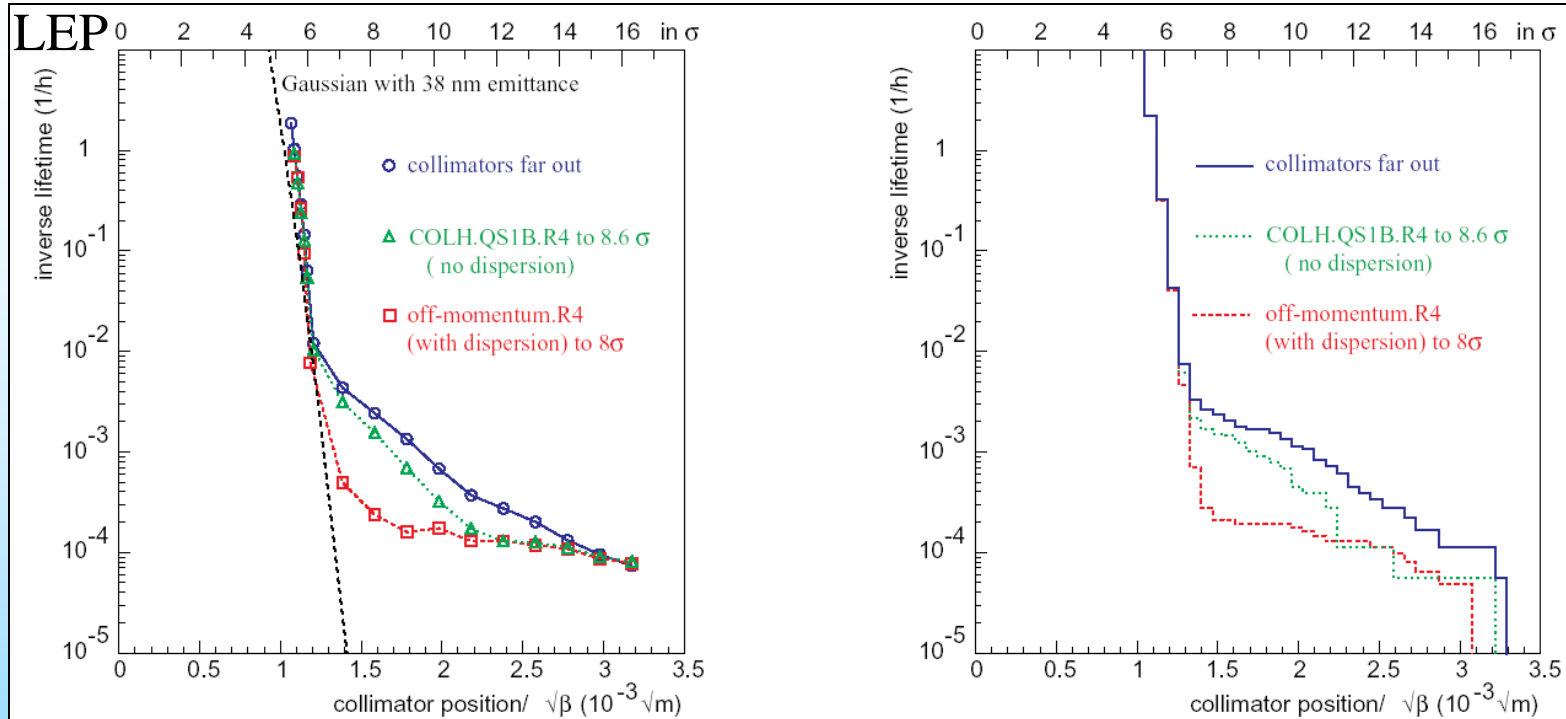


Figure 4: Scraped beam profile in the vertical direction. Red lines are vertical beam profile without setting scrapers, green lines are beam profile with setting scrapers.

# Halo Measurement = Scraping by collimators + BLM



Measurement (left) and simulation (right) of the horizontal beam tails for a beam energy of 80.5 GeV and for different collimator settings at LEP. The simulation is the result of tracking particles after Compton scattering on thermal photons (black body radiation of vacuum chamber).

Measurements were performed by moving one jaw of a collimator closer to the beam in steps. Beam current and beam size measurements were recorded for each collimator setting. The collimators were moved closer until significant lifetime reductions were observed. Lifetimes calculated from beam currents for these points were used to calibrate the loss monitors. This allows to give loss rates directly in terms of equivalent lifetimes

# Other sensitive, high dynamic halo monitors

- Direct measurement by inserting monitor or by an intercepting monitor.  
**No absolute calibration of halo!!!**

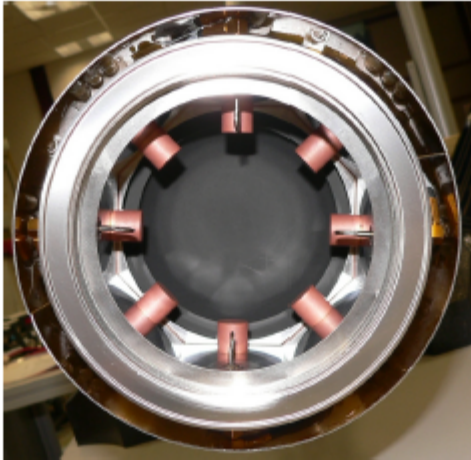
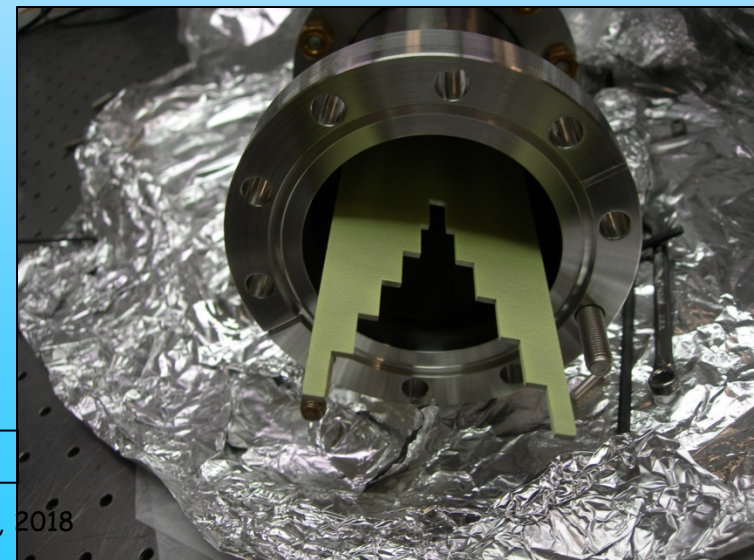
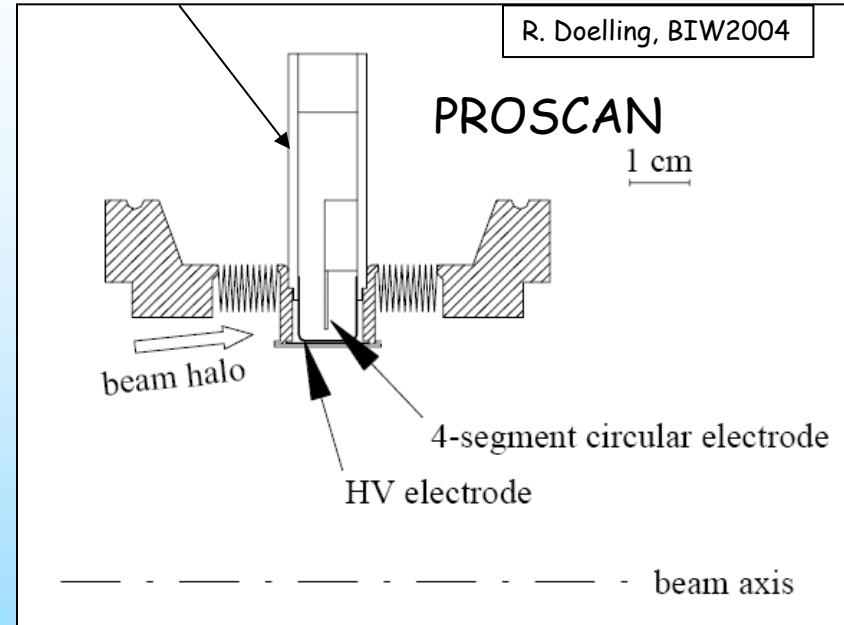


Figure 1: View of the BHM from the dump. The BHM sensors are inside the caps. Four loops of the magnetic-coupled BPM are right in front of the BHM sensors.

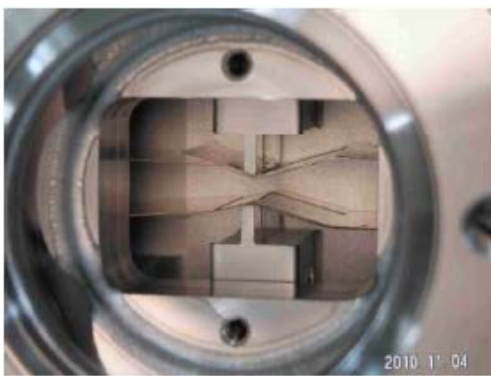
BEAM HALO MONITOR FOR FLASH AND THE EUROPEAN XFEL; A. Ignatenko et al., IPAC2012

## Ion chamber, SEM

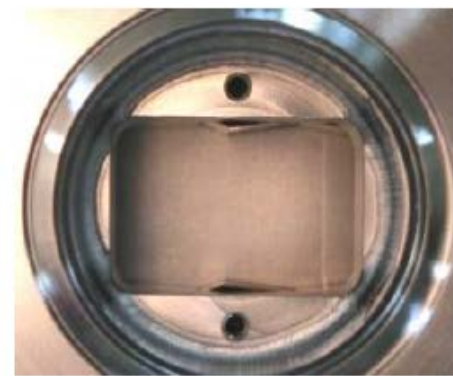


JLab FEL

# Halo measurement by diamonds



(a)



(b)

**Figure 11:** Photograph of the RF fingers with Al windows in (a) active mode and (b) shelter

SACLA XFEL

How to calibrate the 2 monitors?

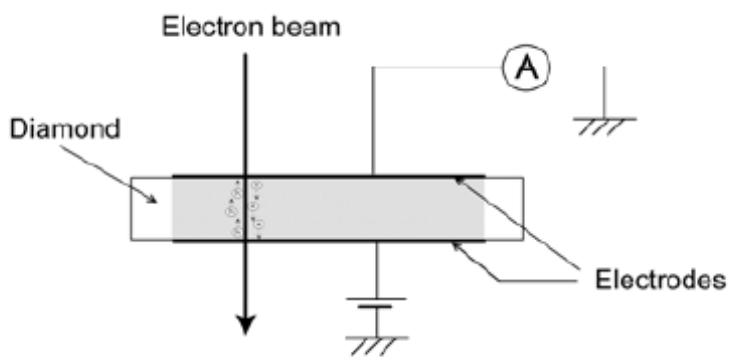


**Figure 2:** Principle of the diamond-based detector.

ELECTRON BEAM HALO MONITORING USING DIAMOND-BASED DETECTORS TO PROTECT UNDULATOR PERMANENT MAGNETS FROM RADIATION DAMAGE  
 Hideki Aoyagi, *Beam Dynamics Newsletter No. 66*, April 2015

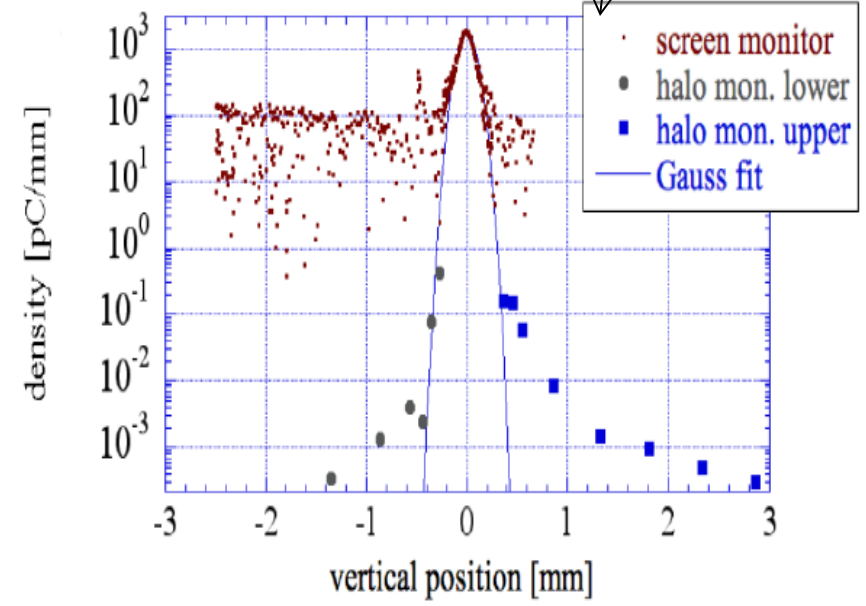


**Figure 17:** Vertical beam profile measurement by using the halo monitor and the screen monitor.

# Halo measurement by diamonds

## In vacuum diamond sensor (DSv) scanner at ATF2

S.Liu et al. In vacuum diamond sensor scanner for beam halo measurements in the beam line at the KEK Accelerator Test Facility ; NIM A832 (2016) 231–242

And very latest results at:

Evaluation of beam halo from beam-gas scattering at the KEK Accelerator Test Facility PHYSICAL REVIEW ACCELERATORS AND BEAMS 21, 051001 (2018)

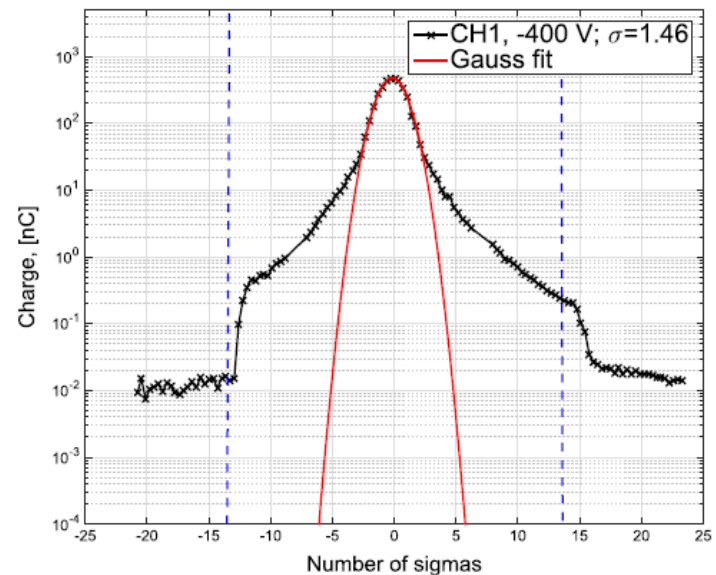
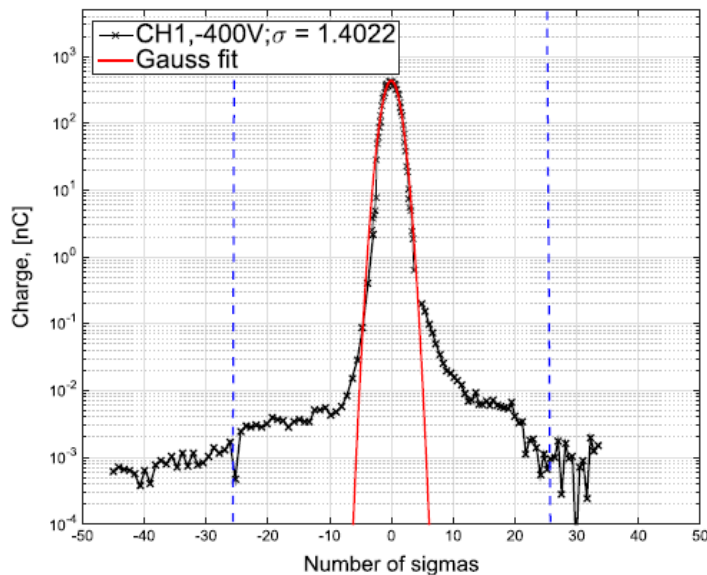
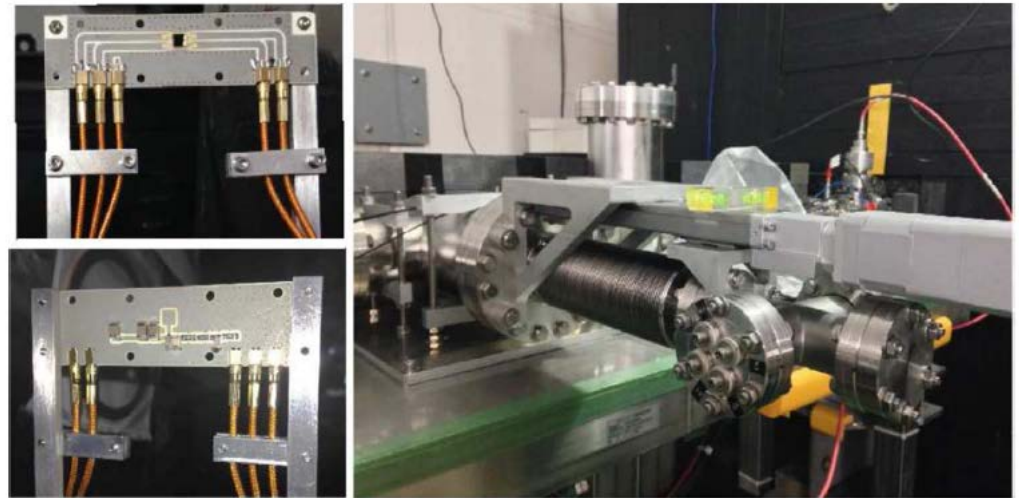


**Fig. 14.** Measured beam core and beam halo distributions using the DSv, with cuts by apertures in the horizontal (left, BX10BY0.5 optics) and vertical (right, BX10BY1 optics) planes. The positions of the cuts obtained in the simulation from the tightest apertures are indicated by dashed lines, for a perfectly aligned and optically matched beam.

# Optical Methods

# YAG:Ce Screen with Slit

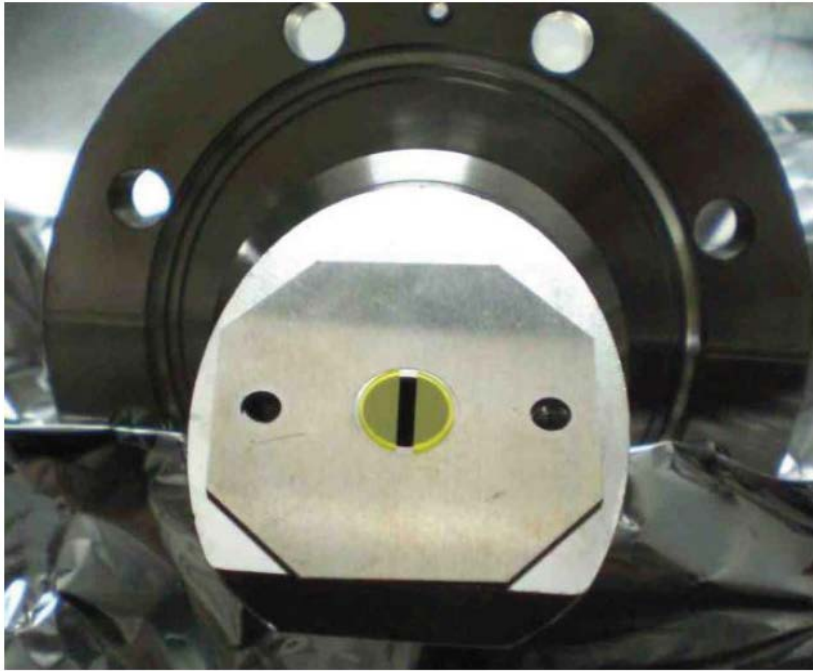


Figure 2: YAG:Ce screen on the actuator holder: The beam core goes through a slit at the center of the screen without any interaction for the scintillator.

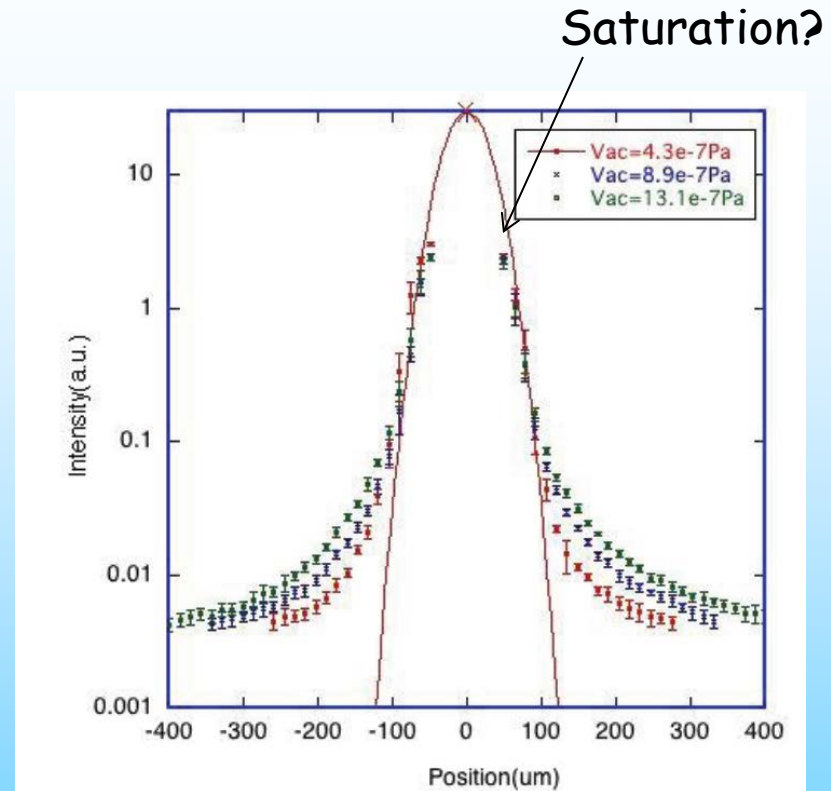
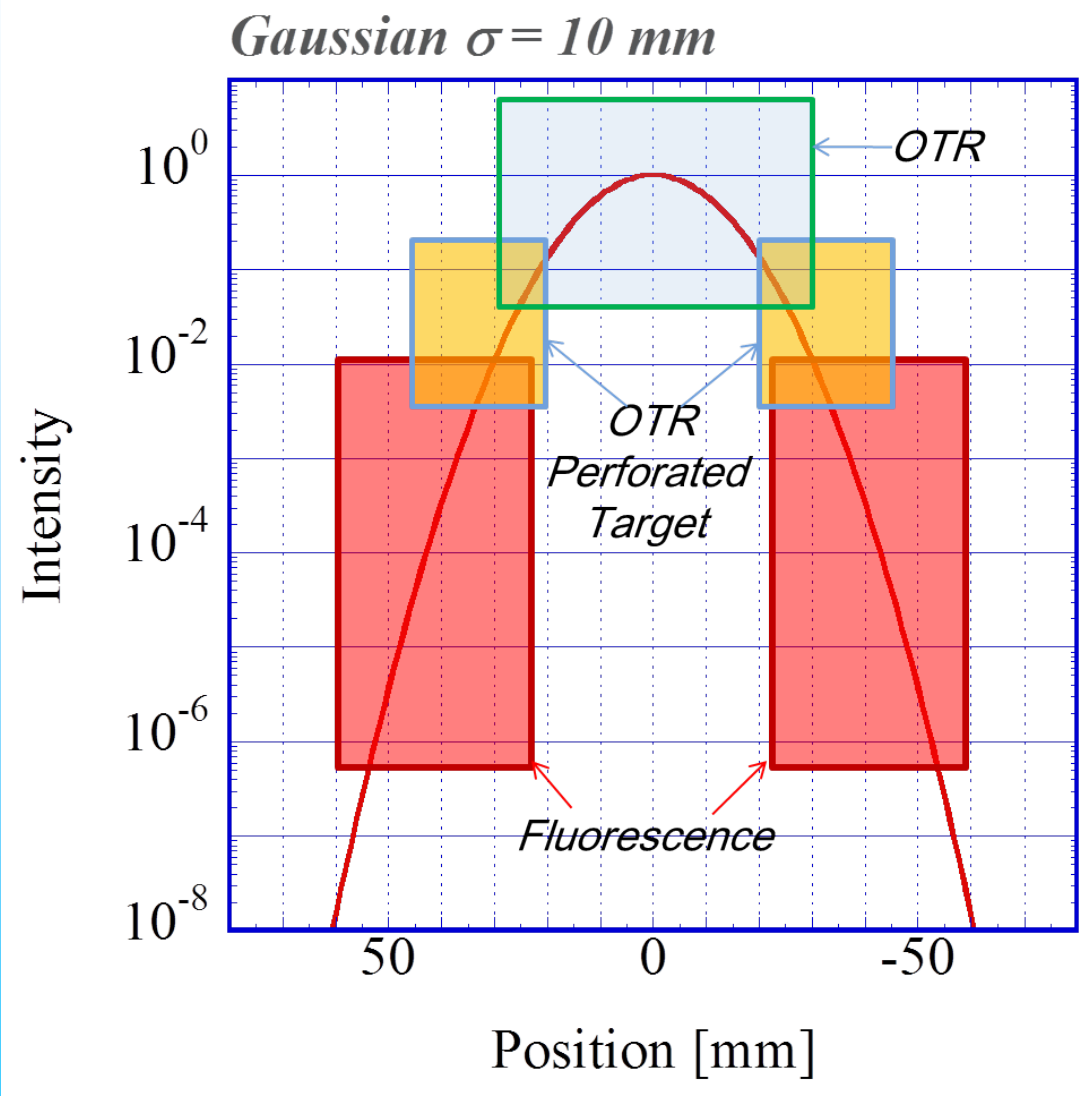


Figure 8: Distribution of the beam halo for the different vacuum condition in the case of the beam intensity  $0.45 \times 10^{10}$  electrons

Beam Halo Measurement Utilizing YAG:Ce Screen  
 T. Naito, T.M. Mitsuhashi  
 IBIC2015, Melbourne, Australia

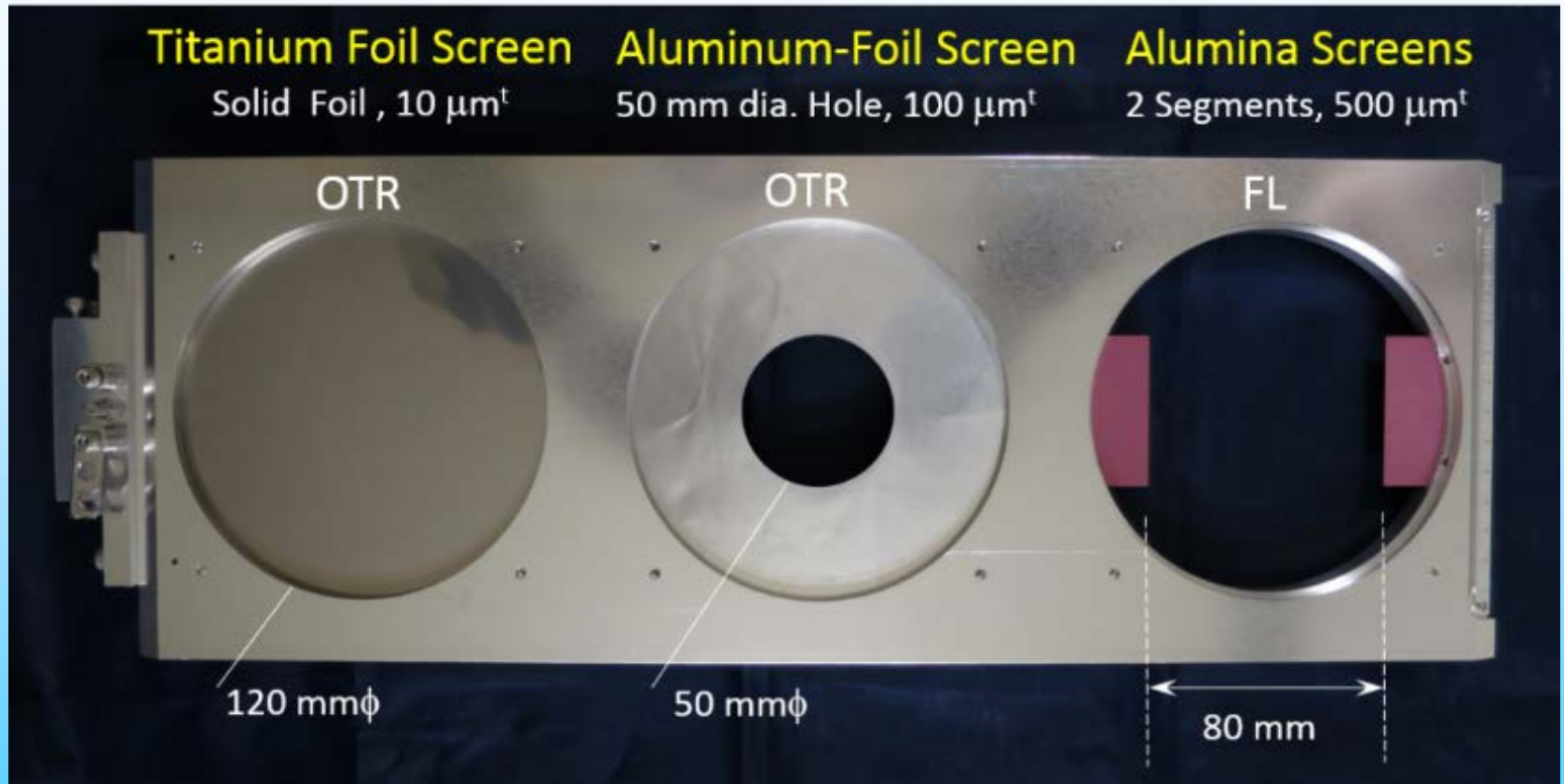
How to calibrate beam core and halo?

# OTR/fluorescence screens



# OTR/fluorescence screens

## Target assembly



Beam center

Tails

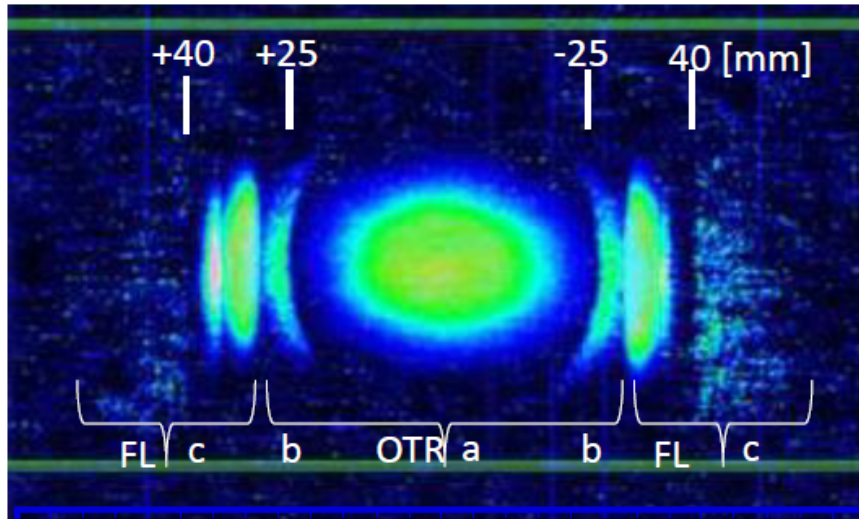
Halo

# OTR/fluorescence screens

## Combination Measurement with OTR and Fluorescence

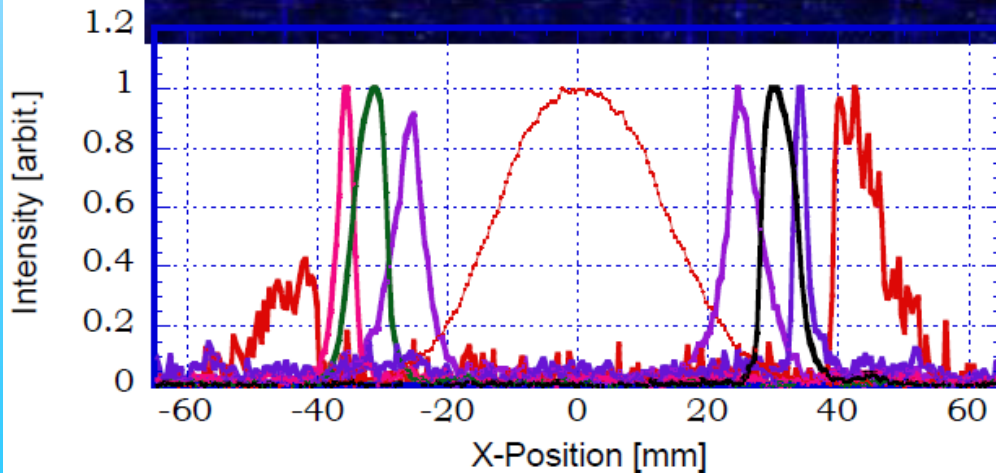
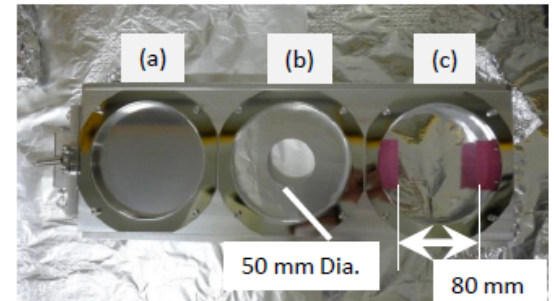


- Intensity :  $9.6 \times 10^{12}$  proton /2bunch
- 2 bunches  $\times$  5 Shots (AVG)
- Image Intensifier Gate:  $10 \mu\text{s}$



Superimposed Profile Image

Multi-screen

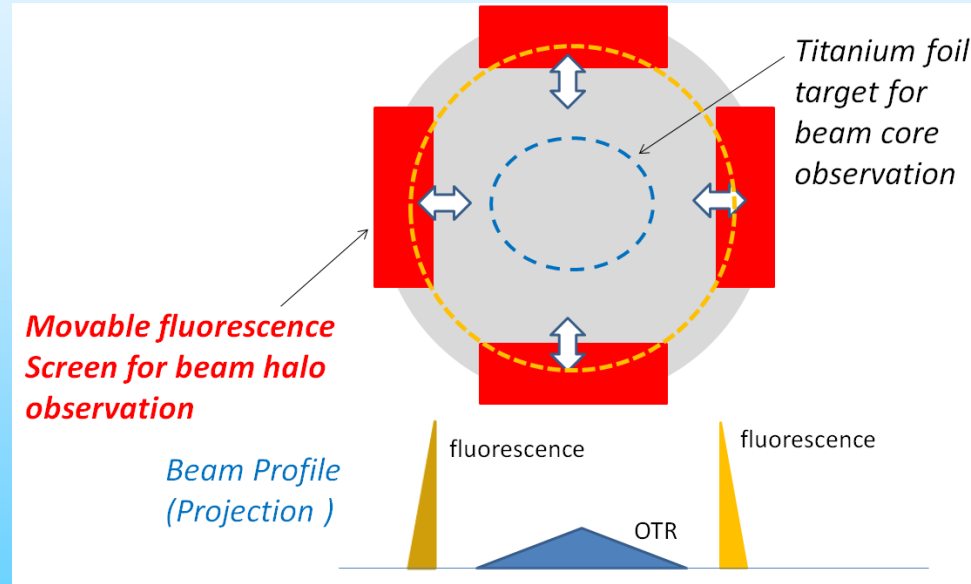
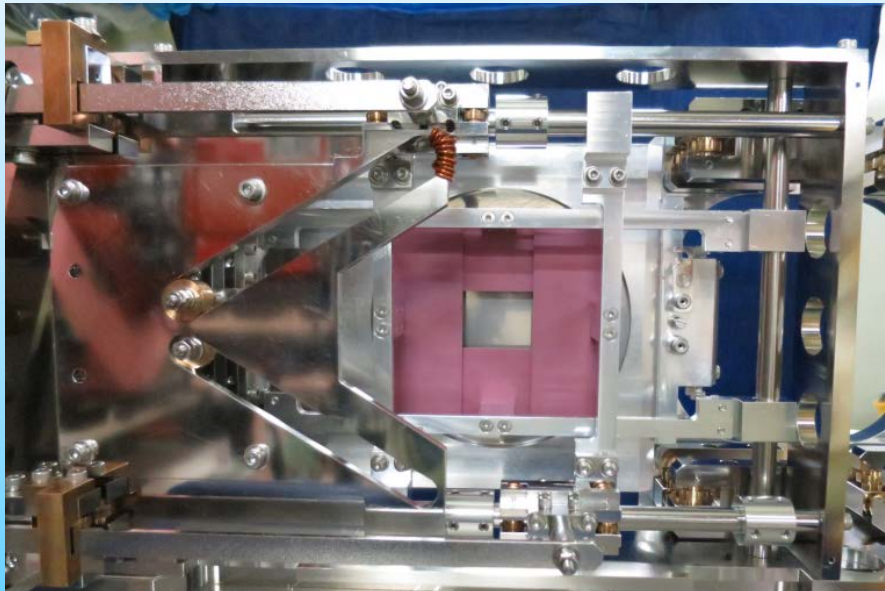


Horizontal Projection (Normalized)

A Development of High Sensitive Beam Profile Monitor Using Multi-Screen  
Y.Hashimoto et al., IBIC2013, Oxford, UK

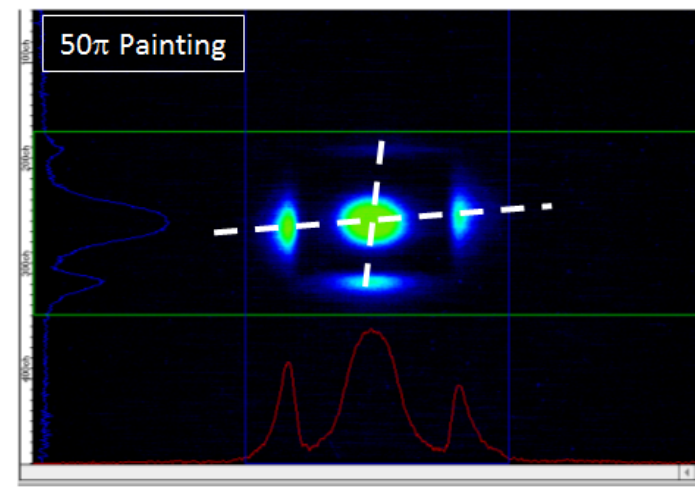
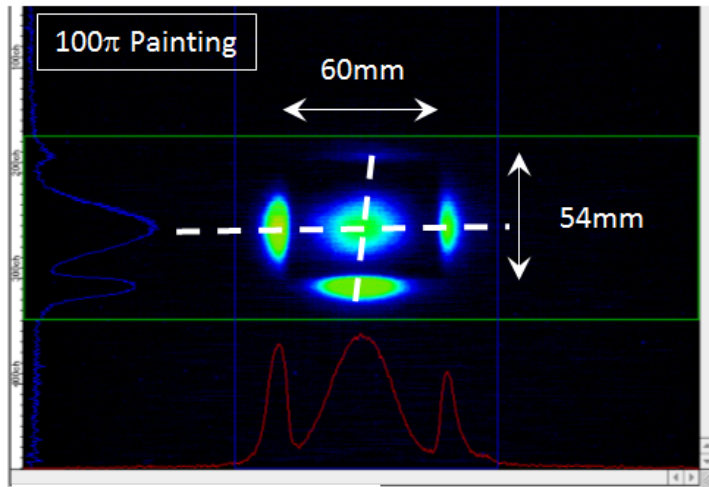
# OTR/fluorescence screens

## A Simultaneous observation of beam core with OTR and fluorescence screen



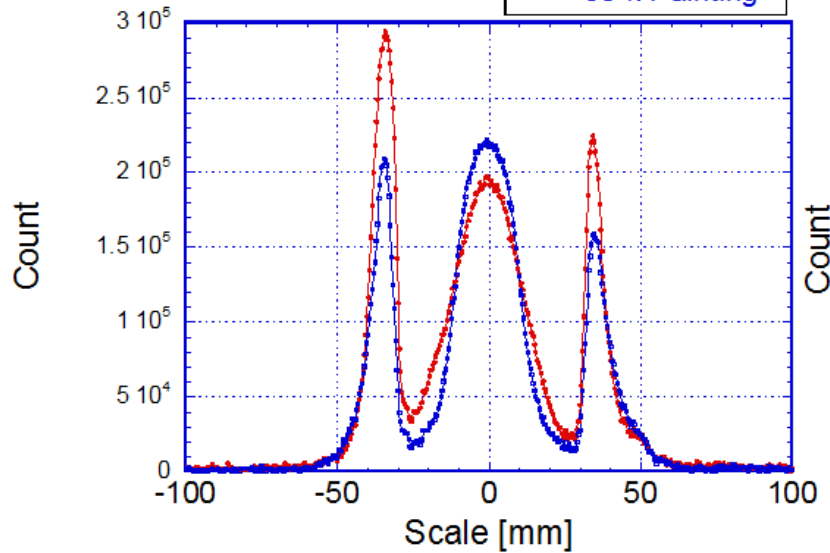
Two-Dimensional and Wide Dynamic Range Profile Monitor Using OTR / Fluorescence Screens for Diagnosing Beam Halo of Intense Proton Beams, Y.Hashimoto et al., HB2014, East Lansing, USA

# OTR/fluorescence screens



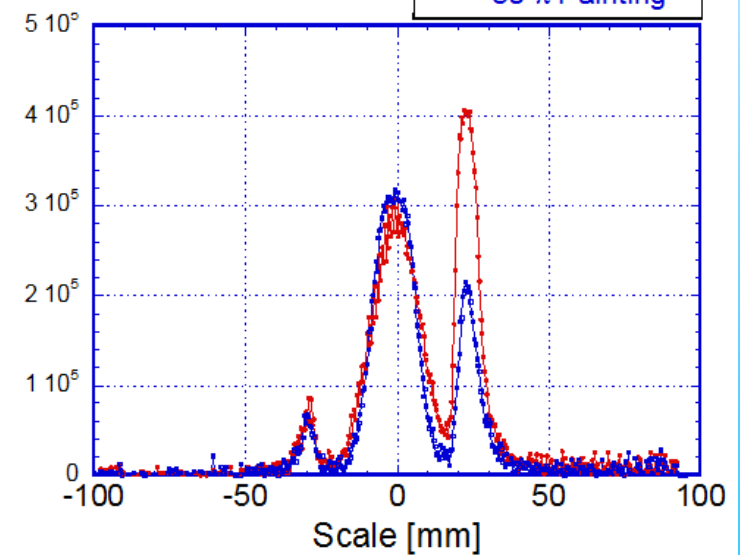
**Horizontal**

—●— 100  $\pi$  Painting  
—●— 50  $\pi$  Painting

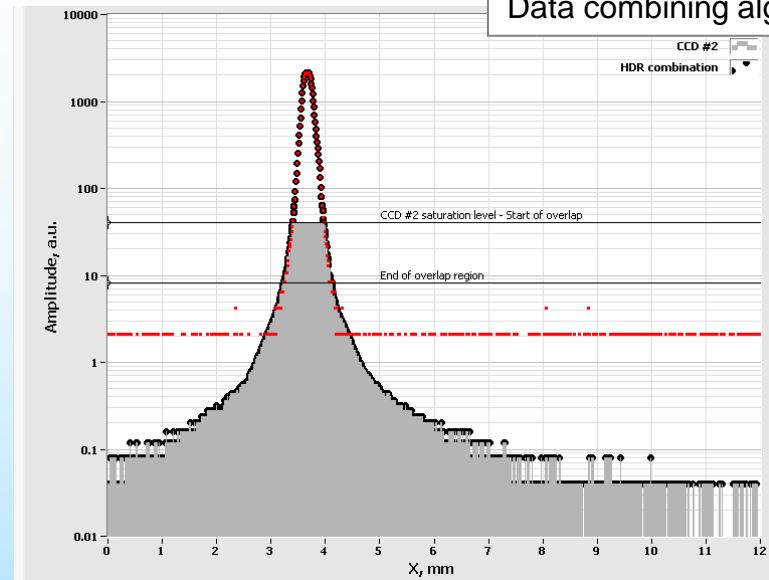
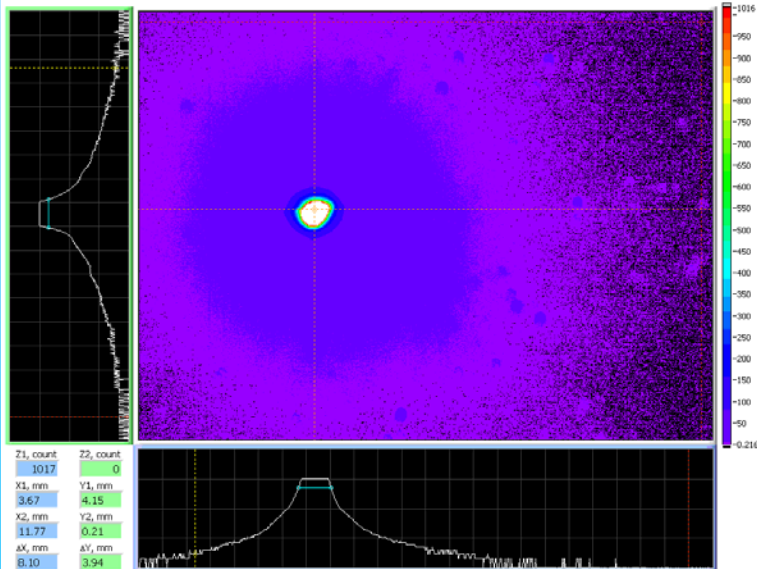
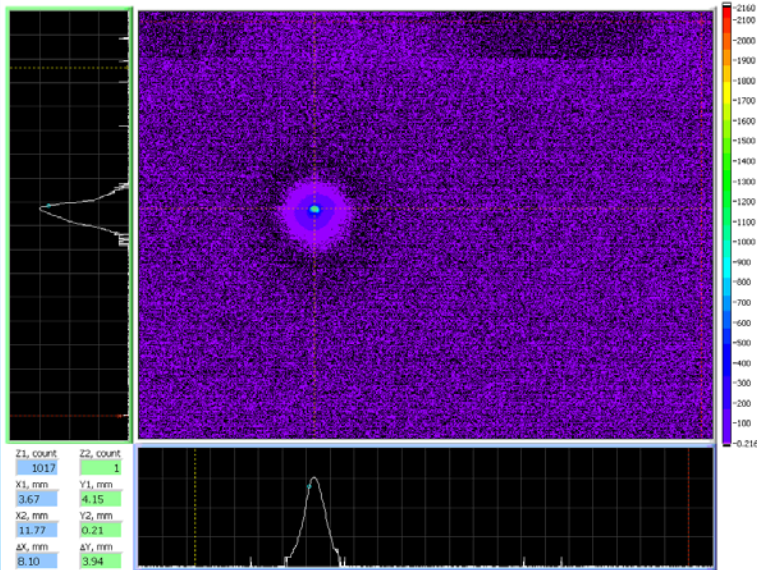


**vertical**

—●— 100  $\pi$  Painting  
—●— 50  $\pi$  Painting



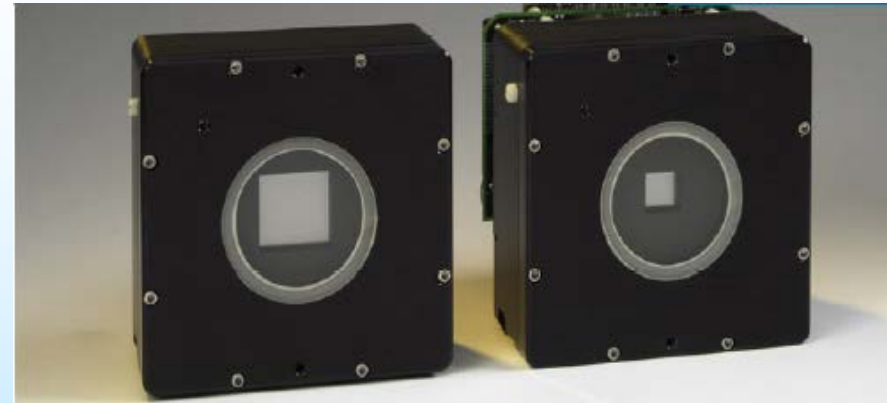
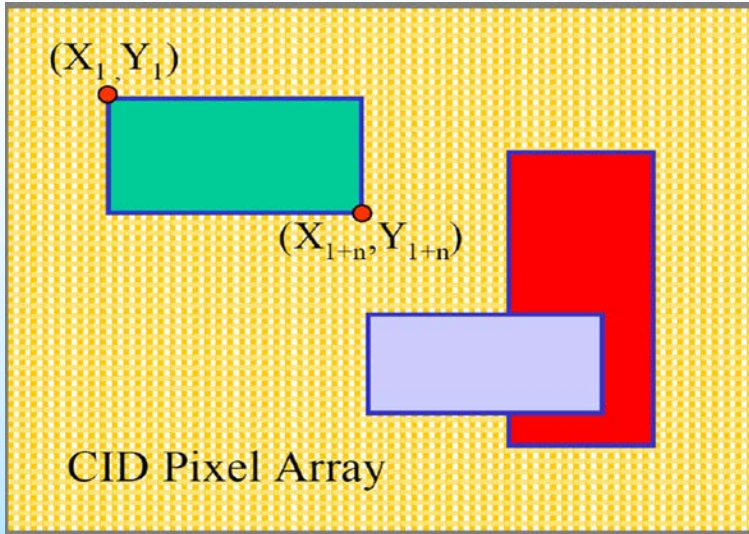
# 2 CCD camera measurements



- ❖ Two images (on the left) measured simultaneously with integration times 20  $\mu$ s and 400  $\mu$ s
- ❖ Background measurements and subtraction is crucial! Made separately for two sensors and subtracted on-line.
- ❖ Combining algorithm is efficient enough to provide 5 Hz repetition rate for 1024x768 images
- ❖ At the time of measurements was limited by the flexibility of DLPC
- ❖ Demonstrated dynamic range of  $\sim 5E+4$  (factor of 100 increase)
- ❖ Integration time is used for normalization and overlap (sufficient)
- ❖ Averaging also improves SNR and therefore DR (beam stability)

High Dynamic Range Beam Imaging with Two Simultaneously Sampling CCDs; , P. Evtushenko, D. Douglas; IBIC2012, Tsukuba, Japan

# CID Camera



Commercial available

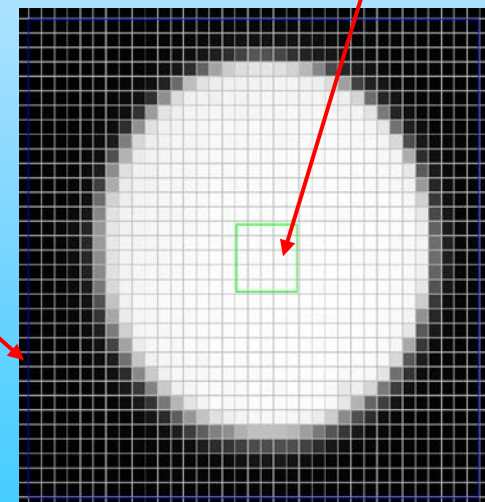
[http://www.thermo.com/eThermo/CMA/PDFs/Product/productPDF\\_26754.pdf](http://www.thermo.com/eThermo/CMA/PDFs/Product/productPDF_26754.pdf)

Each pixel on the CID array is individually addressable and allows for random access non-destructive pixel readout. The *random access integration (RAI)* mode automatically adjusts the integration time from pixel to pixel based upon the real-time observation of photon flux using CID random accessibility and non-destructive readout. With this RAI mode a dynamic range ( $\sim 10^6$ ) can be achieved.

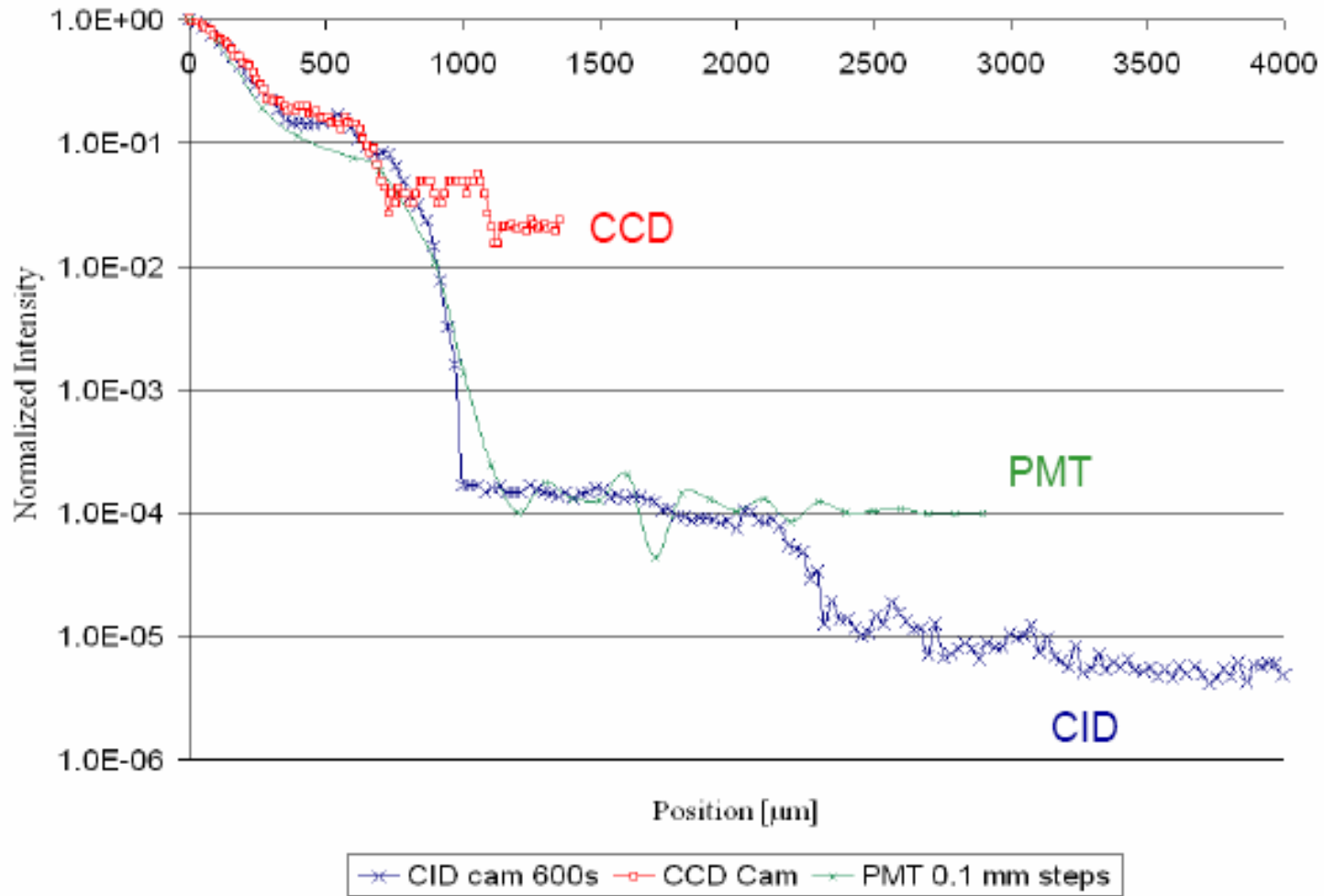
C.P. Welsch et al., CLIC Note 657, 2006

Control Rol

Subarray

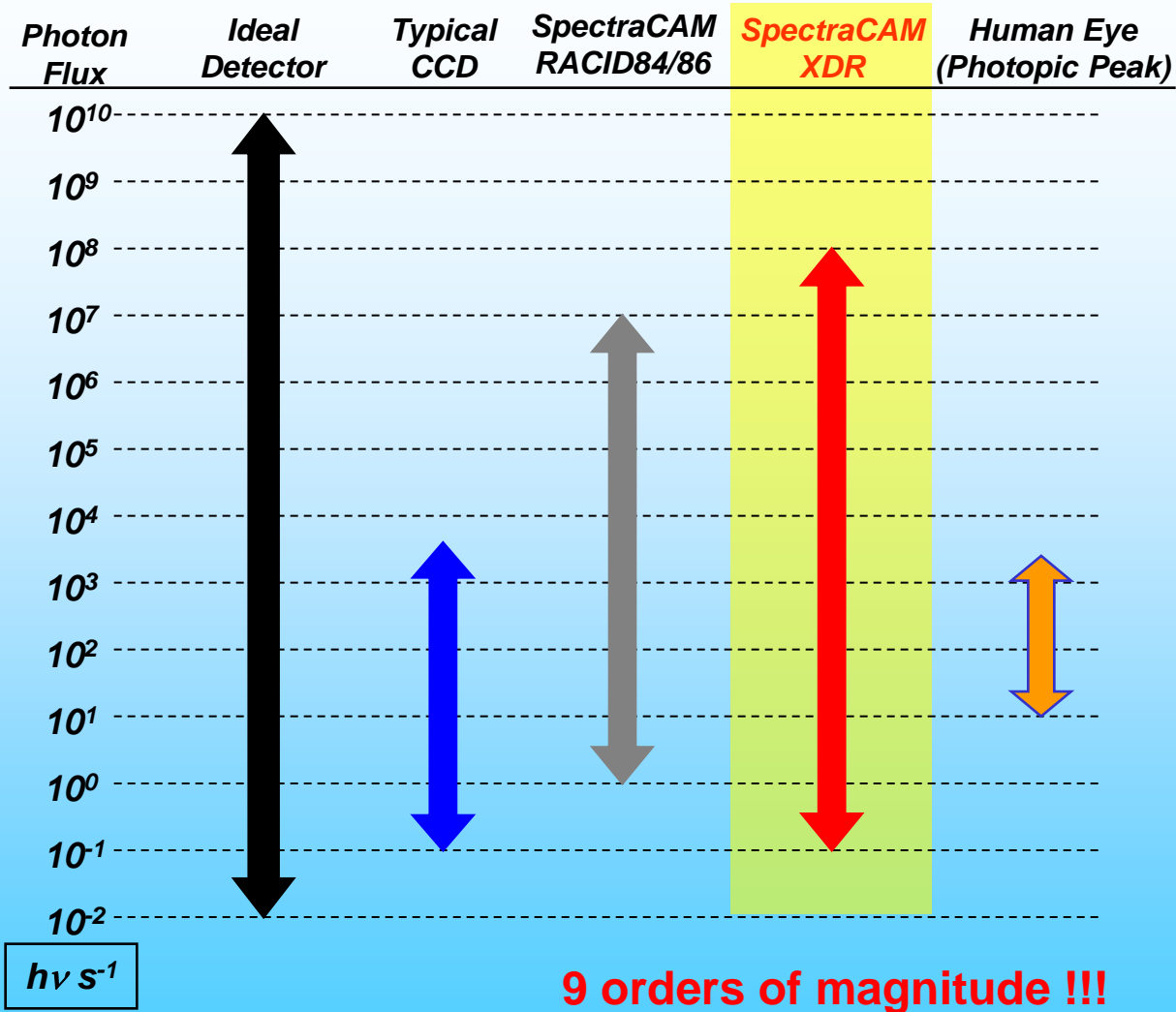


# CID Camera



C.P. Welsch et al, EPAC06

# CID Camera



SPECTRACAM XDR: High resolution scientific imaging camera system using Charge Injection Device capable of extremely high dynamic range and random pixel addressing

# Micro Mirror Array

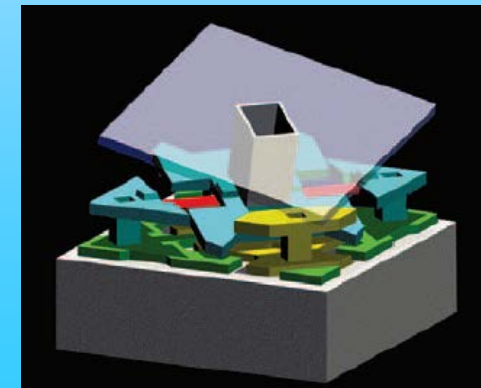
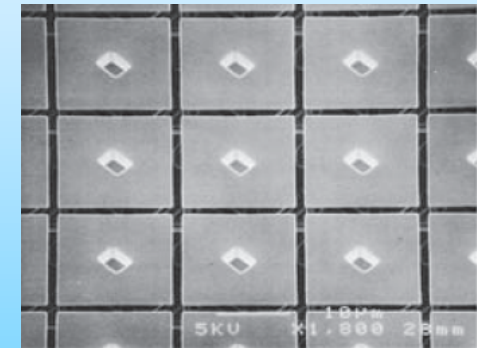
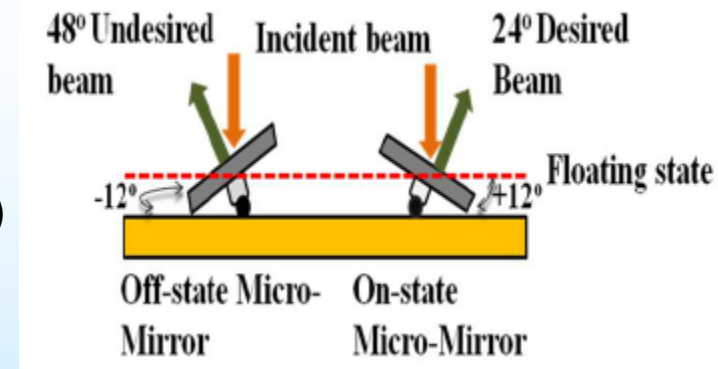
OR Digital Micro-mirror Device (DMD)

- grid of 1920×1080 micro alumina mirrors
- up to 9.600 full array mirror patterns / sec (7.6 Gbs)
- 10.8μm × 10.8μm in size
- optical fill factor of 85%
- +/- 24° of rotation
- Switch of 15-20 μs physically,

The first applications were in digital projection equipment, which has now expanded into digital cinema projectors, with sometimes **more than two million micro mirrors per chip switching at frequencies of up to 5 kHz**. Recently MMAs are finding applications in the large telecommunications market as optical multiplexers and cross-connect switches.

CTF3 Instrumentation, T. Lefevre, BIW08

Beam Halo Monitor Based on an HD Digital Micro Mirror Array  
B.B.D. Lomberg, et al., IBIC2013, Oxford, UK



# Micro Mirror Array

J. Corbett et al., Halo Workshop 2014 at SLAC

Injected Beam Imaging at SPEAR3 with a Digital Optical Mask

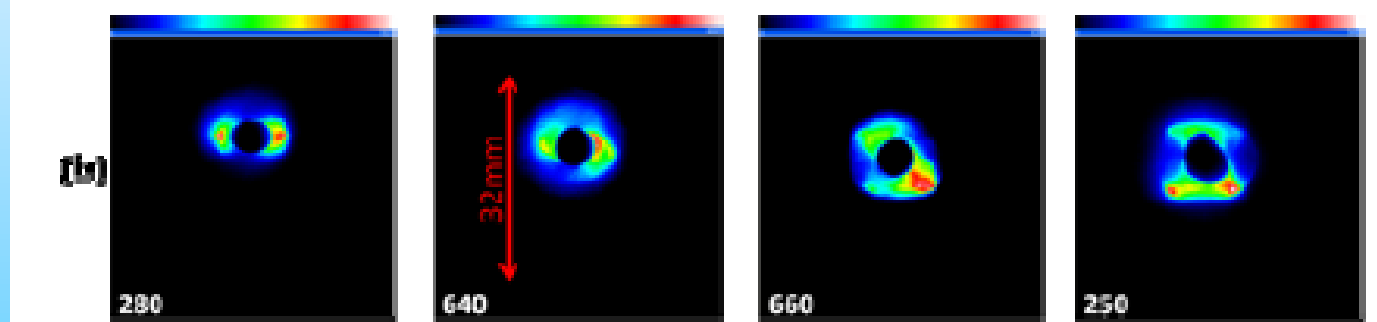
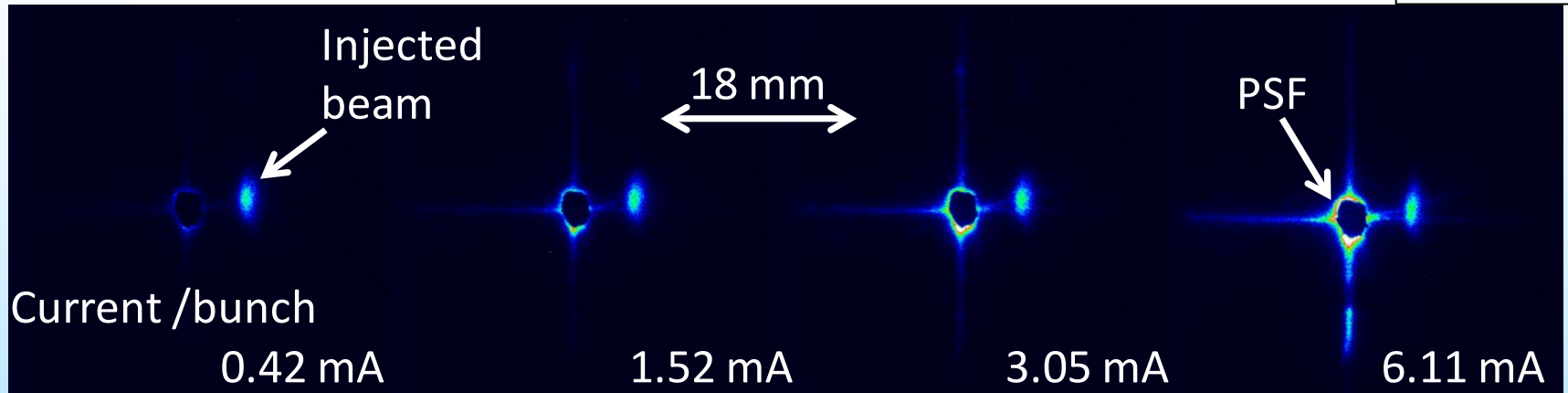


Figure 2: Beam (a) and halo (b) images with quadrupole current variation[5].

UMER: BEAM HALO MEASUREMENTS USING ADAPTIVE MASKING METHODS AND PROPOSED HALO EXPERIMENT, H. Zhang et al., HB2012

# Beam Halo Studies for CTF3

S.T. Artikova ET AL., IPAC'10, Kyoto, 2010.

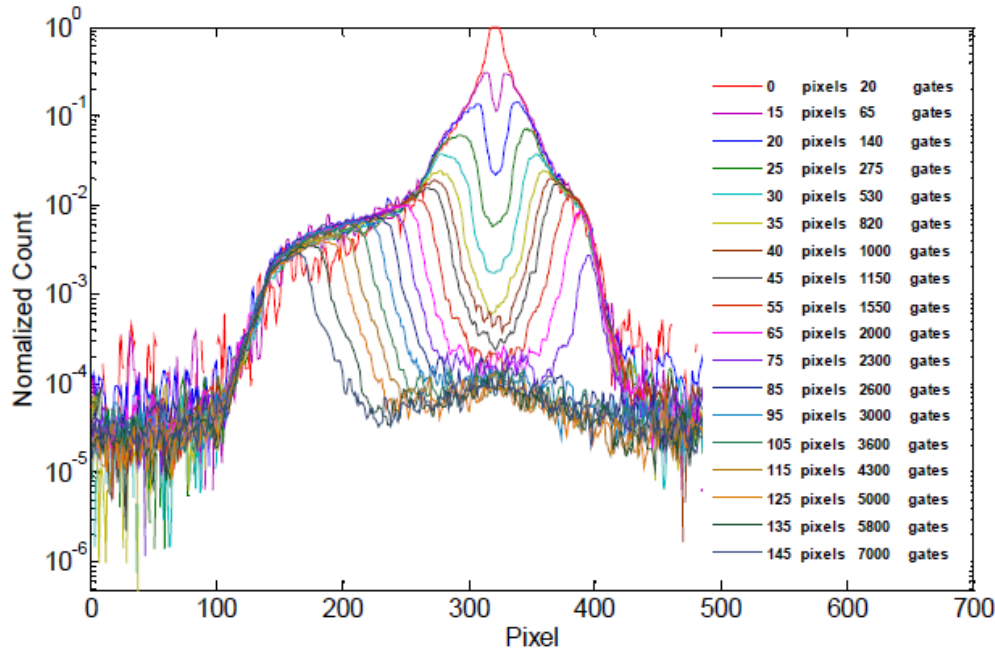


Figure 6: Measured beam profile with different mask sizes. Background subtraction and signal averaging was applied.

The system was then used to monitor the beam profile with different mask sizes. The background obtained when the beam was turned off was subtracted and averaging over 10 pixels was applied to smooth the signal. The signal in the tail of the distribution was increased by extending the measurement time of the ICCD camera progressively for each mask size. The result of these measurements is indicated in Fig 6 and a reconstruction of the beam profile shown in Fig. 7.

# Does It Really Measure Halo?

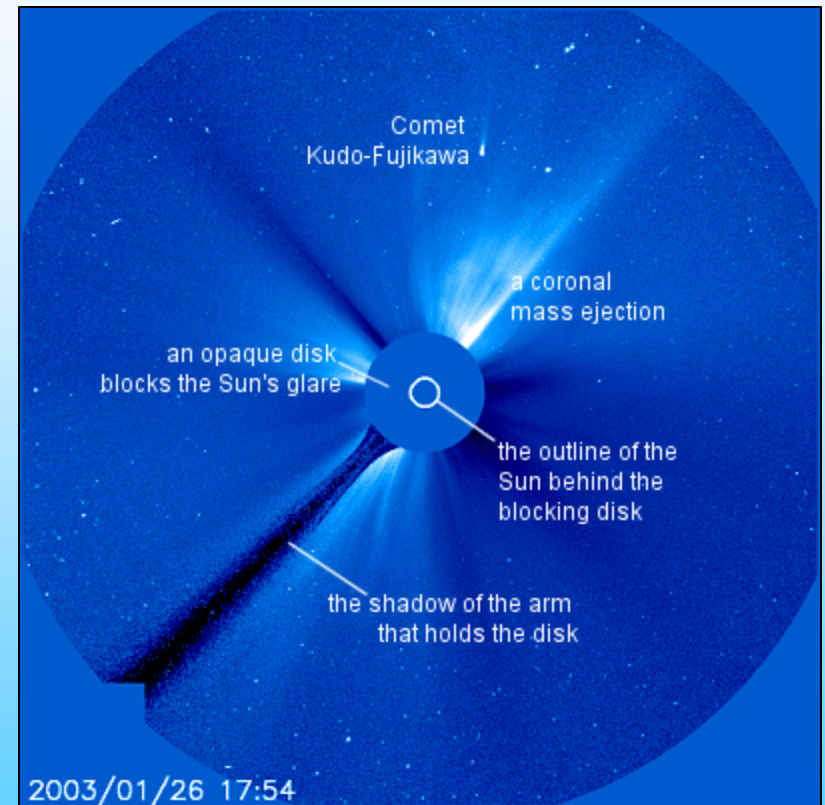
- These ideas can measure over a large dynamic range.
- But...will they measure halo, or will a measurement be dominated by diffracted and scattered light from the core?
- Deconvolution with the point-spread function (transmission pattern of a point source) can correct *some* of this, but:
  - Only if measured with the same optics
  - Each lens or mirror will have unique scatter
  - The beam is not a point source. Its halo is included in any PSF measured with the beam. An independent point source would be needed.
- Also, in a real machine, stray light from bends reflected along the inside of the beampipe will look like halo.
  - A thorough arrangement of baffles to restrict the source region can help.
- **Optical techniques are subject to scatter and diffraction.**
  - **Astronomers have a lot of experience with this problem.**

# Halo measurements with coronagraph

A **coronagraph** is a telescopic attachment designed specifically to block out the direct light from a star, so that nearby objects can be resolved without burning out the telescope's optics. **Most coronagraphs are intended to view the corona of the Sun**, The coronagraph was introduced in 1930 by the astronomer Bernard Lyot.

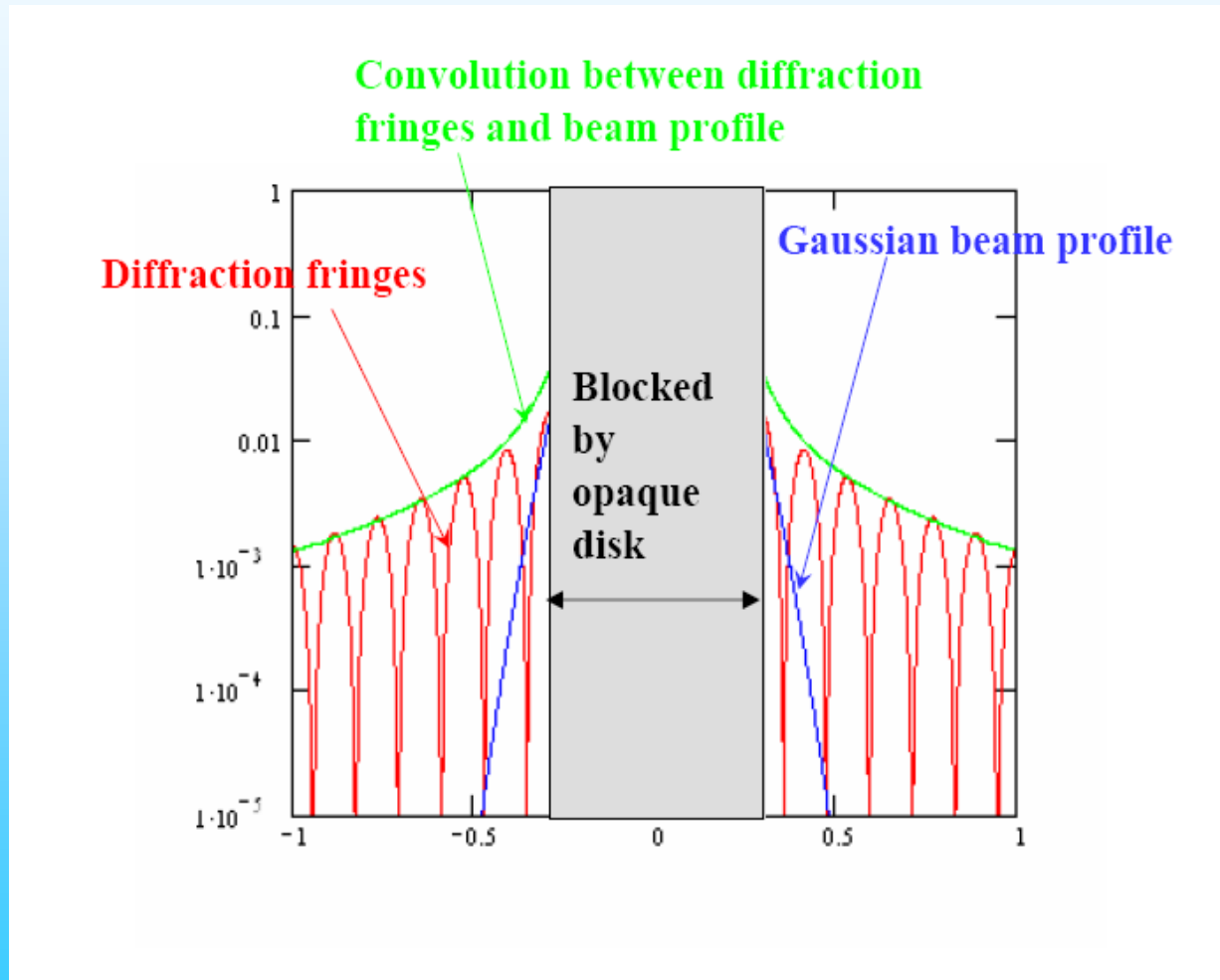
The simplest possible coronagraph is a simple lens or pinhole camera behind an appropriately aligned occulting disk that blocks direct sunlight; **during a solar eclipse, the Moon acts as an occulting disk and any camera in the eclipse path may be operated as a coronagraph until the eclipse is over.**

<http://en.wikipedia.org/wiki/Coronagraph>



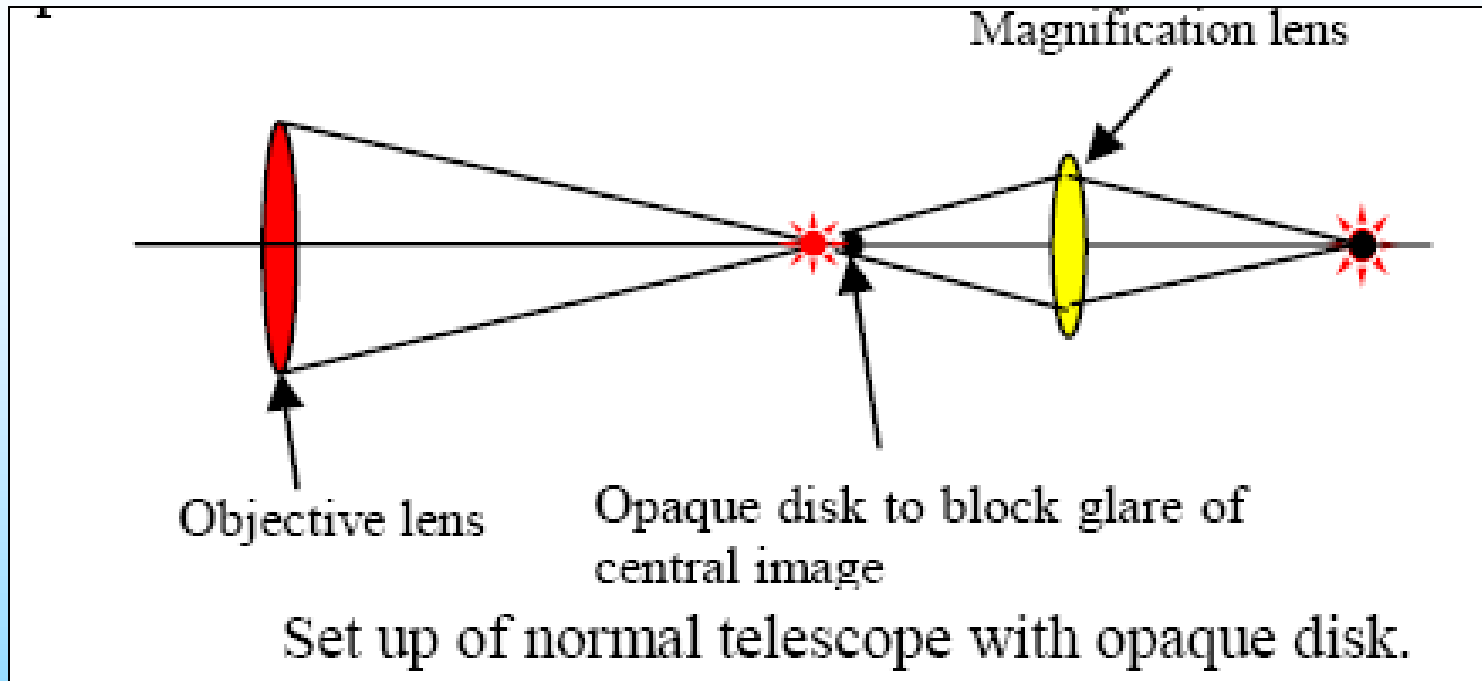
# Optical halo measurements

Directional optical radiation (e.g. Synchrotron radiation or OTR) with small opening angles ( $\approx 1/\gamma$ ) suffer from diffraction limits:



Pictures stolen from T. Mitsuhashi

# Halo measurements with coronagraph



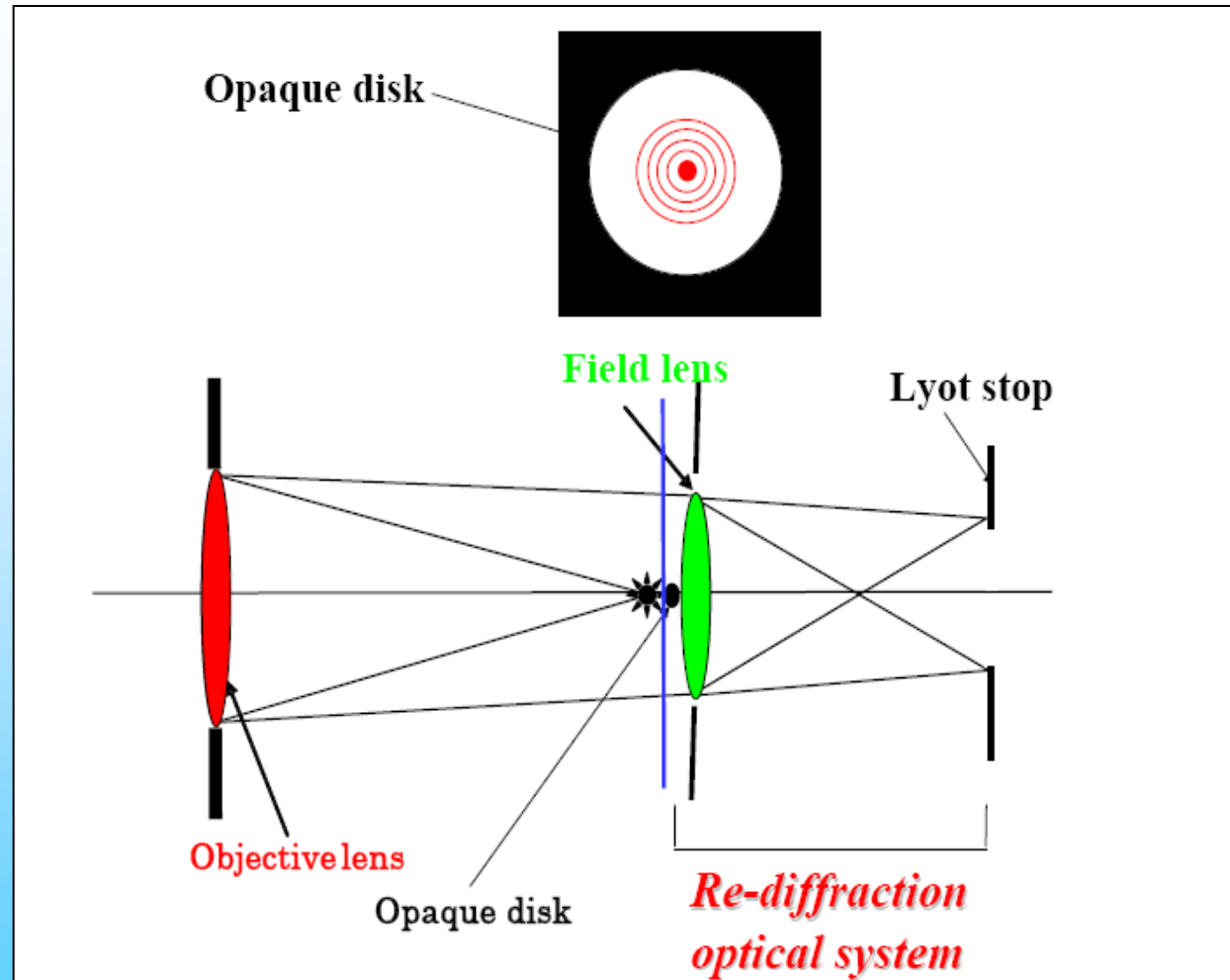
When using OTR or SR (narrow cone) the diffraction fringes makes tail surrounding from the central beam image. Intensity of diffraction tail is in the range of  $10^{-2}$  -  $10^{-3}$  of the peak intensity. The diffraction tail disturb an observation of weak object surrounding from bright central beam

Following pictures from a talk: BEAM HALO OBSERVATION BY CORONAGRAPH. T. Mitsuhashi, DIPAC 2005

# Halo measurements with coronagraph

Lyot's brilliant idea for the coronagraph is to remove this diffraction fringe by a mask, and relay the hidden weak image by a third lens onto the final observation plane

The Lyot stop effectively remove the diffracted light halo that surrounds the target, giving higher contrast improvement.

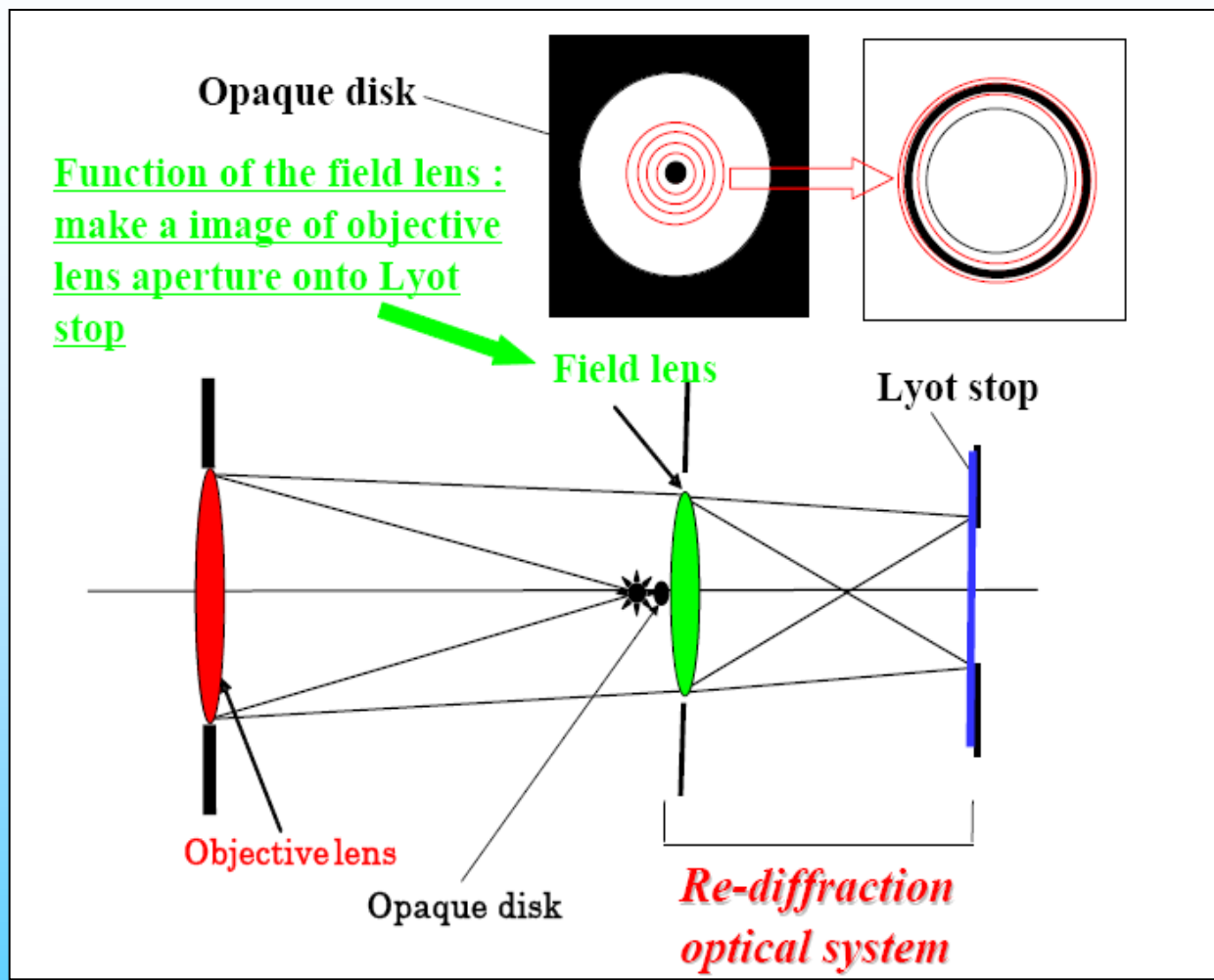


The first lens (objective lens) makes a real image of the object (beam image) on to a blocking opaque disk

# Halo measurements with coronagraph

Lyot's brilliant idea for the coronagraph is to remove this diffraction fringe by a mask, and relay the hidden weak image by a third lens onto the final observation plane

The Lyot stop effectively remove the diffracted light halo that surrounds the target, giving higher contrast improvement.



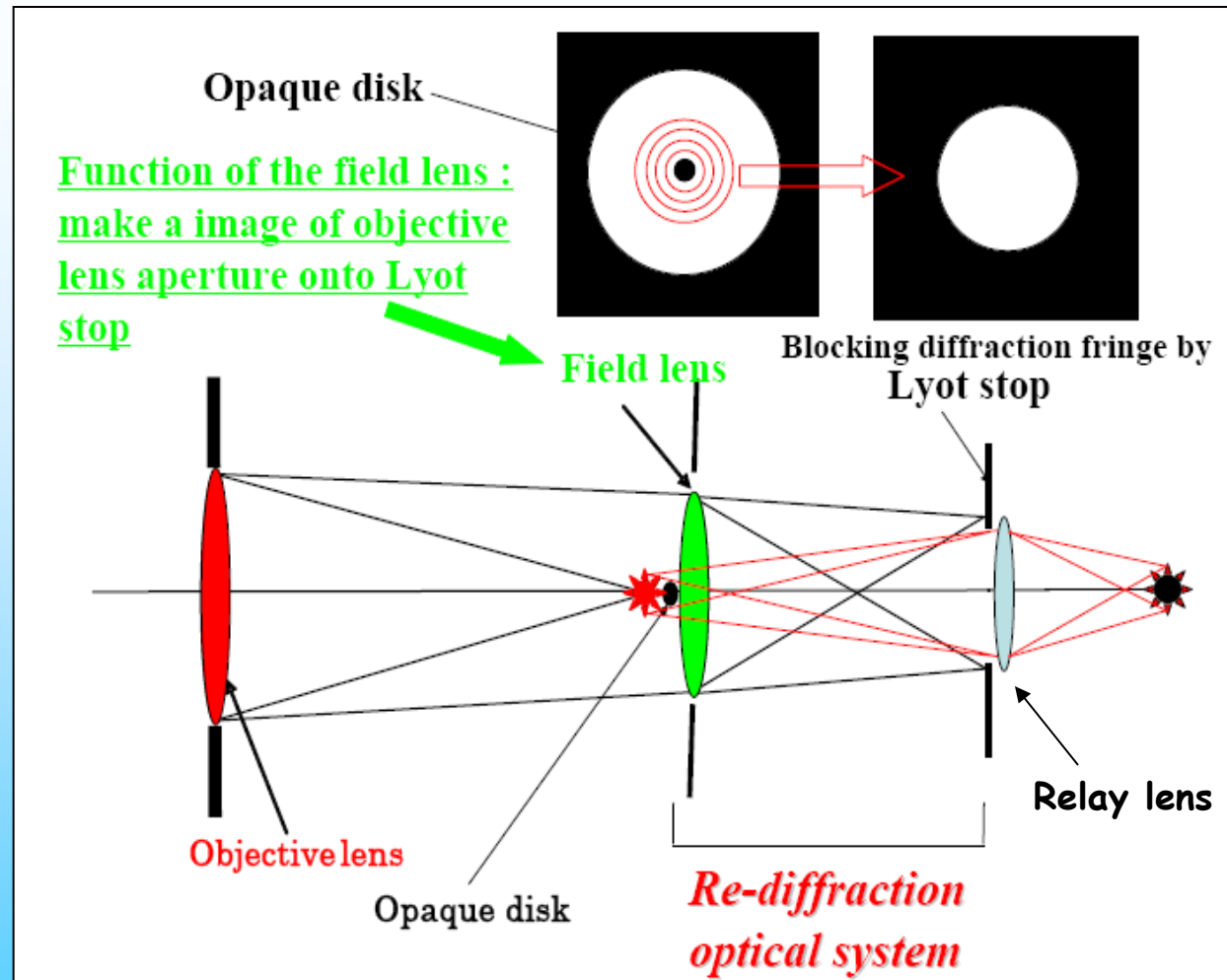
A second lens (field lens) is set just after the blocking disk. The focusing length of the field lens is chosen to make a real image of the objective lens aperture onto a mask (Lyot Stop).

# Halo measurements with coronagraph

Lyot's brilliant idea for the coronagraph is to remove this diffraction fringe by a mask, and relay the hidden weak image by a third lens onto the final observation plane

The Lyot stop effectively remove the diffracted light halo that surrounds the target, giving higher contrast improvement.

Then the re-diffracted light makes another diffraction fringe around the geometrical image of the objective lens aperture in the focal plane of the field lens. The Lyot stop removes this diffraction fringe by a mask, and relay the image by a third lens onto the final observation plane.



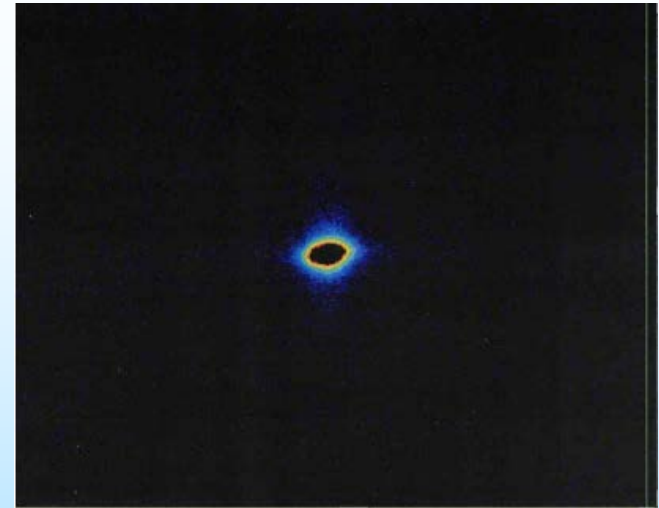
# Halo measurements with coronagraph

expected dynamic range:  $10^6 - 10^7$

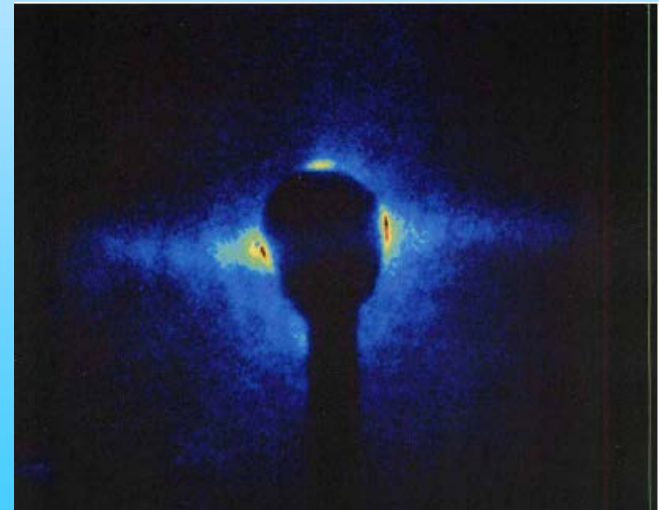


Zoom up of opaque disk.

Shape is cone and top-angle is  $45^\circ$



Beam profile



Beam tail(!)

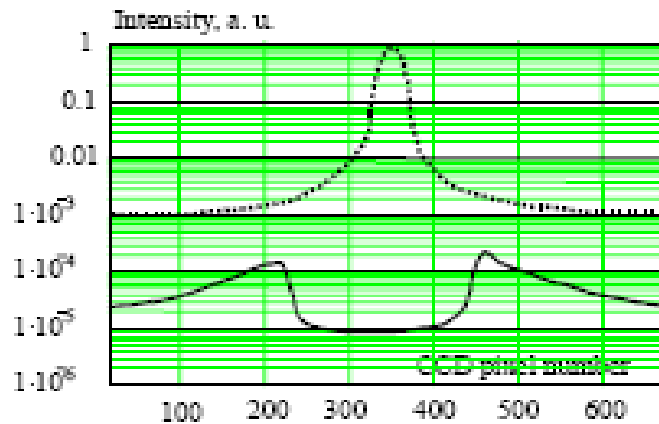


Figure 2: Coronagraph test. Upper curve is a source image. The down curve is the source obscured by mask.

VEPP3

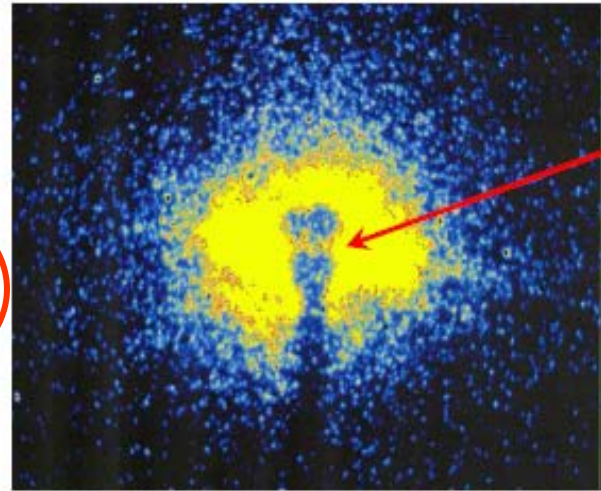
STUDY OF  
BEAM TAILS  
WITH THE  
OPTICAL  
CORONAGRA  
PH  
O. I.  
Meshkov et  
al., EPAC04

# Halo measurements with coronagraph

## Observation for the more out side

Single bunch  
65.8mA

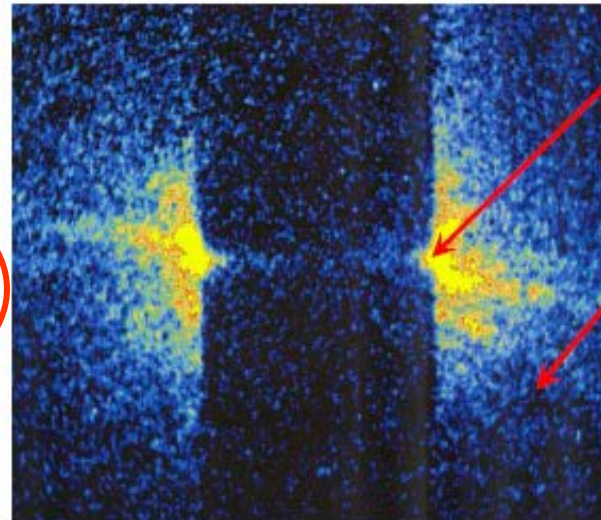
Exposure time  
of CCD : 3msec



Intensity  
in here :  
 $2.05 \times 10^{-4}$   
of peak  
intensity

Far tail

Exposure  
time of CCD :  
100msec



$2.55 \times 10^{-6}$

Background  
level : about  
 $6 \times 10^{-7}$

# Halo measurements with coronagraph

## Background sources

1. Scattering by defects on the lens surface (inside) such as scratches and digs.
2. Scattering from the optical components (mirrors) near by coronagraph.
3. Reflections in inside wall of the coronagraph. Cover the inside wall with a flock paper (light trapping material).
4. Scattering from dust in air. Use the coronagraph in clean room.

A background level of  $6 \cdot 10^{-7}$  and a spatial resolution of  $50 \mu\text{m}$  was achieved.

## LIMITATIONS

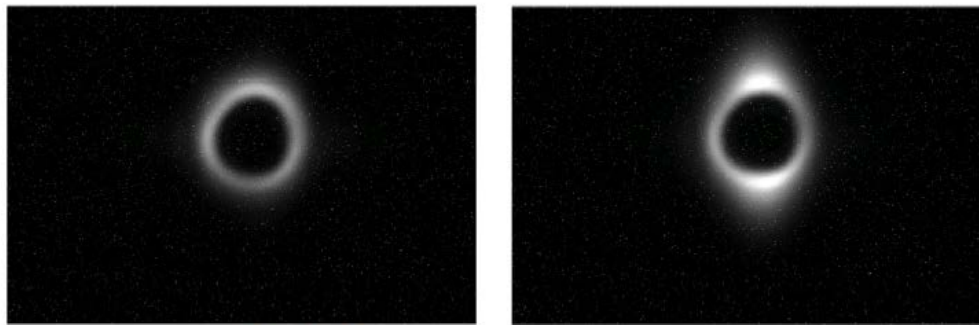
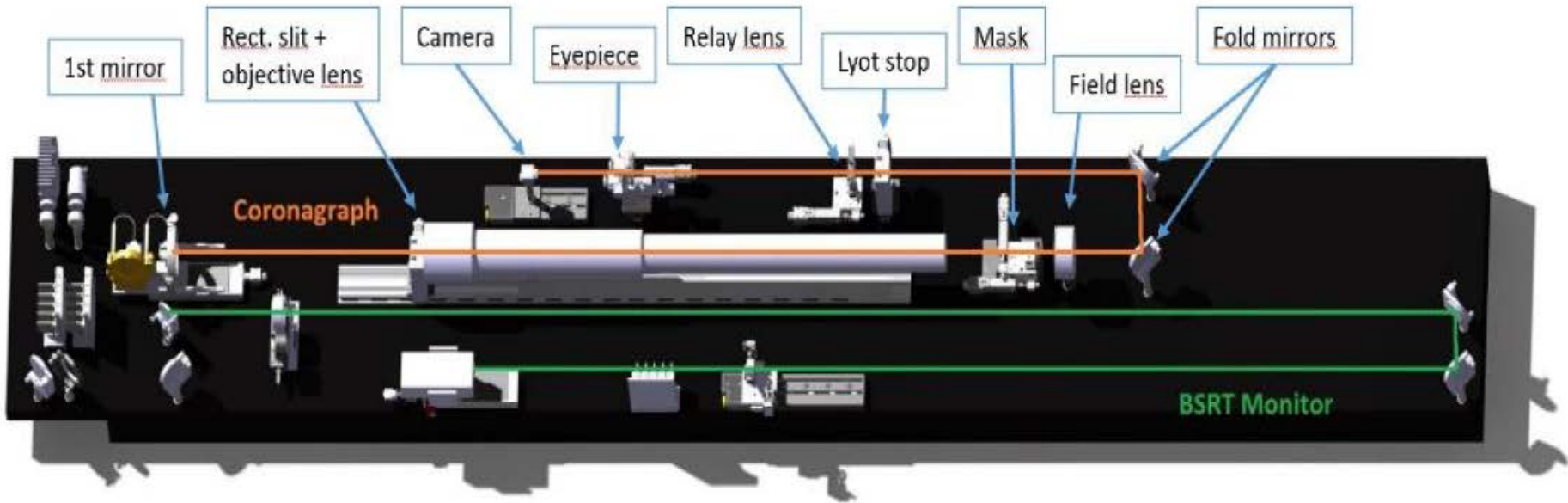
- OTR light intensity was not intense enough to explore further the halo distribution (CTF3).
- The masking technique must follow the beam position and halo size to avoid the saturation of the camera.

Mie Scattering: Dust and impurities on lenses

BEAM HALO MONITORING AT CTF3  
T. Lefèvre et al, EPAC04



# LHC coronagraph

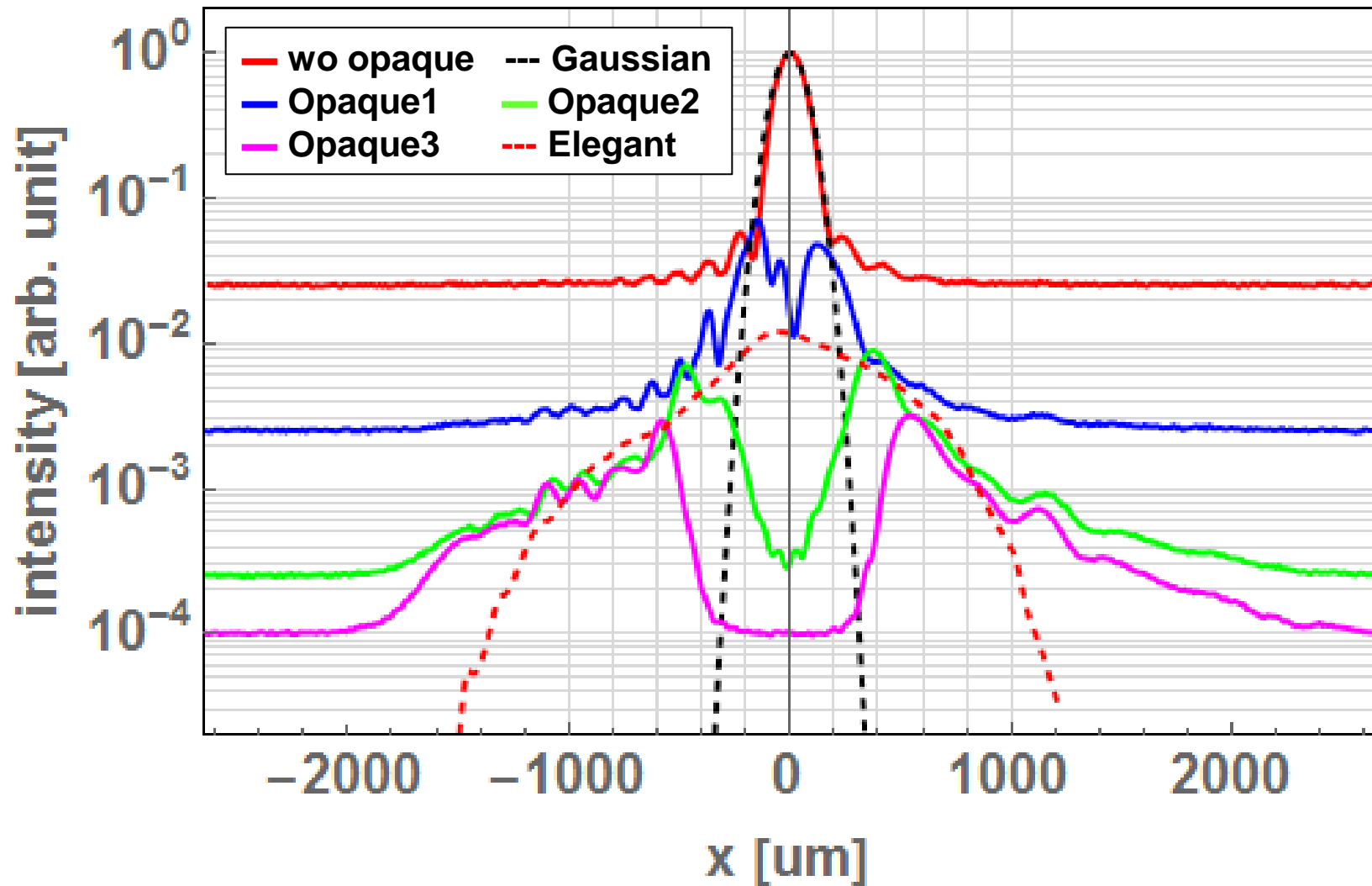


(a) (b)

Figure 8: Result of two images taken by coronagraph for vertical, (a) original beam profile (no excitation of blow up) and (b) blow up to 10 μm.

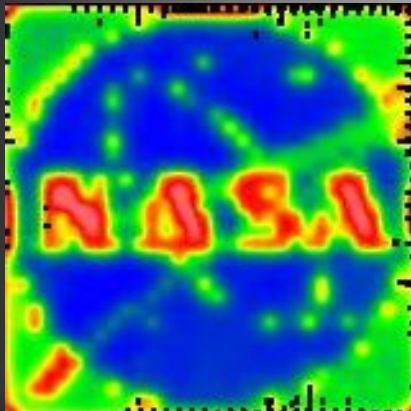
First Observation of the LHC Beam Halo Using a Synchrotron Radiation Coronagraph, T.M. Mitsuhashi et al., IPAC'17, Copenhagen, Denmark

# Beam test with PPRE bunch

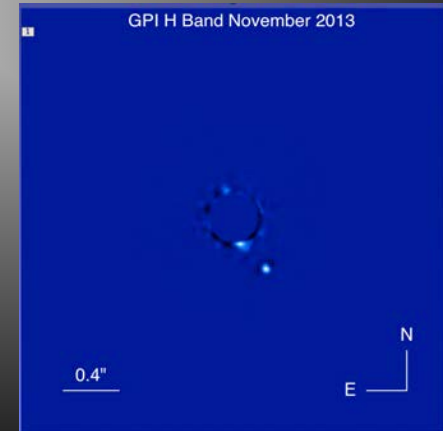


# High-Contrast Imaging and the Direct Detection of Exoplanets

Sandrine Thomas, Ruslan Belikov, and many collaborators



Beam Halo Workshop  
SLAC, Friday 19th  
September 2014

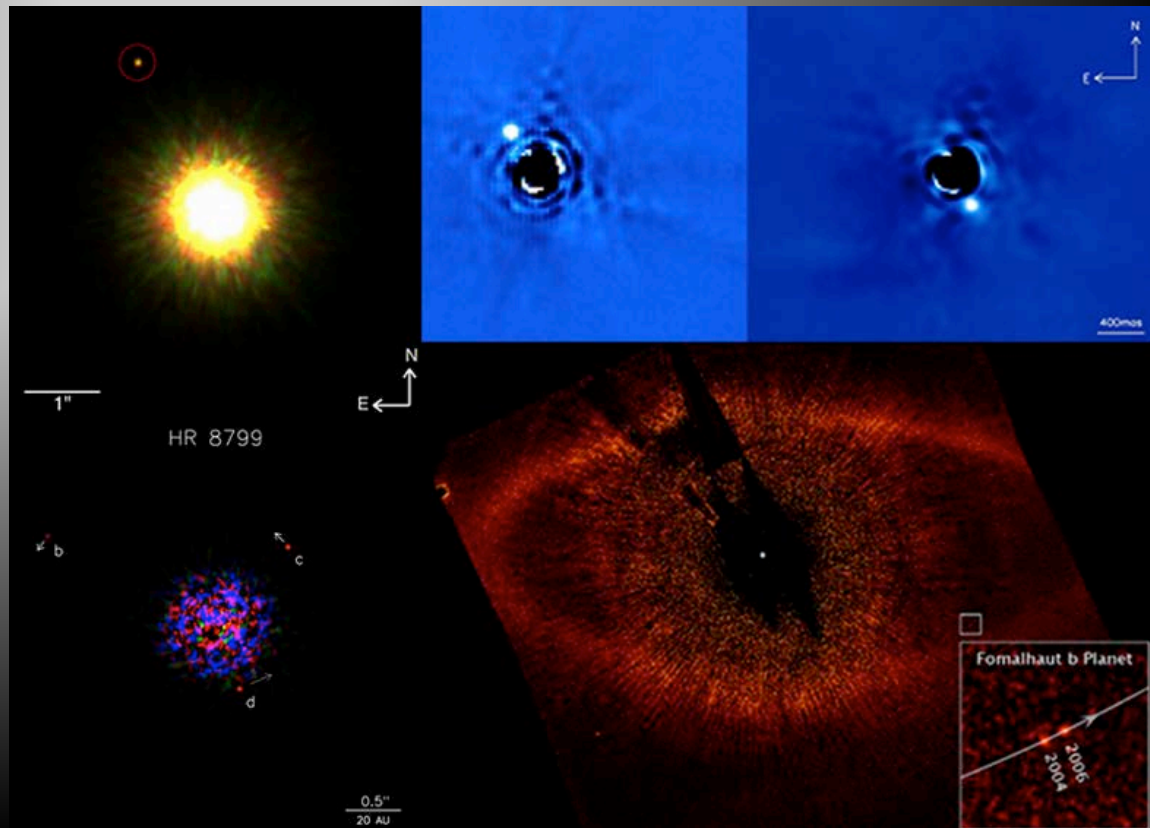


# High Contrast Imaging



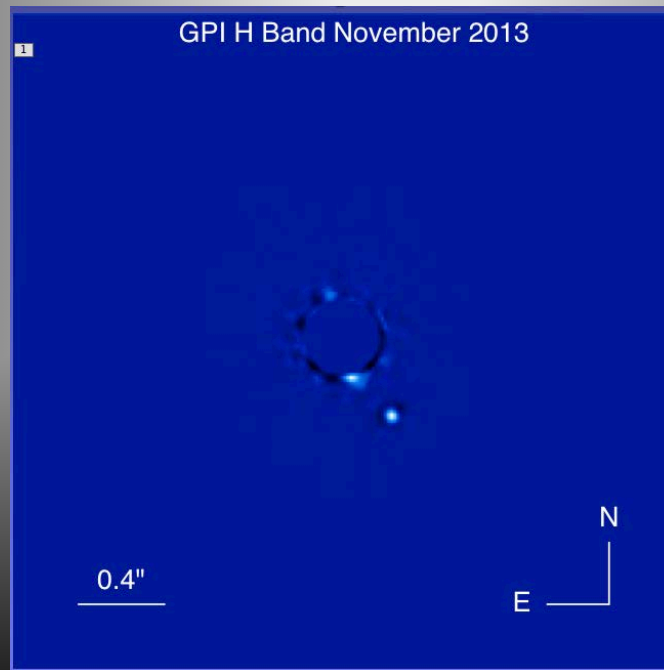
Like searching for a firefly next to a lighthouse in San Francisco from Boston  
=> Very faint and small in comparison

- Upper Scorpius
  - Lafreniere et al 2008
- Beta Pictoris b
  - Lagrange et al 2010
- HR 8799
  - Marois et al 2008
- Fomalhaut b
  - Kalas et al 2008



# Conclusion

- Similar issues are seen by your groups and coronagraphy for astronomy.
- Need a translation between astronomy and particle physics



# Outline

- Halo diagnostic:
  - What is Halo?
  - Halo Quantification
- Transversal Halo Measurements with:
  - Wire Scanners and Scrapers (slow)
  - Optical Methods (fast)
- Longitudinal Halo
  - **Bunch Purity:** Time-Correlated Single Photon Counting (TCSPC)
  - "Beam in Gap"
  - Coasting Beam

# Bunch Purity Measurements

Measurement of the sometimes special fill pattern of synchrotron light sources (rings) is important for the time-resolved experiments. **The adjacent buckets must not have any stored particles or, in reality, as few as possible.** A method with very good time resolution ( $\ll 1\text{ ns}$  for a 500 MHz RF-System) and high dynamic range (more than six orders of magnitude) is necessary.

## *Mechanism of loosing electrons*

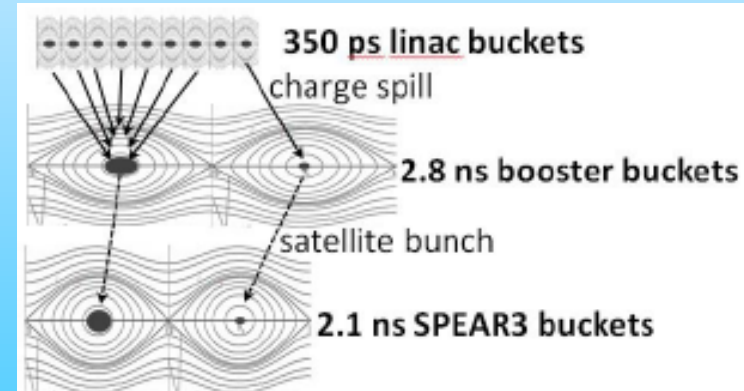
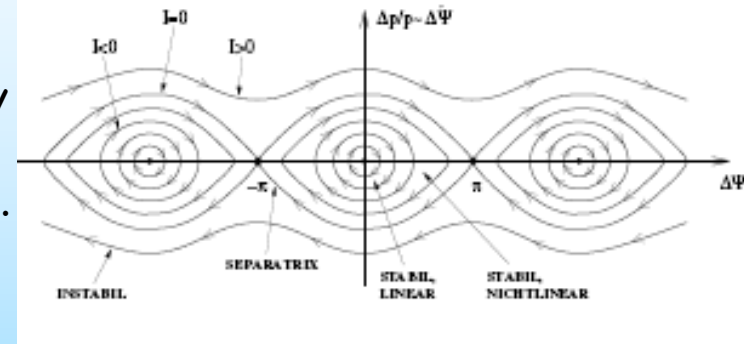
1) Quantum lifetime. An electron is lost from a bucket by emitting a photon having a momentum larger than bucket height  $\eta_{RF}$  and can be captured by the backward buckets.

2) Lifetime determined by the vacuum pressure.

Electrons lose energy by collisions with residual gas molecules in the vacuum chamber.

3) Touschek effect. Electrons in a bunch execute betatron oscillation with transverse momenta. When two electrons are scattered elastically (Moller scattering), the transverse momenta can be transferred to longitudinal ones.

4) Injection errors (energy, timing,). At top-up a source of impurity growth on the both time sides of the main rf buckets.



A typical measurement is: Time-Correlated Single Photon Counting (TCSPC)

Measurement of the longitudinal bunch structure in the Photon Factory positron storage ring with a photon counting method, Obina T. et al., NIM A Vol.354, Nr. 2

Electron Bunch Pattern Monitoring via Single Photon Counting at SPEAR3, B. Xu, et al., IBIC2017, Grand Rapids, MI, USA

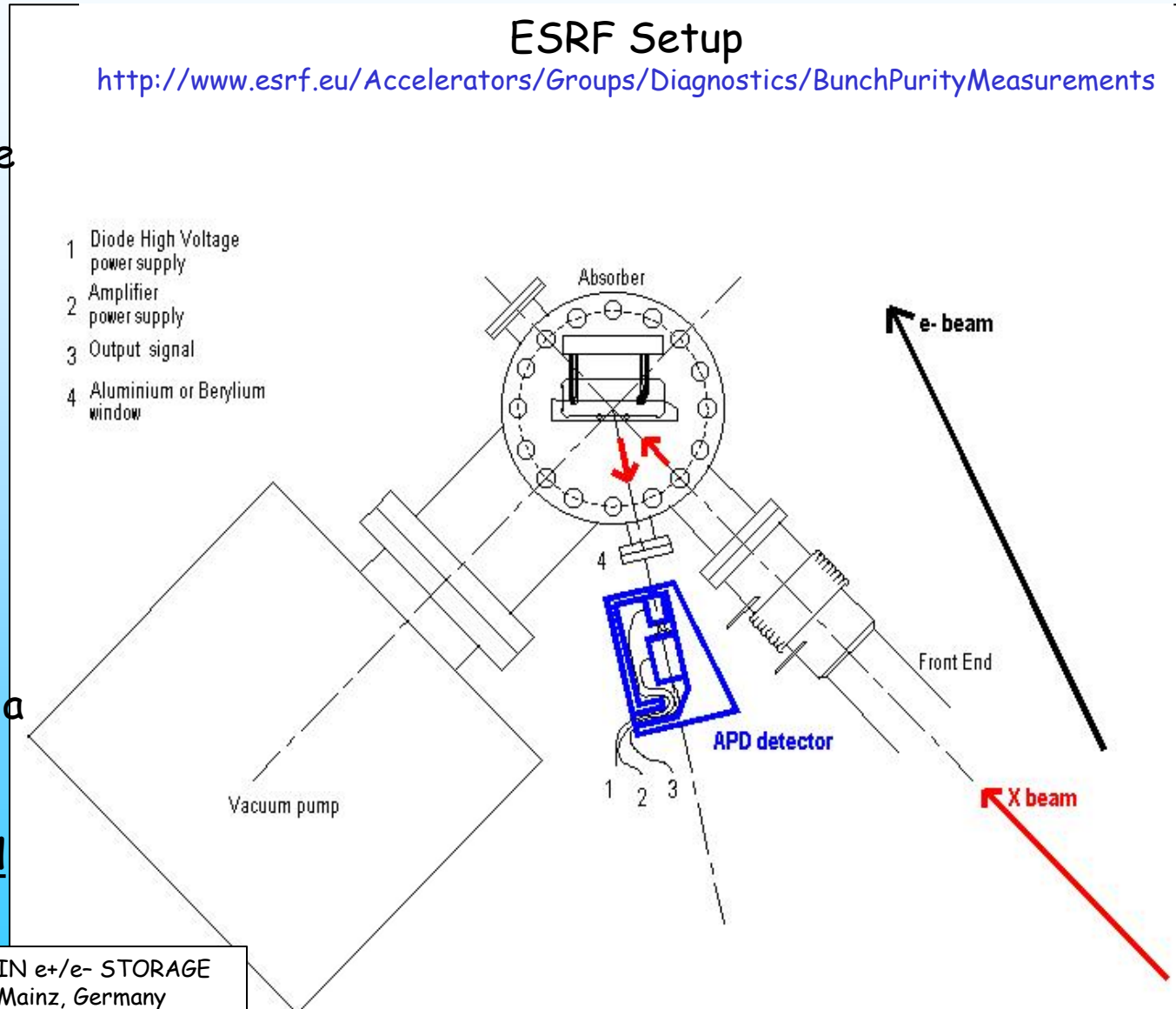
# TCSPC

## Time-correlated single photon counting method

PETRA II setup:  
 "The parasitic bunch measurement is achieved by an avalanche-photo diode (APD) detecting scattered X-rays from a 1 mm thick graphite foil. It is located in the PETRA beamline 31.3 m downstream of a dipole used as x-ray source. The detector signals are amplified close to the diode by a fast amplifier."  
The detector must be carefully shielded against stray light.

### ESRF Setup

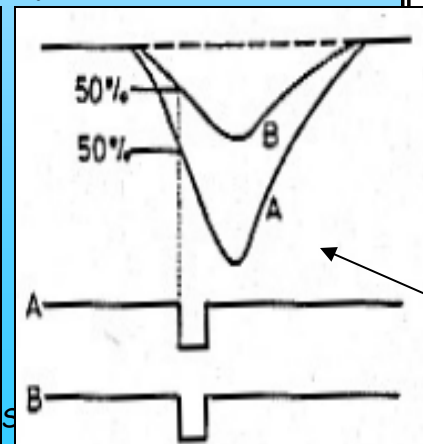
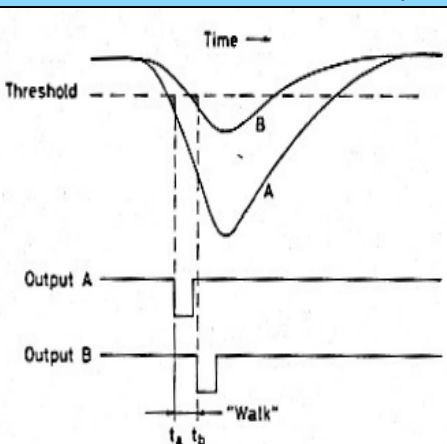
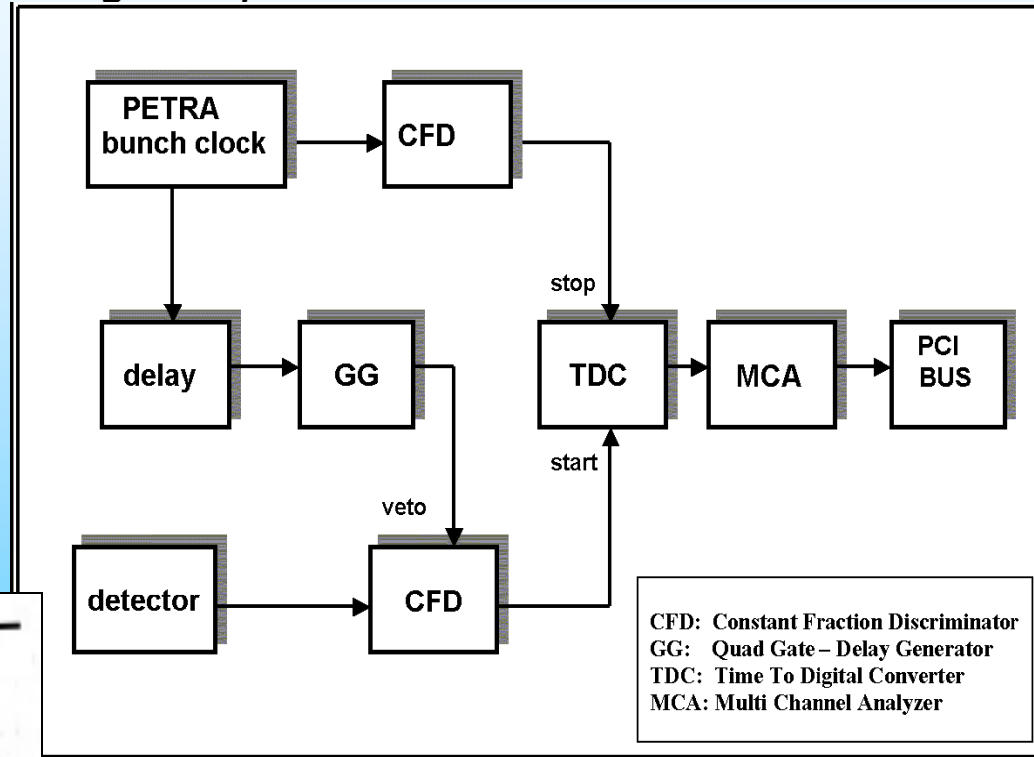
<http://www.esrf.eu/Accelerators/Groups/Diagnostics/BunchPurityMeasurements>



# TCSPC

The **arrival time of single photons** emitted by the electron bunches passing through a particular dipole in the storage ring is **measured**. The photon arrival time is measured relative to a clock pulse which is **synchronized to the bunch revolution frequency** via the storage ring RF system.

The amplified signal is analyzed using a time-to-digital-converter (**TDC**) and a multichannel-analyzer (**MCA**). To reduce the influence of the so-called "walk" and to reduce the background due to electronic noise the amplified detector signal is filtered by a **constant-fraction-discriminator (CFD)**.



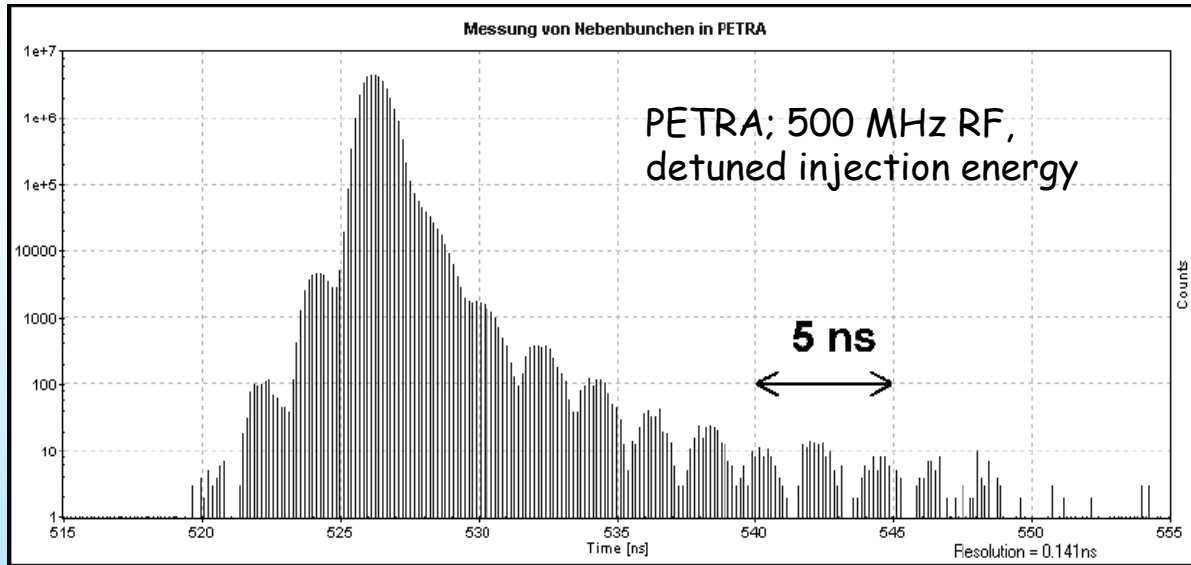
# TCSPC

The TDC-board offers 4096 channels with minimum width below **40 ps** and can work at **count rates up to 3 MHz** (300 ns recovery time).

To measure a histogram not affected by recovery-time and pile-up effects, the detector count rate should be limited to below 1.5% of the sync rate.

Bunch distance = 10 MHz, count rate = 10 kHz, expected dynamic range:  $10^7$   
=> time to resolve  $1/10^7 = 100$  sec, with better statistic => 1000 s  $\approx 16$  min!!!!

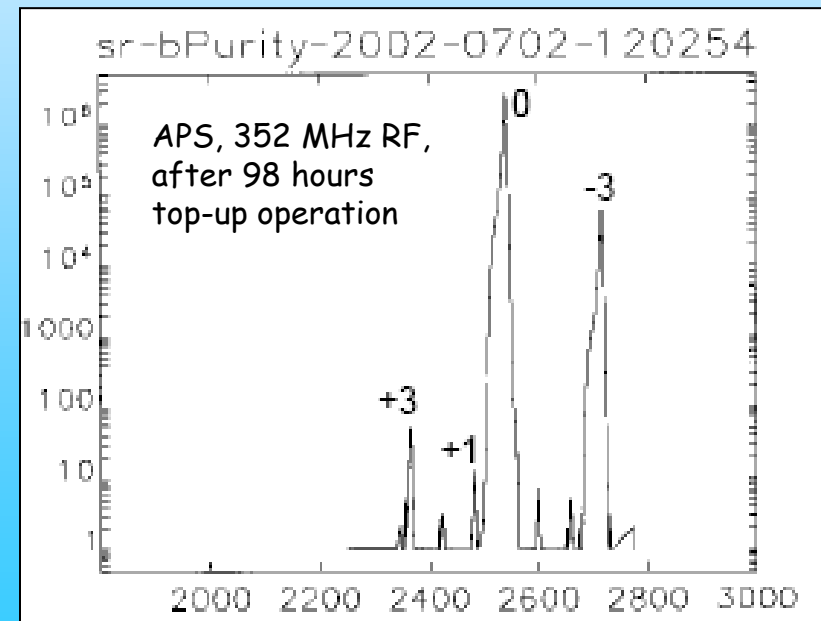
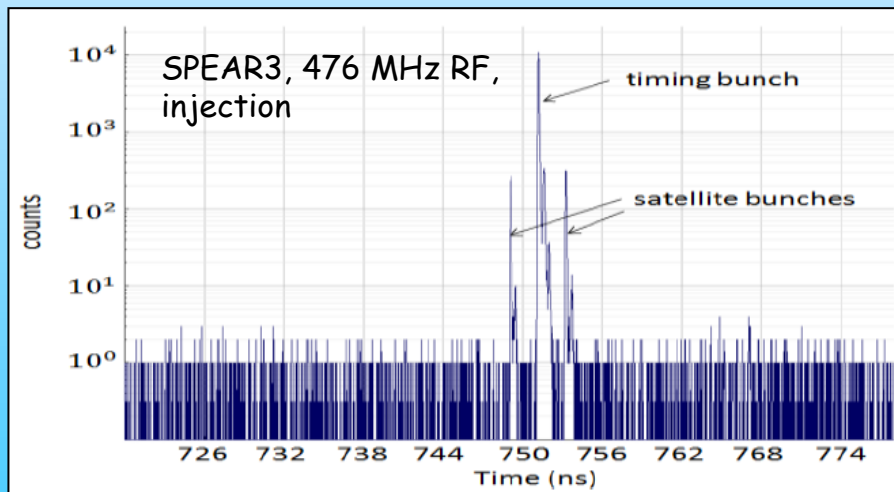
# TCSPC



PARASITIC BUNCH MEASUREMENT IN  $e^+/e^-$  STORAGE RINGS, H. Franz et al., DIPAC 2003 - Mainz, Germany

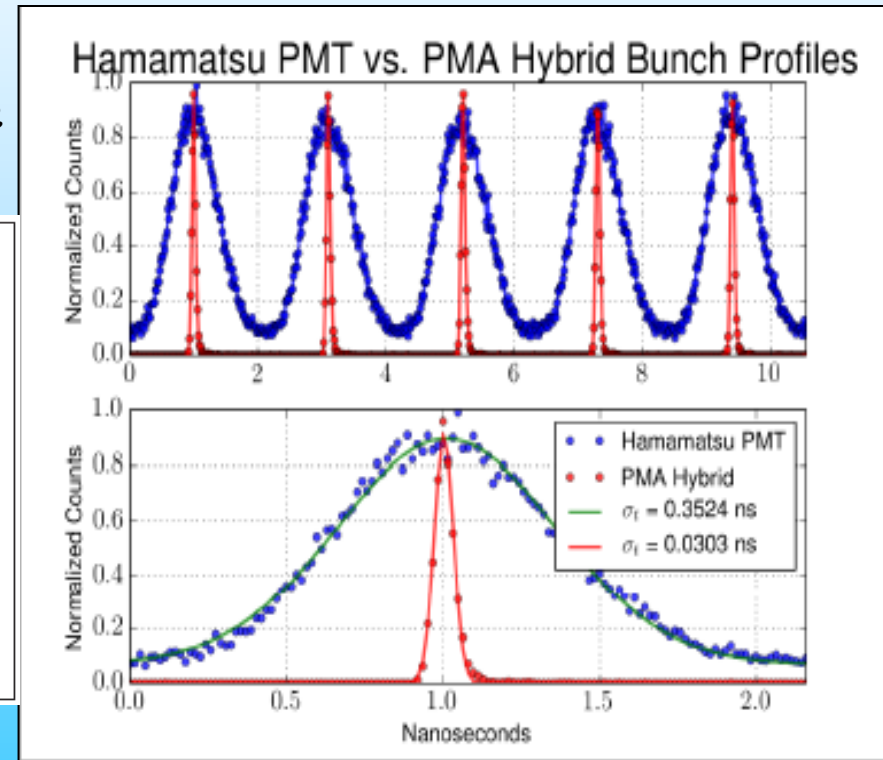
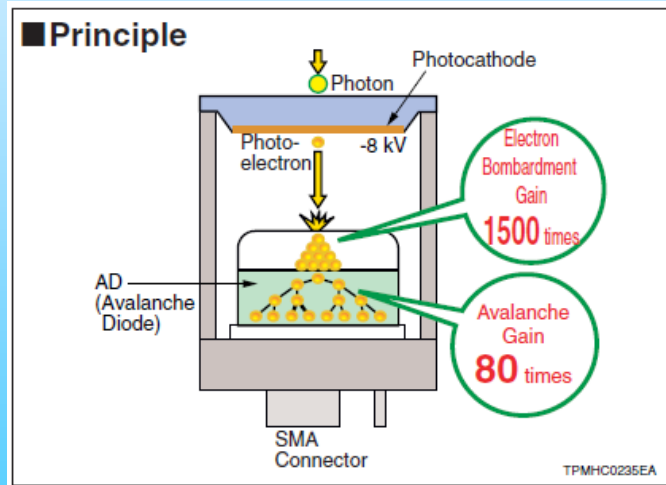
Bunch Purity Evolution during APS Storage Ring Top-up Operations, A.H. Lumpkin, et al, PAC03

Electron Bunch Pattern Monitoring via Single Photon Counting at SPEAR3, B. Xu, et al., IBIC2017, Grand Rapids, MI, USA



## Improvements:

- 1) **Better TDC:** e.g. HydraHarp 400 ps event timer & TCSPC .The system features a time resolution down to **1 ps**,... A common sync input for all channels permits to use the system for TCSPC in forward start-stop mode at stable excitation sources up to **150 MHz**.
- 2) **Well suited PMT:** R10467 from Hamamatsu (with APD), PMA Hybrid serie with 50 ps resolution.



## 3) MCP-PMT for better detector timing

[http://www.picoquant.com/\\_instrumentation.htm](http://www.picoquant.com/_instrumentation.htm)

Upgrades to the SPEAR3 Single-Photon Bunch Measurement System, T.M. Cope, et al., IPAC16, BEXCO, Busan Korea

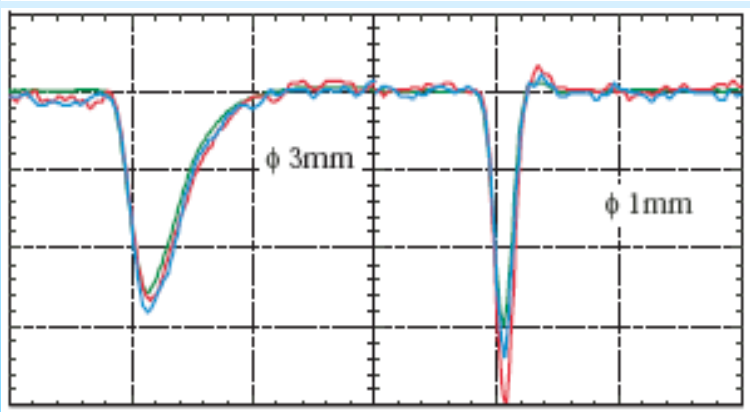
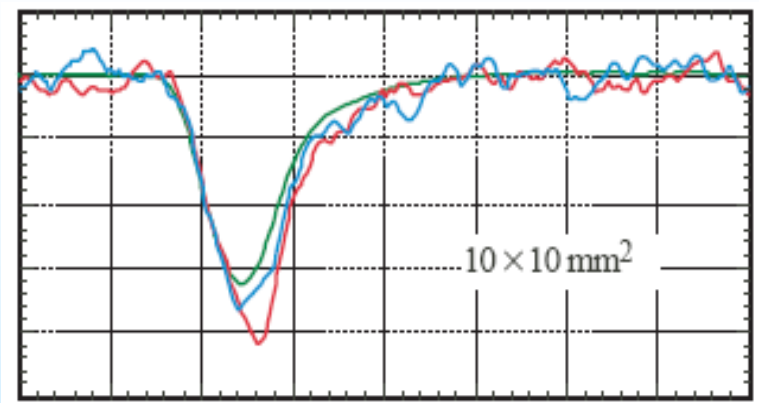
# APD (C30703F) (534X LC)



vs.

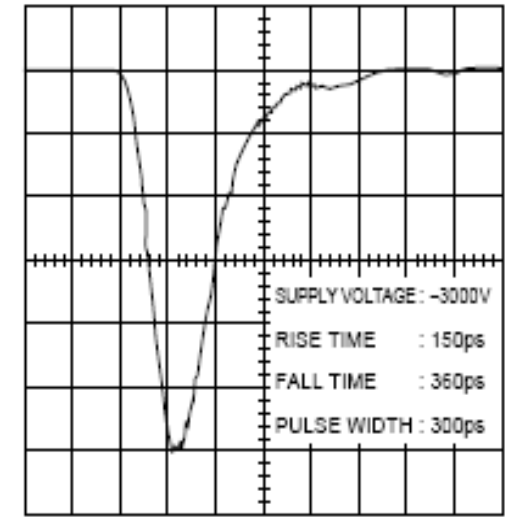


# MCP-PMT (R3809U-50)



APD: The average over many events is shown (smooth curve) as well as two single-photon events to show an indication of the noise level  
Scale: 50 mV (upper) 100 mV (lower) and 5 ns /div.

TPMH80183EA Ø 11 mm

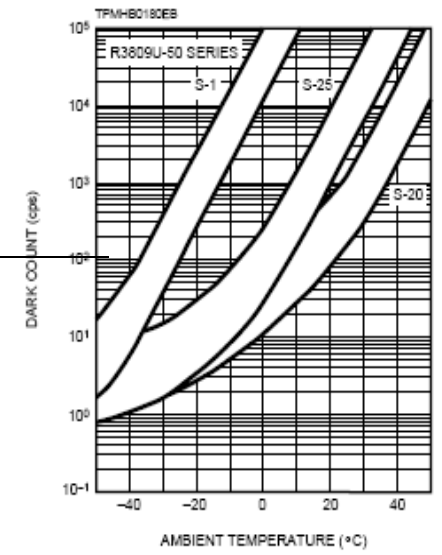


0.2 ns/div

Dark count rate limits the dynamic range in a 100 ns interval to  $\approx 10^7$

100 c/s ←

Figure 5: Variation of Dark Counts Depending on Ambient Temperature

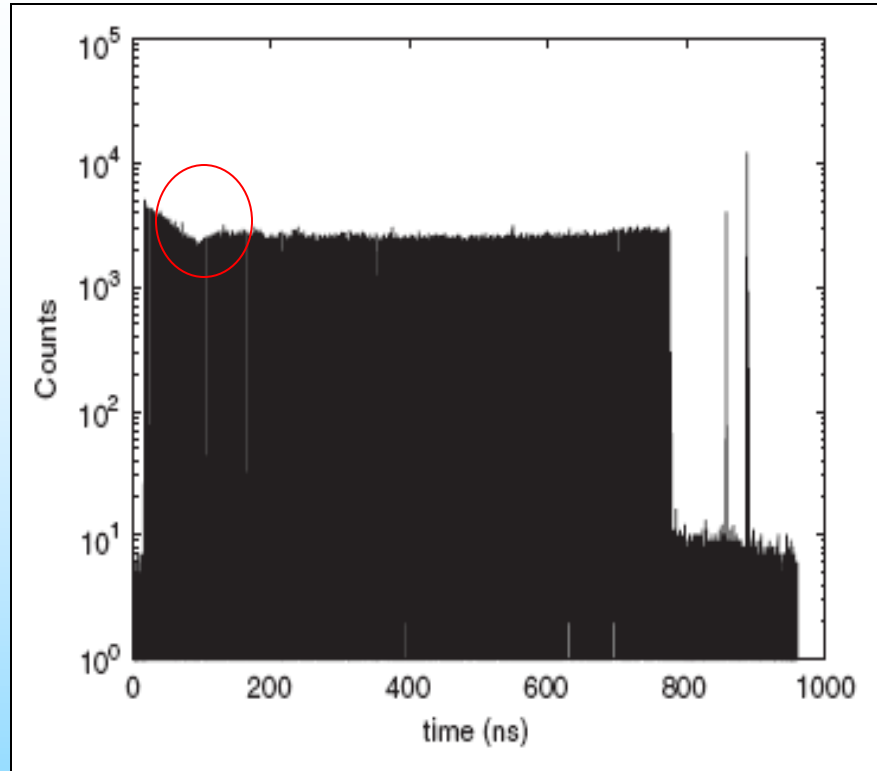


typ. dark count rate 20-500 c/s

Two Notable APDs for Fast X-ray Detection  
A.Q.R. BARON, et al,  
[http://www.spring8.or.jp/pdf/en/ann\\_rep/99/p149-150.pdf](http://www.spring8.or.jp/pdf/en/ann_rep/99/p149-150.pdf)

<http://datasheet.digchip.com/190/190-01565-0-R3809U-50.pdf>

Pile up:



The number of electrons is nearly the same in the bunches of the train, but the measurement shows a decreasing number in the first bunches, down to a minimum value, followed by a flat top for the rest of the bunches. This effect is due to a **too high count rate** of  $4.5 \cdot 10^6$  counts/s. At this rate, a photon arrives every 220 ns on average: this is **comparable to the dead time** of the PicoHarp 300 (95 ns). As a result the probability of a photon from one of the first pulses to be detected is significantly larger than for the rest of the train.

Instrument response function:

MCP-PMT after pulses

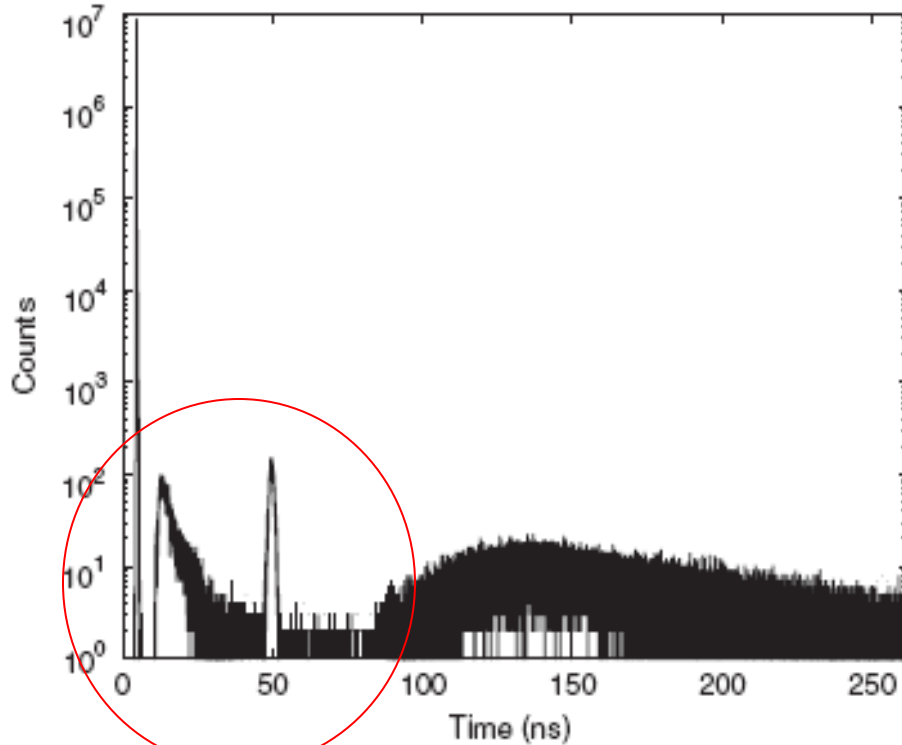


Fig. 4. Full scale of the IRF recorded with the 35 ps diode, with approximately 1 count/s noise.

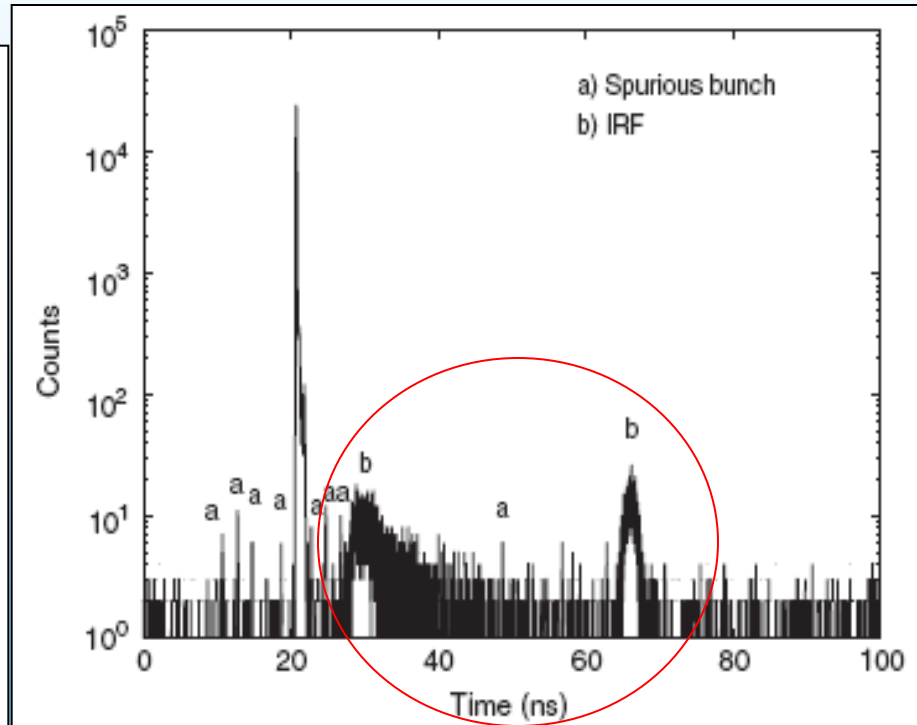


Fig. 5. SRS single bunch mode pattern at 600 MeV. Due to a small current (4 mA) the count rate is only 3000 and the background is 100 counts/s. Spurious bunches (a) can be seen in the adjacent buckets of the main bunch, and the after-pulses of the MCP-PMT (b) as observed in the IRF.

C.A. Thomas et al., Bunch Purity Measurement for Diamond, NIM A,566(2) 762766, October 2006.

# TCSPC

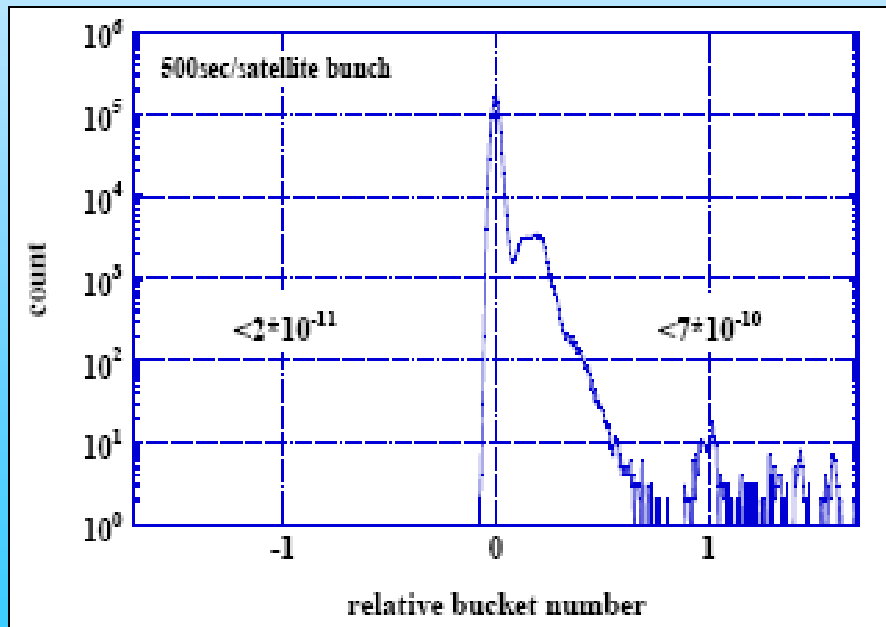
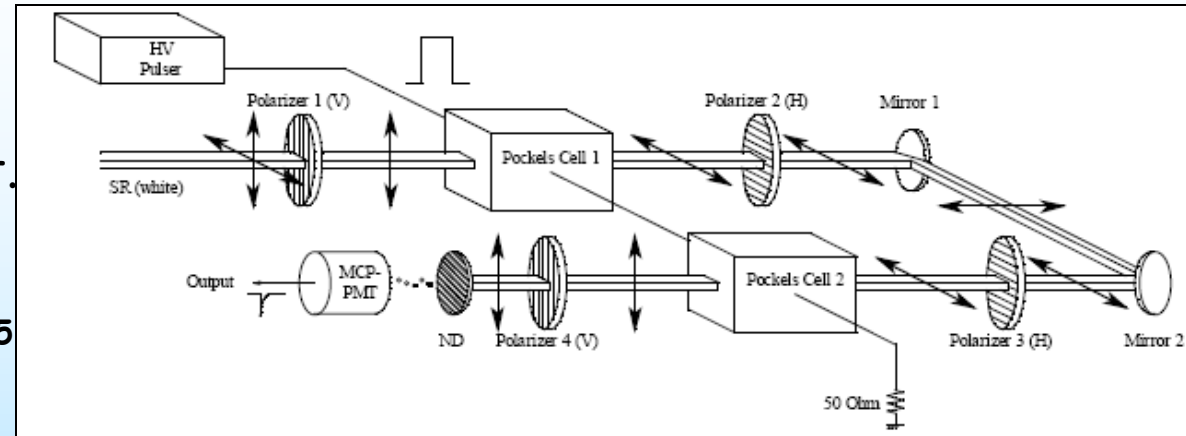
Spring-8:

Huge dynamic range with fast optical light shutters (Pockels cells), selecting only one bucket.

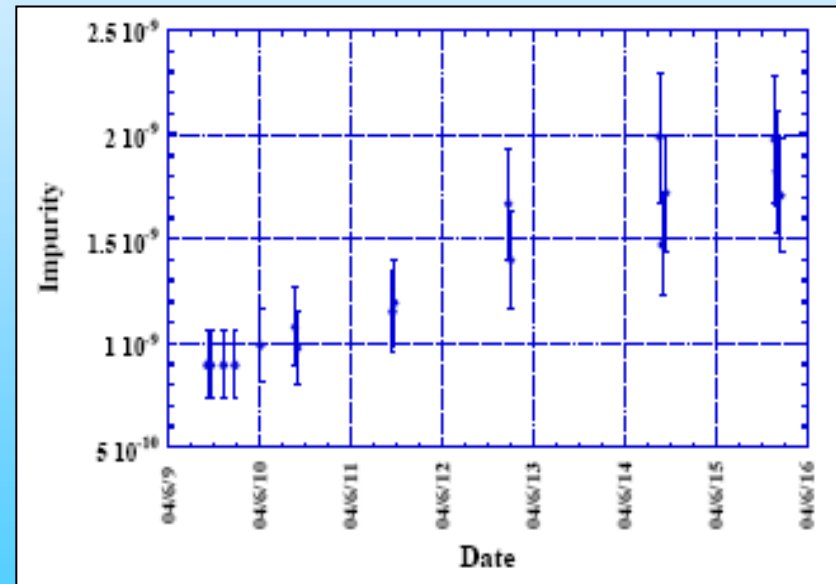
Measuring time: 500 s for satellites.

Main peak is suppressed by  $10^{-5}$  due to shutter efficiency.

=> Dynamic range  $\approx 10^{10}$ !



K. Wittenburg, DESY, Beam Halo Monitoring, CAS Beijing

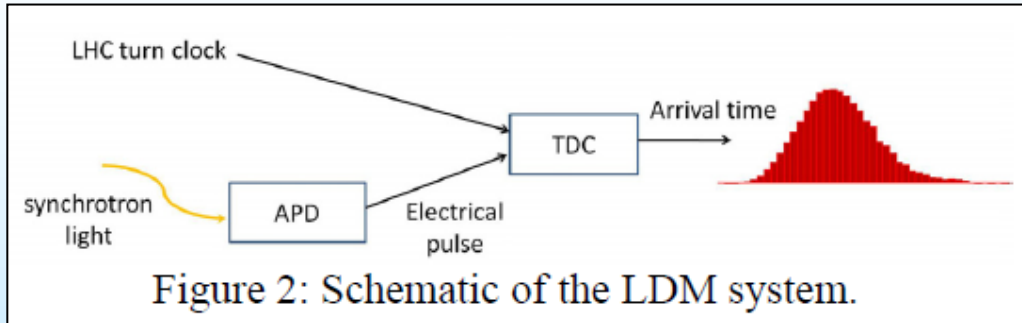


Growth of bunch impurity during top up at Spring-8

SINGLE BUNCH PURITY DURING SPRING-8 STORAGE RING TOP-UP OPERATION, K. Tamura, et al., Proceedings of the 1st Annual Meeting of Particle Accelerator Society of Japan and the 29th Linear Accelerator Meeting, Funabashi, Japan

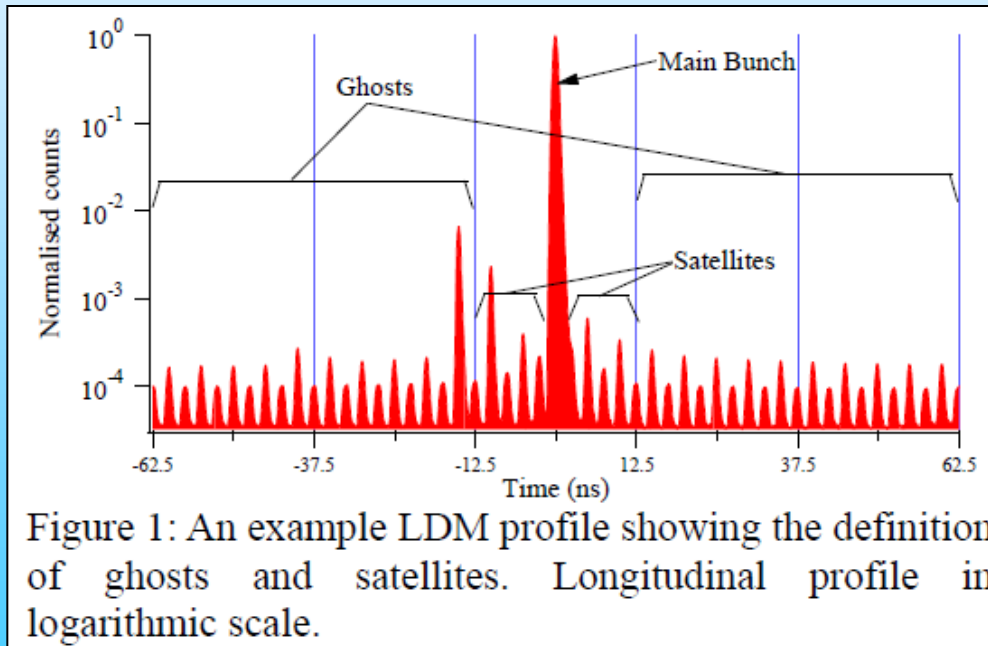
# Beam in Satellites

## Proton Synchrotron Light (LHC)

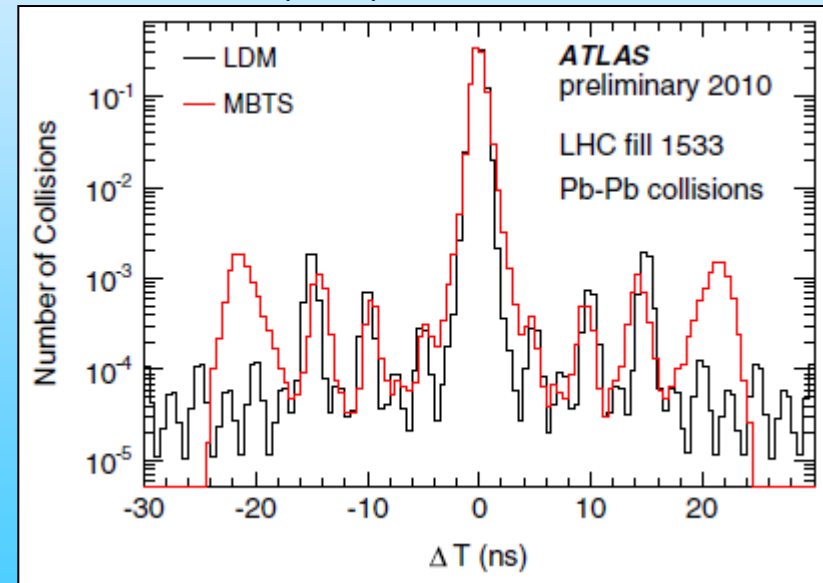


Longitudinal Density Monitor (LDM) with APD and TDC

These satellite and ghost bunches can collide at the interaction points and create background noise for the Experiments.



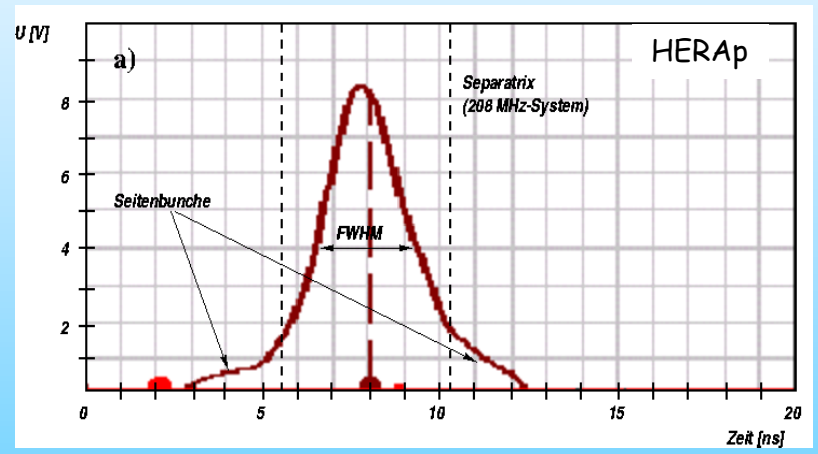
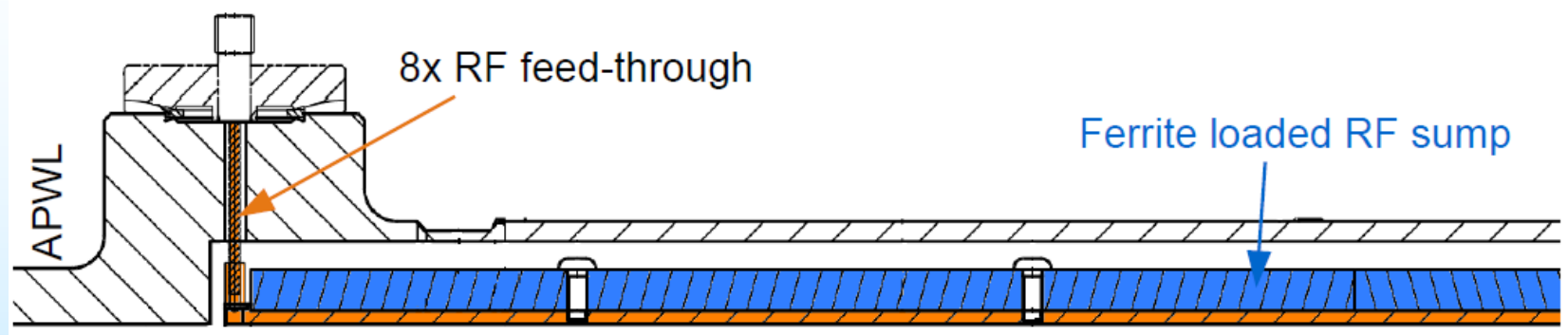
Measured by Experiment:



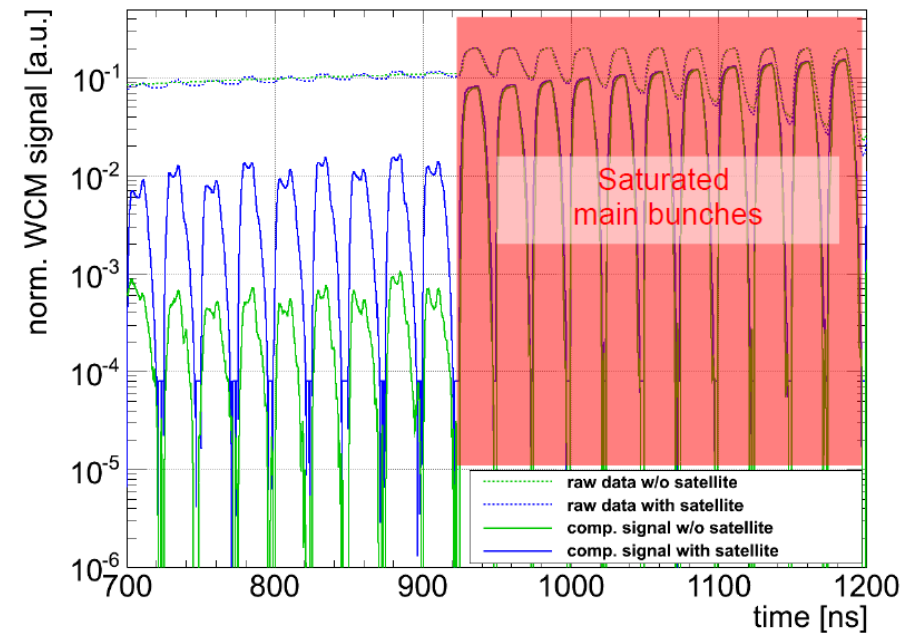
Measurement of Satellite Bunches at the LHC, A. Jeff, et al., , IPAC12, New Orleans, Louisiana, USA and Longitudinal density monitor for the LHC, A. Jeff, et. al., Phys. Rev. ST Accel. Beams » Volume 15 » Issue 3

# Bunch impurity

Another method: Fast wall current monitor (protons)



After full post-processing chain of smoothing and removing background:



More precise estimates measuring bunch populations below the  $10^{-3}$  level require the compensation of the non-linear phase-delays, signal attenuation and recovery of the zero baseline, particularly if several bunches are circulating.

K. Wittenburg, DESY, Beam Halo Monitoring, CAS Beam Instrumentation, 2018

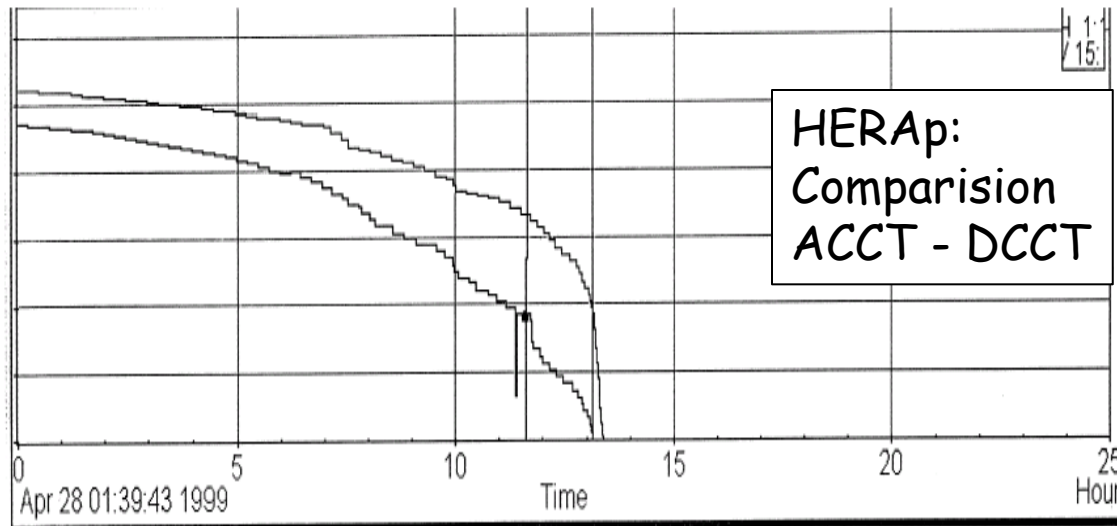
Wall-Current-Monitor based Ghost and Satellite Bunch Detection in the CERN PS and LHC accelerators; R.J. Steinhagen, BIW12, 2012

# Outline

- Halo diagnostic:
  - What is Halo?
  - Halo Quantification
- Transversal Halo Measurements with:
  - Wire Scanners and Scrapers (slow)
  - Optical Methods (fast)
- Longitudinal Halo
  - Bunch Purity
  - "Beam in Gap" } By Temporal Loss Distribution
  - Coasting Beam } or Synchrotron Radiation

# Coasting beam

Hadron (!) beams only, rings



DC current (upper) and total bunch current (lower)

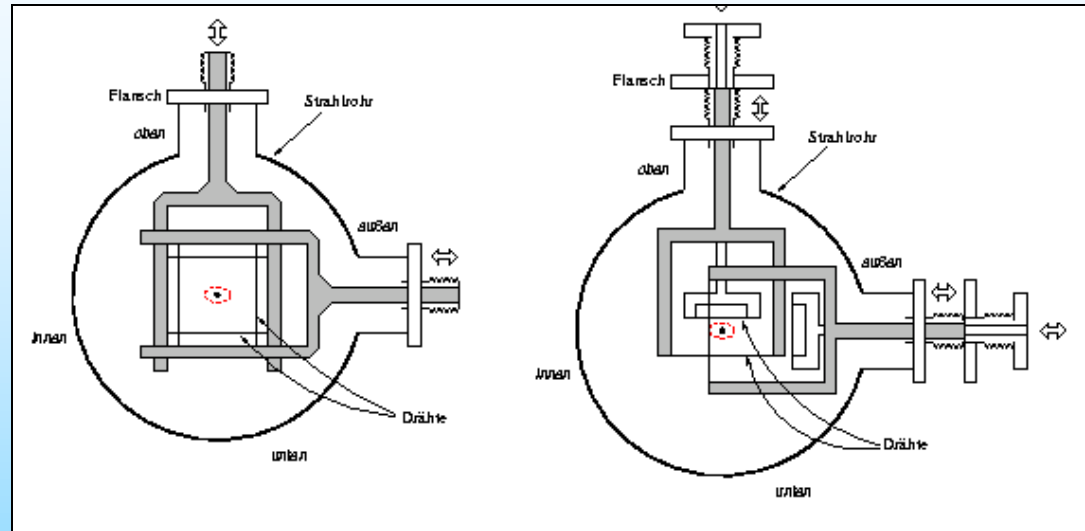
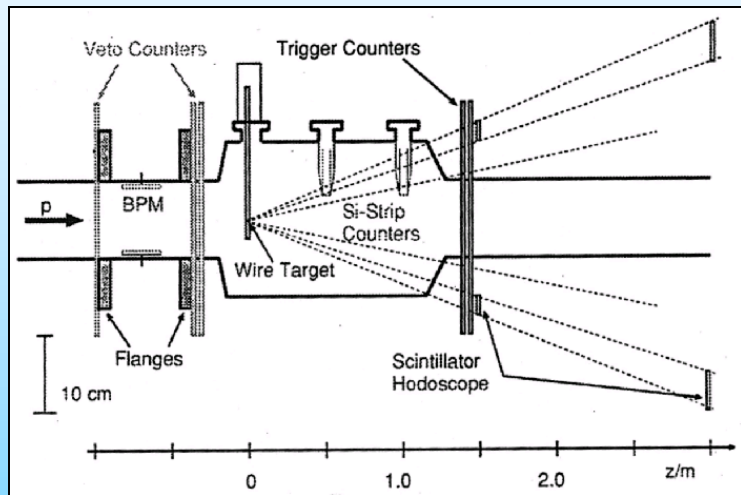
**Tevatron:** 980 GeV protons and antiprotons lose about 9 eV/turn due to the SR. For **uncaptured beam particles**, this energy loss is not being replenished by the rf system, so they **slowly spiral radially inward and die on the collimators**, which determine the tightest aperture in the Tevatron during collisions. The typical time for an uncaptured particle to reach the collimator is **about 20 minutes**. The **total uncaptured beam intensity is a product of the rate at which particles leak out of the main bunches and the time required for them to leave the machine.**

Generation and diagnostics of uncaptured beam in the Fermilab Tevatron and its control by electron lenses, Xiao-Long Zhang et al, PRST-AB 11, 051002 (2008)

# Coasting beam

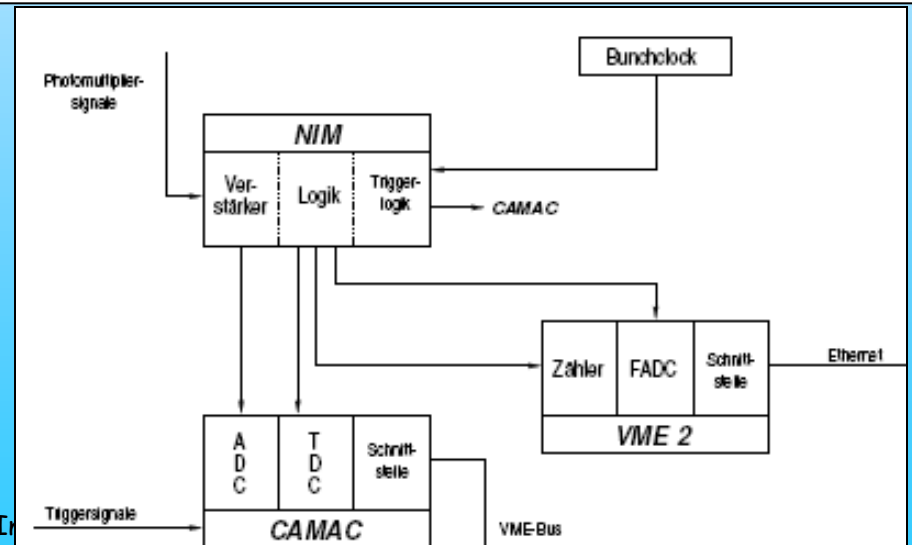
Measured by temporal beam loss distribution

HERA-B experiment: Wire scanners + Counters + TDC (only in beam tails)



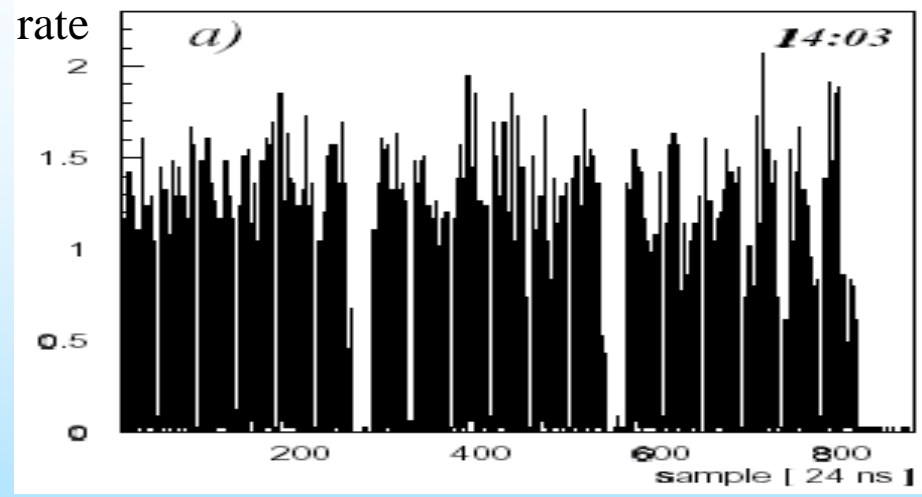
Detection efficiency > 50%

Observation of coasting beam at the HERA proton ring.  
 K. Ehret et al. Nucl.Instrum.Meth.A456:206-216,2001  
 And  
 Bestimmung der Wechselwirkungsrate des HERA-B Targets und  
 Untersuchung des Coasting Beam am HERA Protonen-Ring, S. Spratte  
 Fachbereich Physik d. Universität Dortmund Juni 2000



# Coasting beam

## Detection of coasting beam



1 h ↓

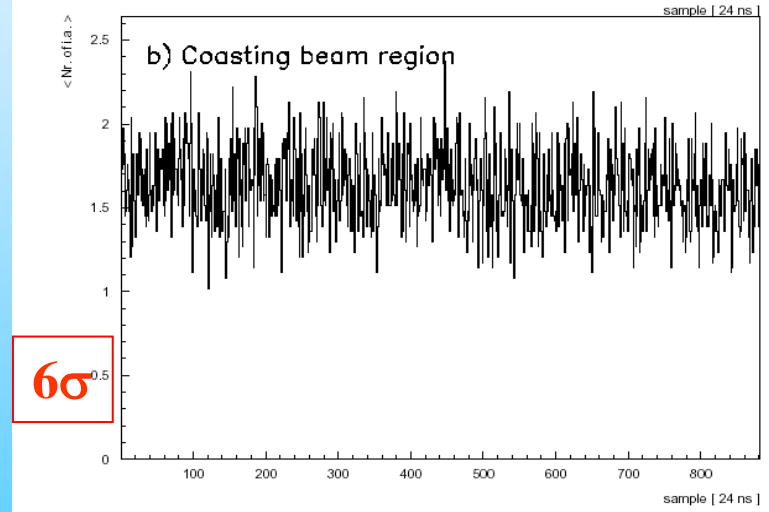
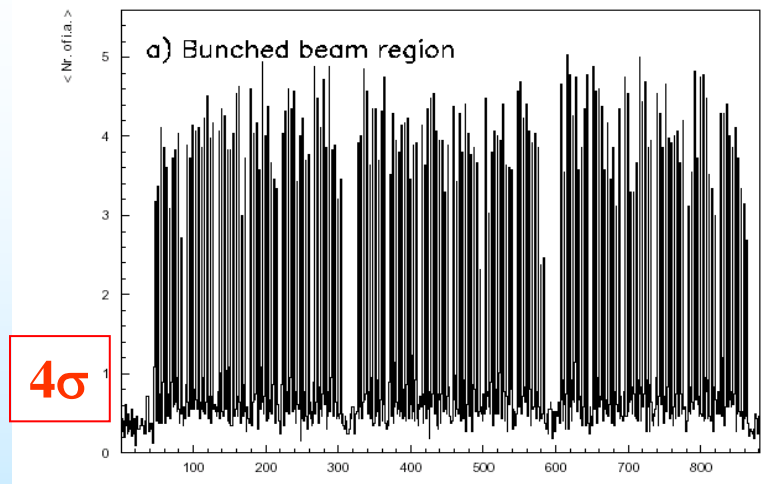
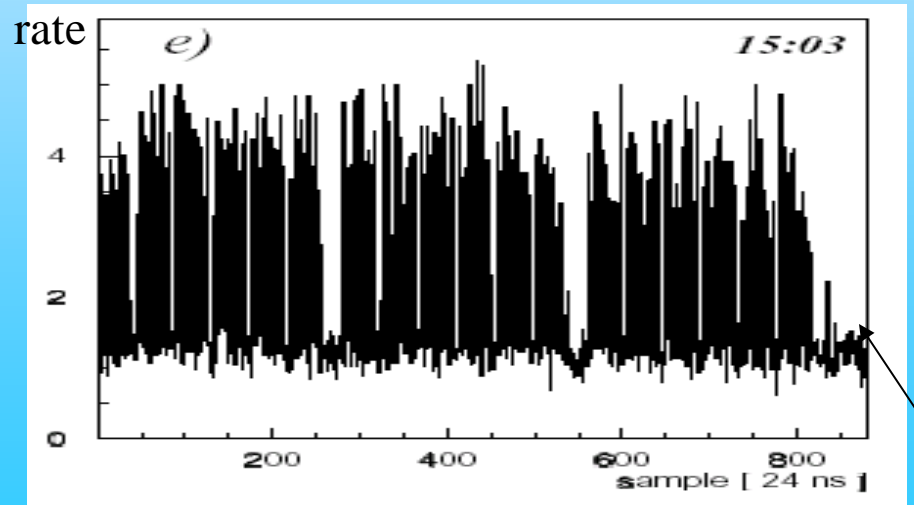
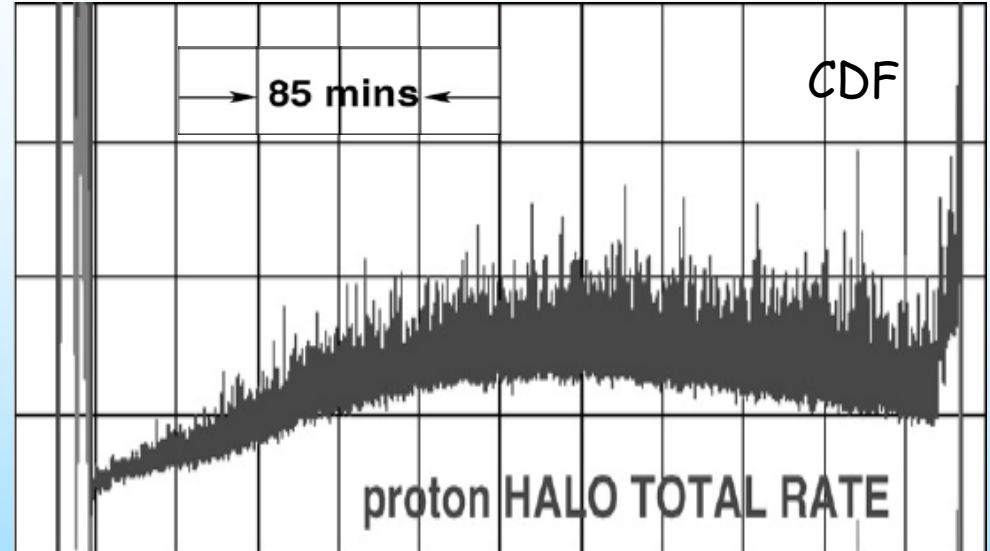
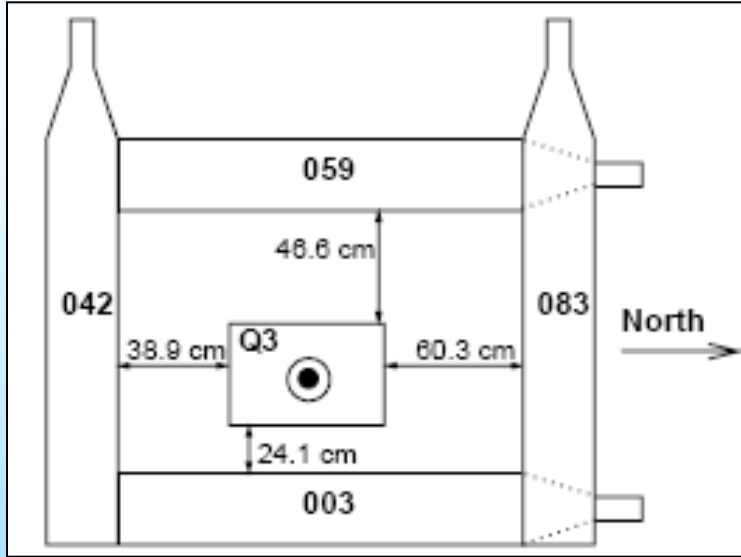


Figure 11.2: The time structure of the proton interaction for an outer target wire at different distances of the wire to the beam center: a) wire  $\approx 4\sigma$  from the beam center and b) wire  $\geq 6\sigma$  from the beam center.

Note the increased rate in the Bunch gaps (=coasting beam)

# Coasting beam

CDF experiment (FNAL): "normal" losses + Counter + variable Trigger delay



Beam halo monitoring at CDF.  
Muge Karagoz Unel et al., Nucl.Instrum.Meth.A506:7-19,2003

- Halo diagnostic:
    - What is Halo?
    - Halo Quantification
  - Transversal Halo Measurements with:
    - Wire Scanners and Scrapers (slow)
    - Optical Methods (fast)
  - Longitudinal Halo
    - Bunch Purity,
    - "Beam in Gap"
    - Coasting Beam
- } not mentioned: Abort Gap Cleaning by Kickers (fast or resonant)  
Electron lens

# Summary

## Transversal Halo

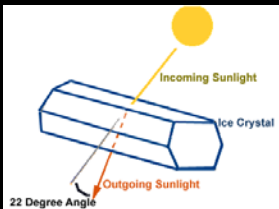
- Wire scanners still “state of the art” instruments for very high dynamic range up to  $10^8$  or more.
- SR with CID and coronagraph has potential to more dynamic range.
- IPM etc. are sufficient for profiles but background and instrumental issues limit their use for halo.
- Laser work well for  $H^-$  beams.

## Longitudinal Halo

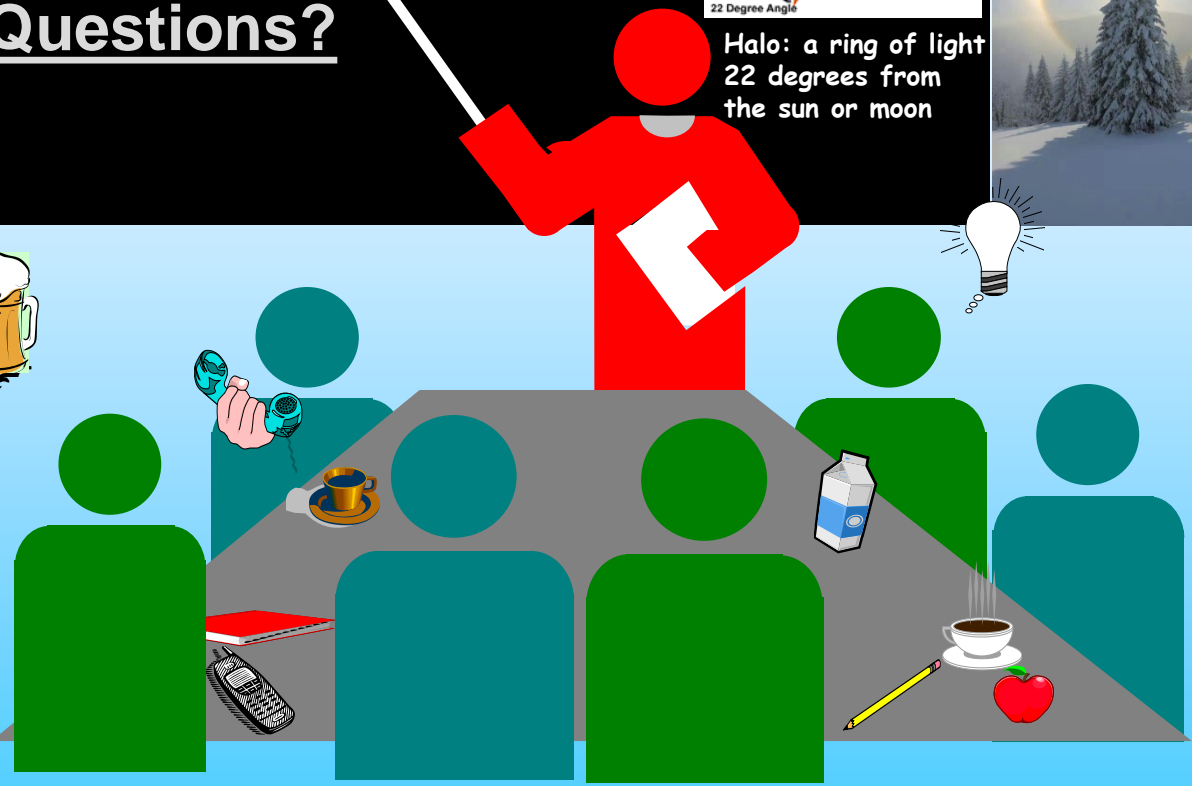
- Bunch purity: Measurements with  $>10^{10}$  dynamic range (Electrons)
- Beam in Gap and LDM: SR limited to high energy beam (Protons/Ions) but more methods are under study.
- DC beam: Compare ACCT and DCCT; Wire scanners are very sensitive, applicable in trans. halo only

# The End

Questions?



Halo: a ring of light  
22 degrees from  
the sun or moon

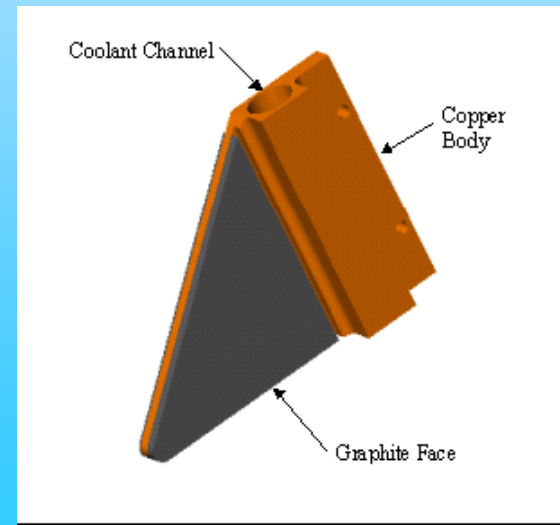


More:  
Wire Scanner + Scraping  
Vibrating Wire Scanner  
Halo Collimation  
Beam in Gap

# Wire Scanners

## To 1: Scraper data are spatially differentiated and averaged

As the scraper marches inward, it intercepts an ever increasing segment of the beam. It is therefore necessary to **differentiate the scraper signal** to determine the transverse distribution. Take scraper data with N-times finer steps than used for the wire scan. This finer stepping allows the **differentiation algorithm to smooth the data**. The numerical derivative can be computed as the difference between two N-point averages on either side of the point in question divided by the spatial separation between them. Larger values of N improve the signal-to-noise ratio, but at the cost of additional time to complete the scrapes.



# Wire Scanners

to 2: Wire and scraper data are acquired with sufficient spatial overlap

The first step in joining the scraper data to the wire scanner data is determining where the data sets overlap. The overlap region consists of wire scanner locations ranging from where the wire scanner signal-to-noise ratio is greater than 2 to the maximum insertion location of the scraper.

to 3 and 4: Differentiated scraper data are normalized to the wire beam core data and

Normalize data to axis

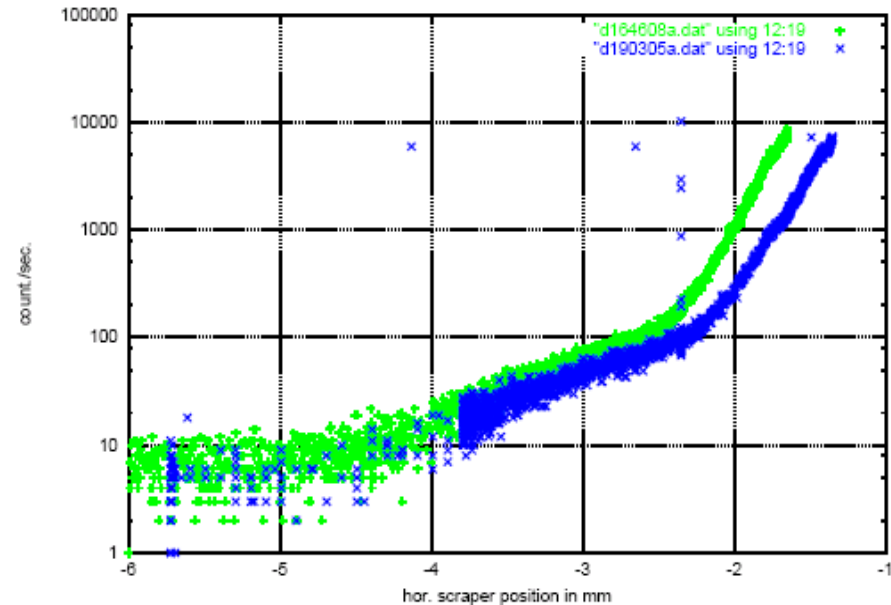
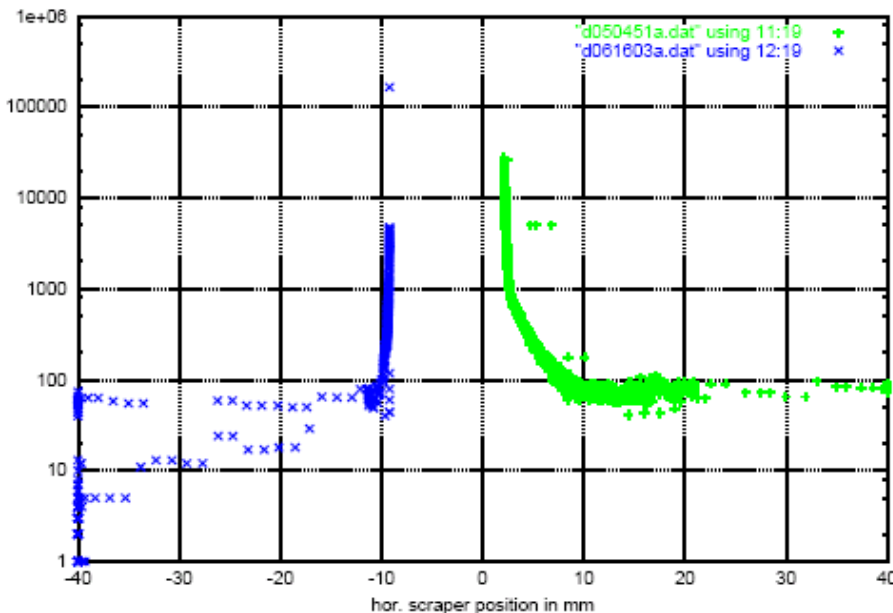
Once the region of overlap has been determined, the scraper data must be normalized to attach it to the wire scanner data. The scaling factor is the average of wire scanner to halo scraper signal ratios at two of the three most-inboard points in the overlap region (the most inboard point is excluded). Once scaled, the entire scraper data set is thinned by keeping only every  $N^{\text{th}}$  scraper point and attached at the connecting points.

Measurements of wire to scraper distances were carried out in Lab. with an uncertainty of 0.25 mm. This implies a positional attachment uncertainty of 0.25 mm. At this point, the resulting three distributions have been combined into a single distribution with uniform step size.

# Wire Scanners and others

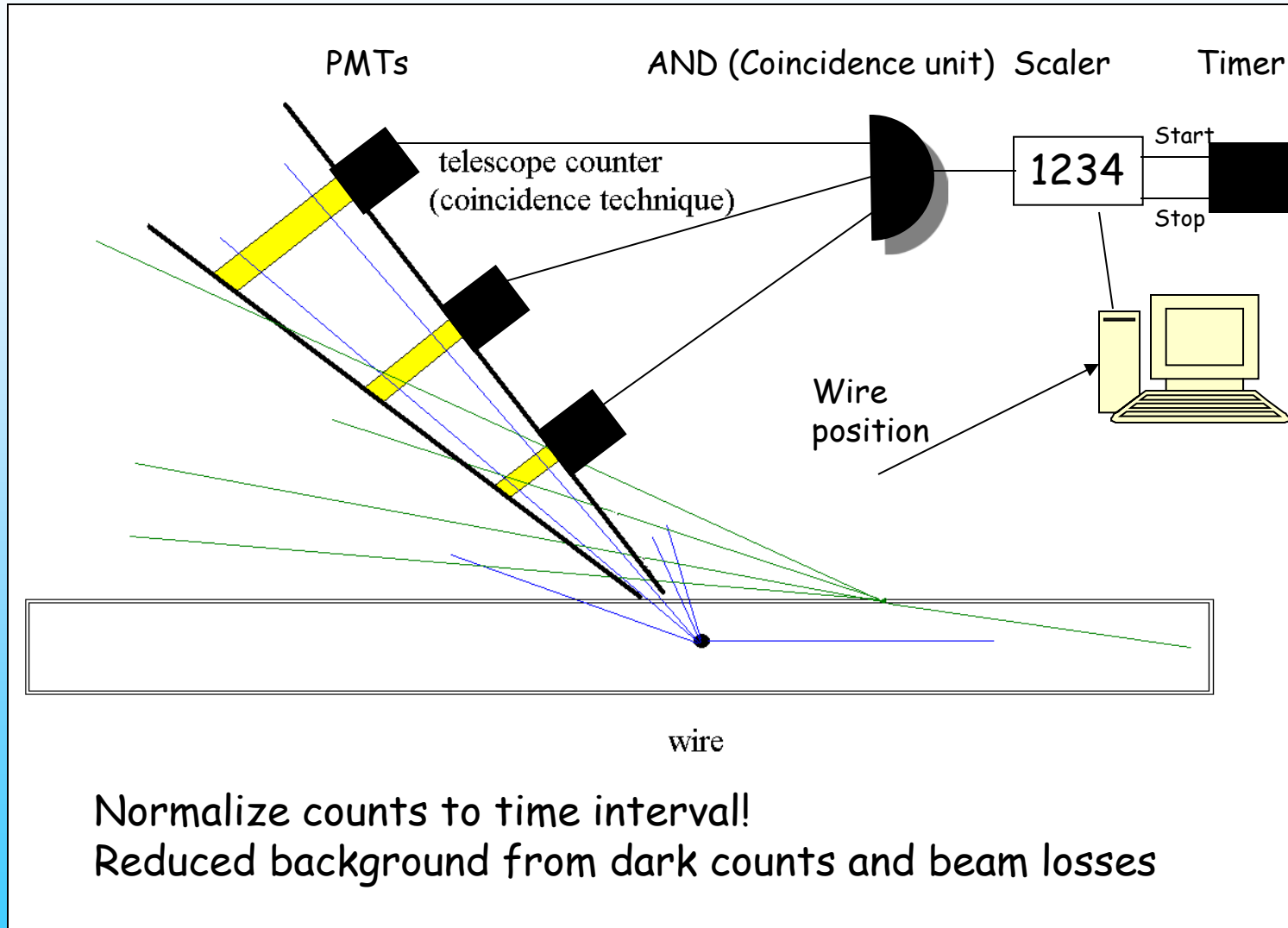
to 5: Normalize data to beam current and beam position

Each data point has to be normalized to the measured beam current and beam position for each measurement.



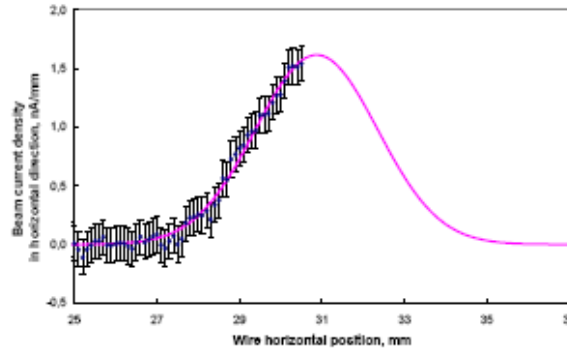
*Beam loss rates versus scraper position, black: first measurement, grey: second measurement. During the second measurement the orbit moved about 0.30 mm in 4721 s.*

# Wire Scanners

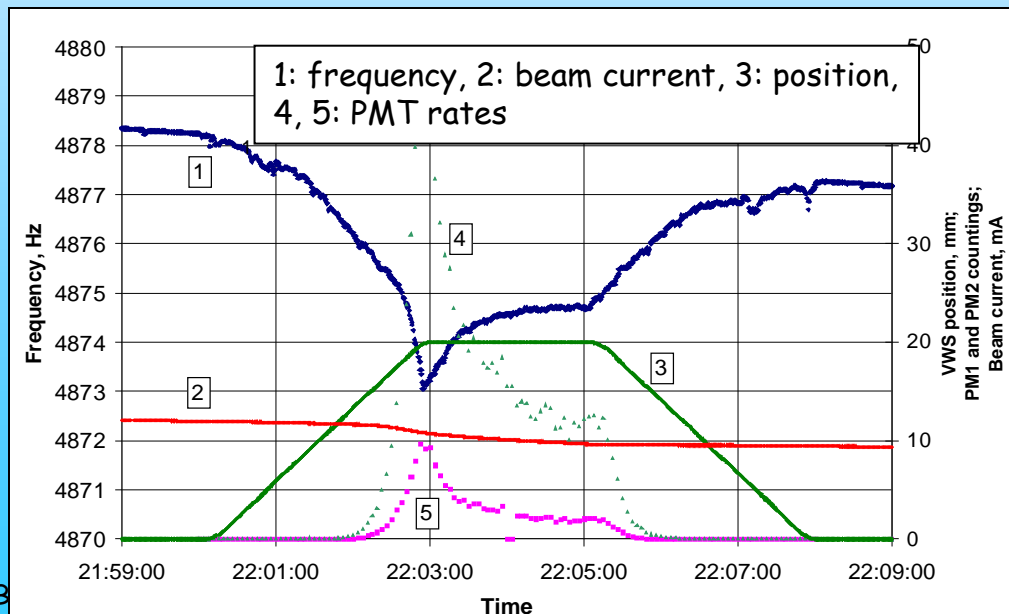
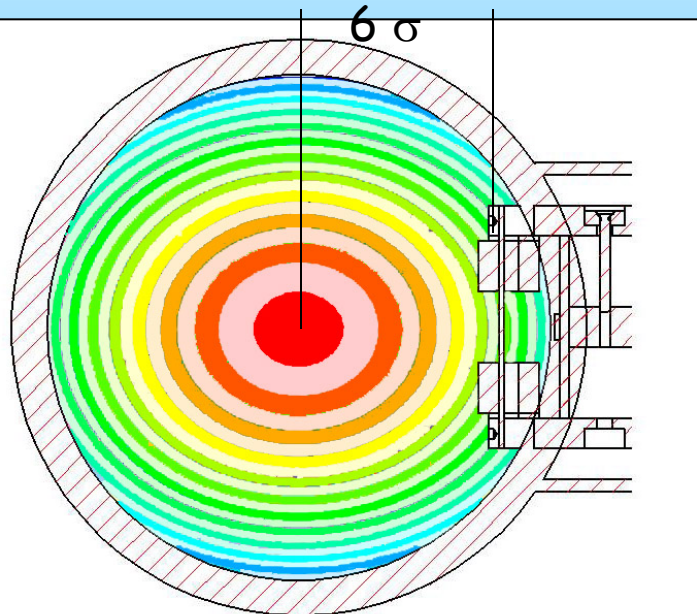
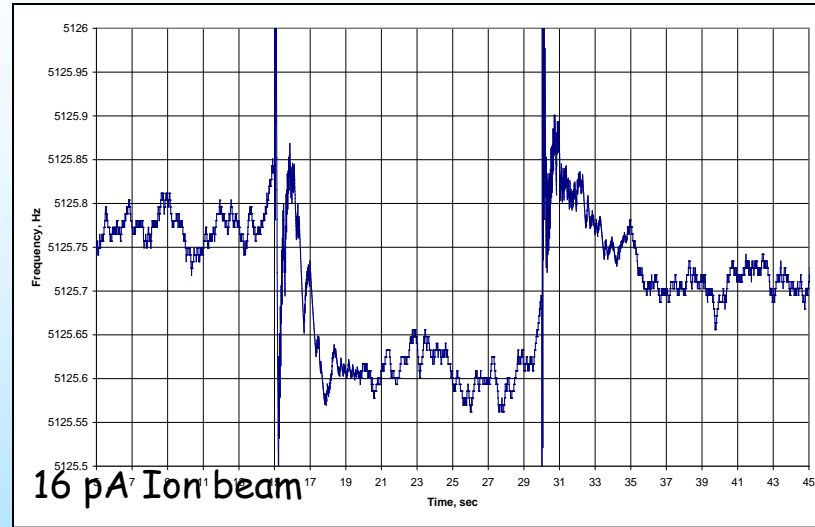


# Vibrating wire scanner

WWS mounted on the vacuum below with 1  $\mu\text{m}$  step motor feed



Scan of the electron beam at the Injector of Yerevan Synchrotron with an average current of about **10 nA** (after collimation) and an electron energy of 50 MeV



# Vibrating wire scanner

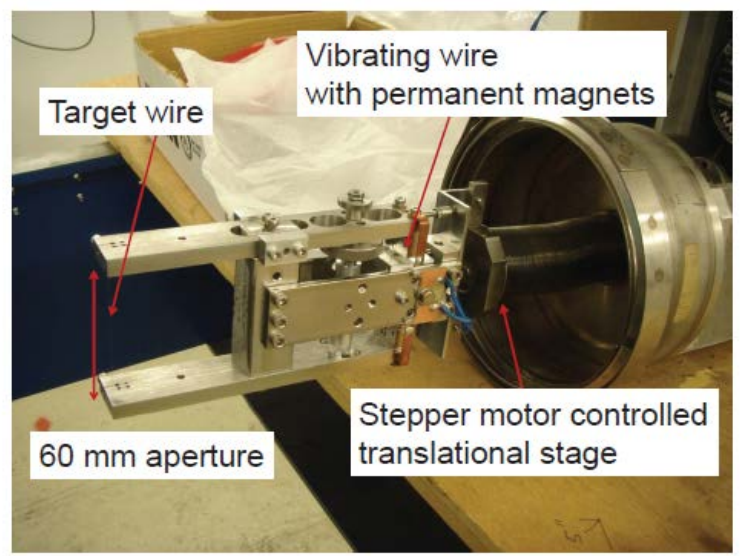
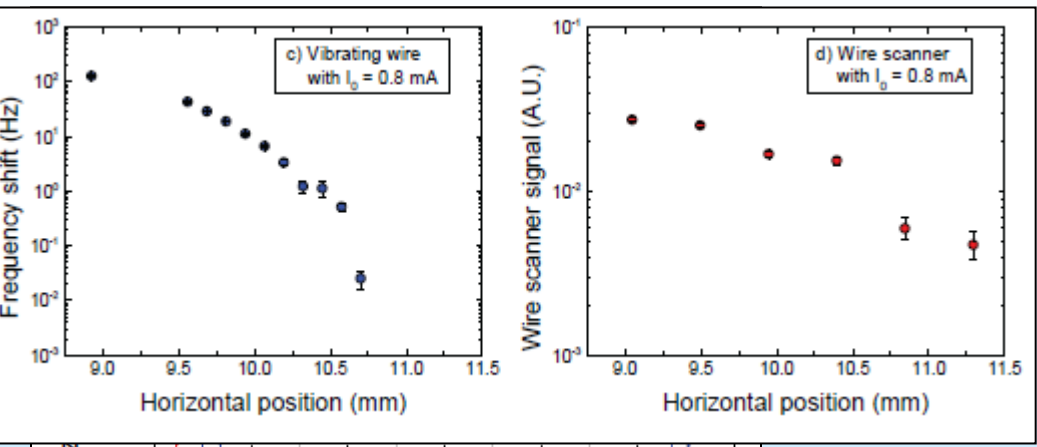
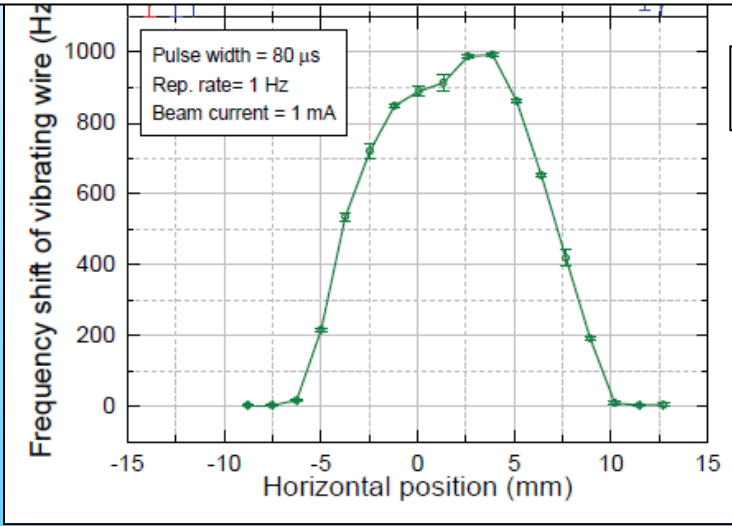
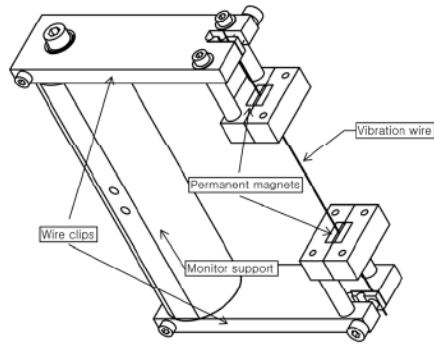
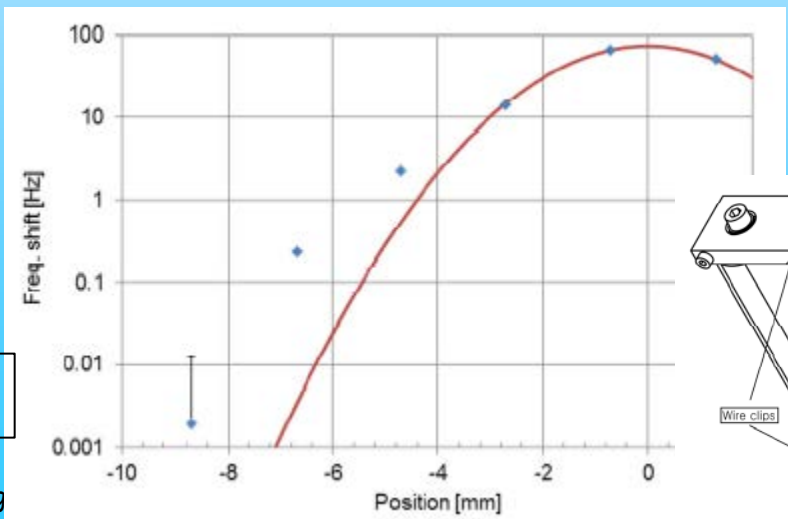


Figure 1: Picture of the large aperture vibrating wire monitor assembly.



HINS: M. Chung et al. IPAC13

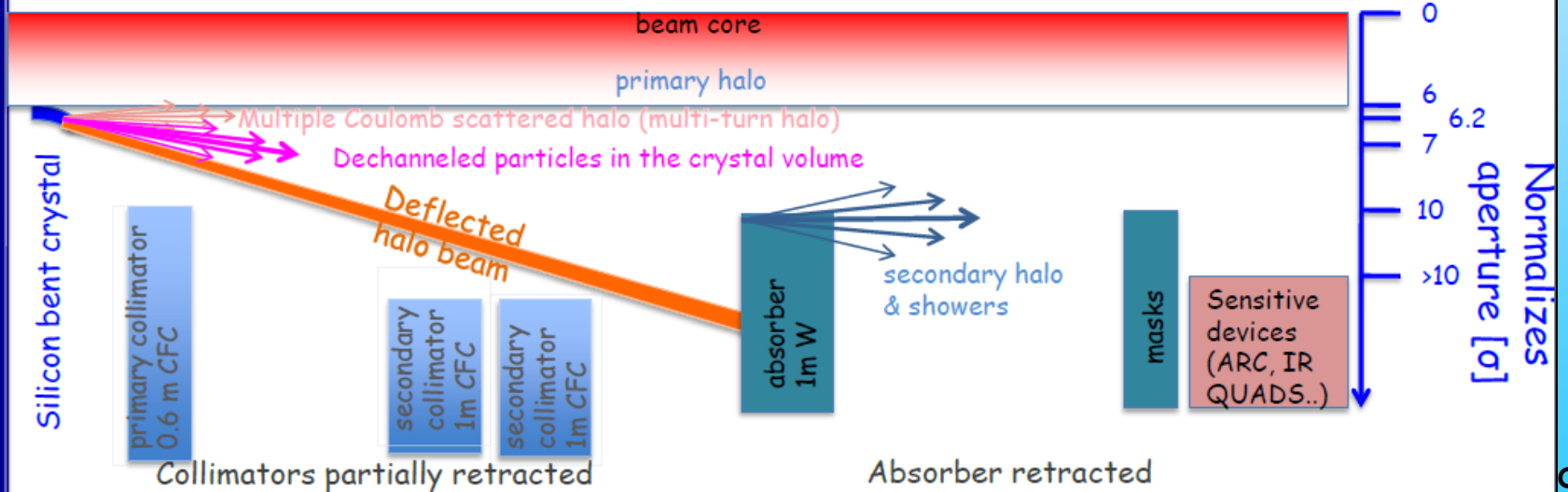
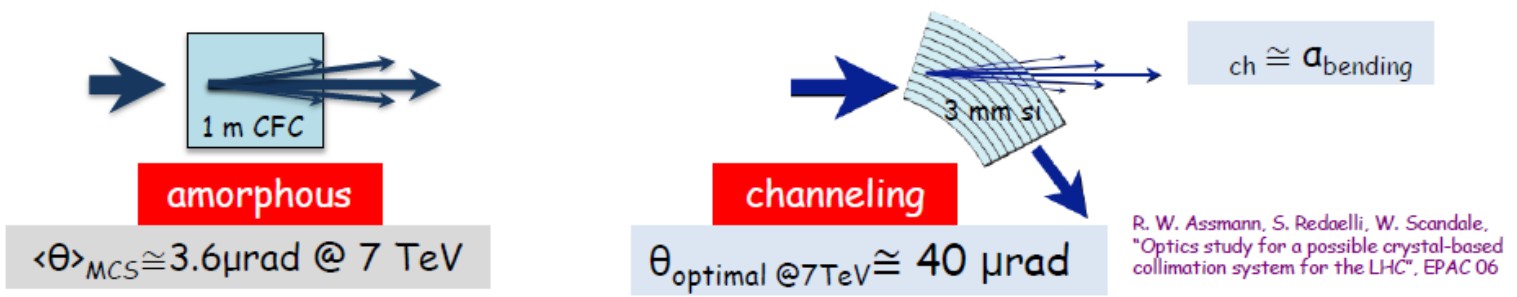
J-PARC L3BT:  
K. Okabe et al, IPAC13



## Crystal assisted collimation

- ❑ Bent crystals work as a "smart deflectors" on primary halo particles
- ❑ Coherent particle-crystal interactions impart large deflection angle that minimize the escaping particle rate and improve the collimation efficiency

W. Scandale  
IPAC11



# Halo scraping by collimators

## Concept

The hollow electron beam collimator is a cylindrical, hollow, magnetically confined, possibly pulsed electron beam overlapping with the beam halo (Fig. 3).

Electrons enclose the circulating beam. Halo particles are kicked transversely by the electromagnetic field of the electrons. If the hollow charge distribution is axially symmetric, the core of the circulating beam does not experience any electric or magnetic fields.

BEAM HALO DYNAMICS AND CONTROL WITH HOLLOW ELECTRON BEAMS\*  
G. Stancari et al. HB2012

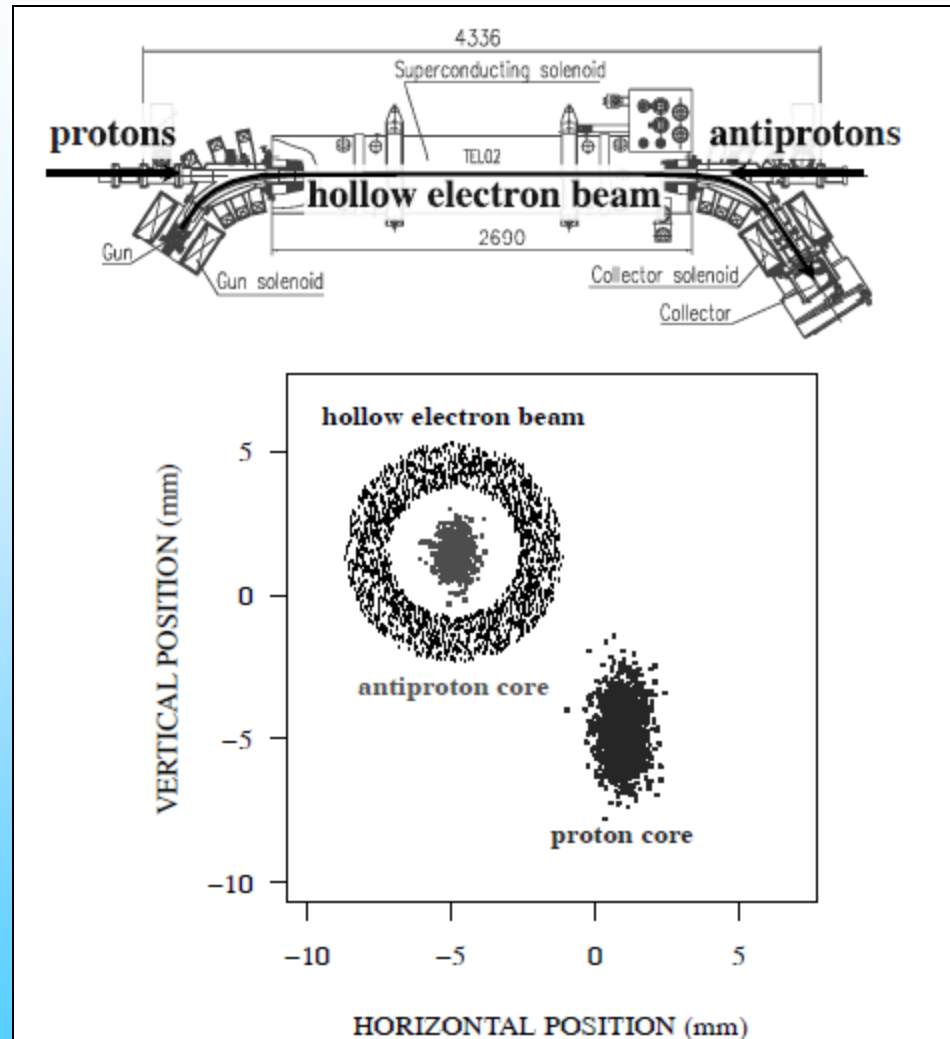


Figure 3: Schematic diagram of the beam layout in the Tevatron hollow electron beam collimator.

# Beam in Gap

## Hadron storage rings

Beam in Gap (hadrons) due to:

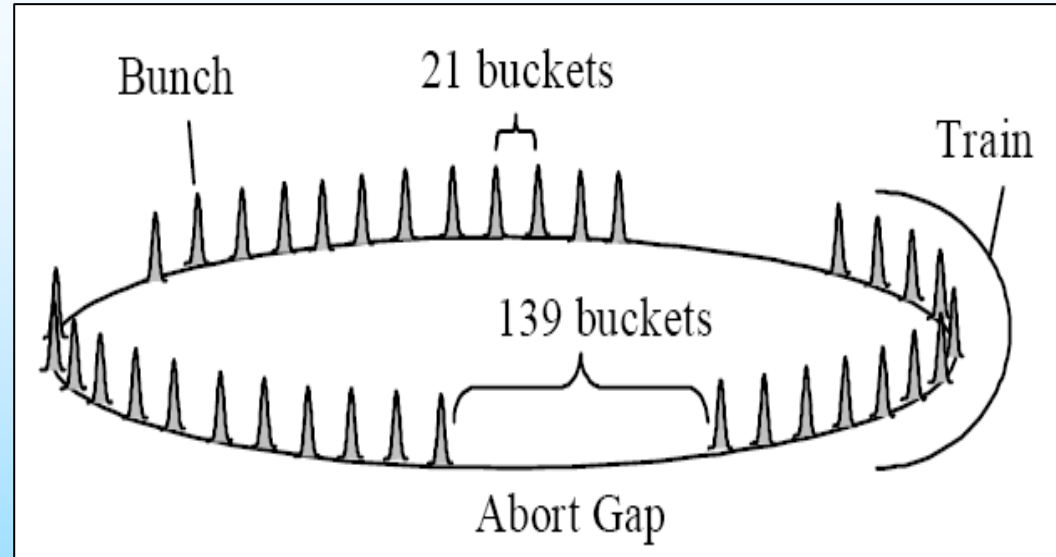
- Injection errors (timing)
- debunching
- diffusion
- RF noise/glitches
- ...

If beam (AC or DC) in gap, extraction kicker ramp will spray beam.

→ Will result in:

- Quenches (SC-magnets)
- activation
- spikes in experiments
- equipment damage
- ...

Therefore a continuous determination of the amount of beam in the gap is necessary to either clean the gap or dump the whole beam before major problems arise.

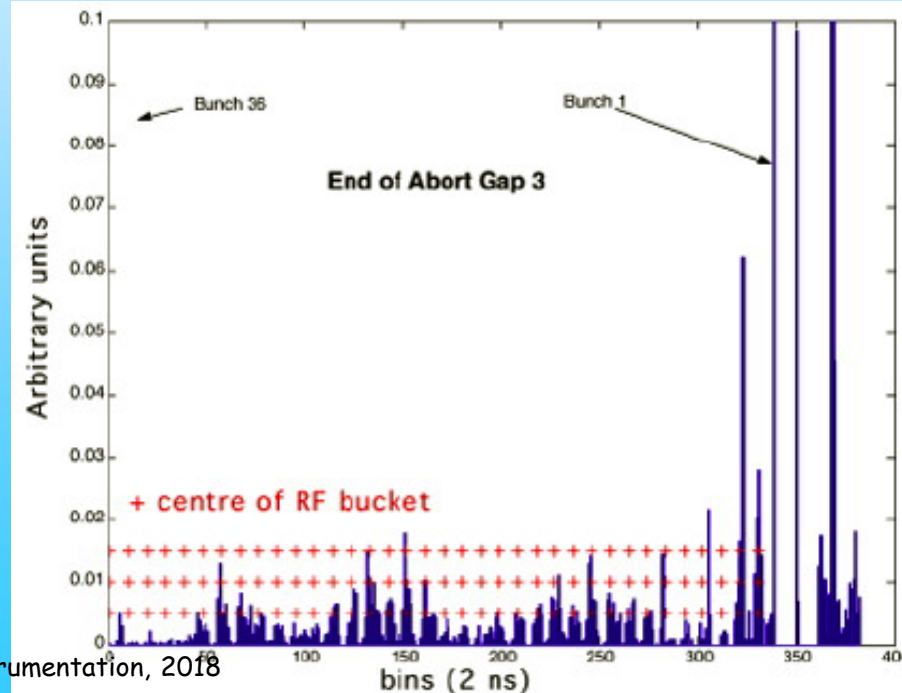
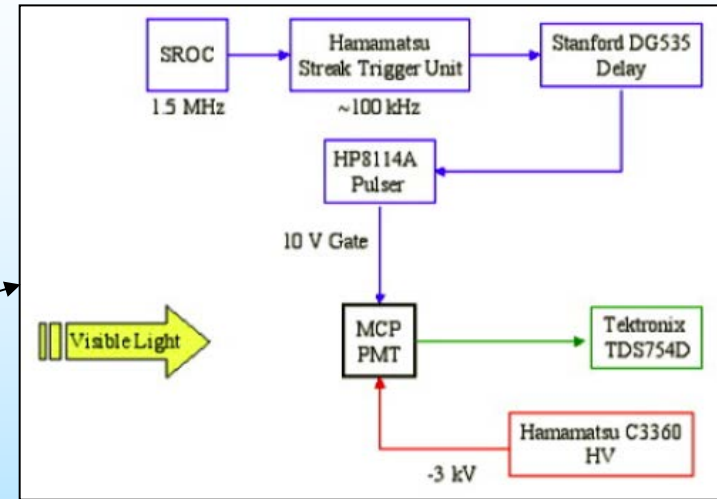
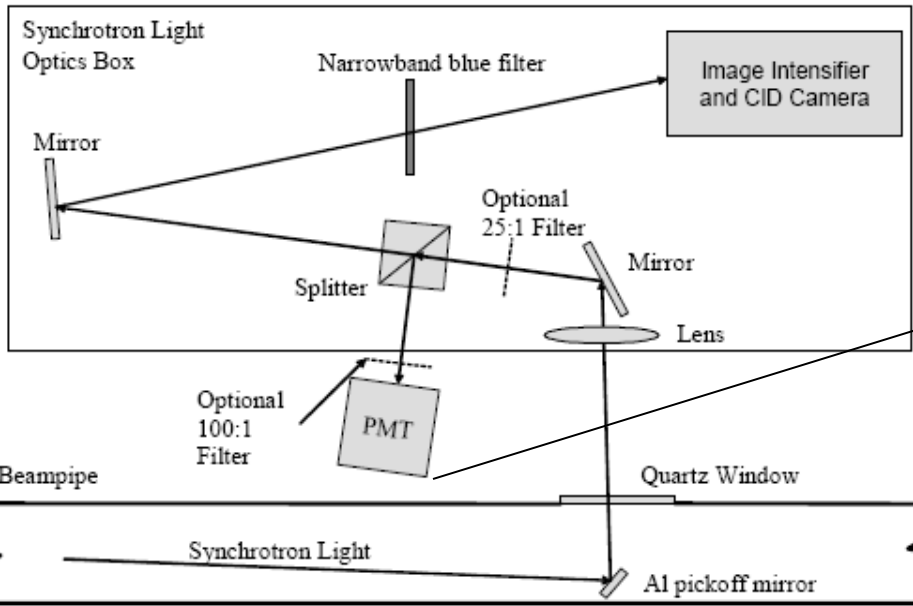


Measurement of the intensity of the beam in the abort gap at the Tevatron utilizing synchrotron light. R. Thurman-Keup, FERMILAB-CONF-05-139

Development of an abort gap monitor for the Large Hadron Collider. J.F. Beche, LBL-55208 (04/07, rec. Nov.)

# Beam in Gap

## Proton Synchrotron Light (Tevatron, LHC)



Depending on the amount of protons measured in the gap, a software alarm is sent that would trigger Radio-Frequency dampers, which would clean the abort gap to acceptable levels, before the beam is dumped.

First Operation of the Abort Gap Monitor for LHC, T. Lefèvre, et al., IPAC'10, Kyoto

LARP Note 1, 2005, Design of an Abort Gap Monitor for the Large Hadron Collider; J.-F. Beche et al.

# Beam in Gap

Note that in principle any other fast process, e.g. Beam Induced Gas Scintillation, Secondary Electron Emission or beam loss monitor signals (e.g. at halo scrapers or at wire scanners) can serve as a signal source, which are not limited to very high beam energy. A fast and gate-able detector which is synchronized by the revolution frequency is most useful to avoid saturation due to the signal of the main bunches.

## Measurement at J-PARC with fast Kickers + Scintillator-BLM:

"We first found that (supposed to be) empty bucket contains  $10^{-5}$  level of the main pulse. ... Any existing beam monitor could not detect this level of the beam. Surprisingly, it is accelerated both in the RCS and the MR without any monitor signal as a invisible beam."

**LHC:** New studies with Diamond based detectors are ongoing by monitoring the gap population with beam  $\leftrightarrow$  gas interactions.

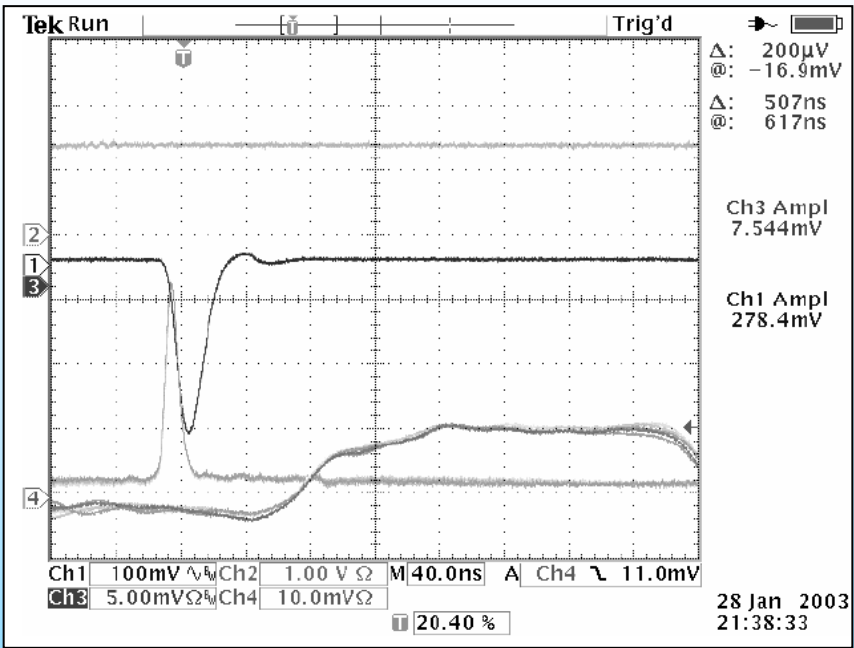


Measurements of Proton Beam Extinction at J-PARC  
K. Yoshimura, et al, IPAC'10

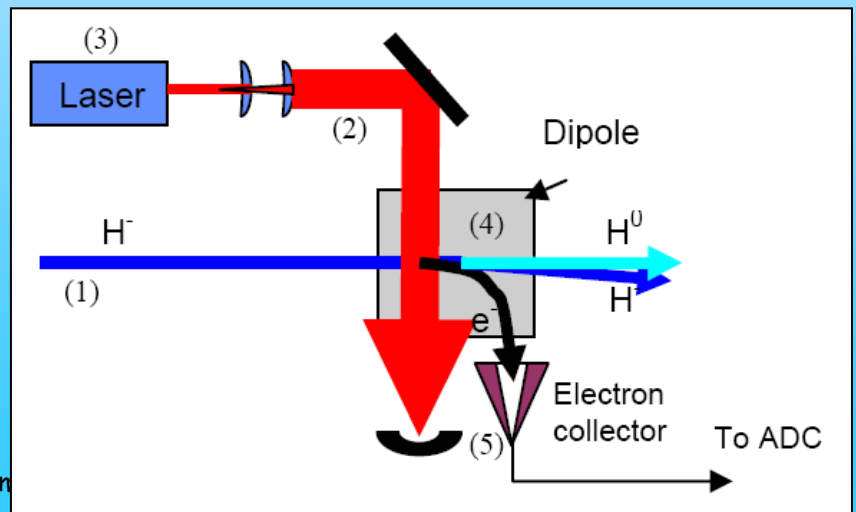
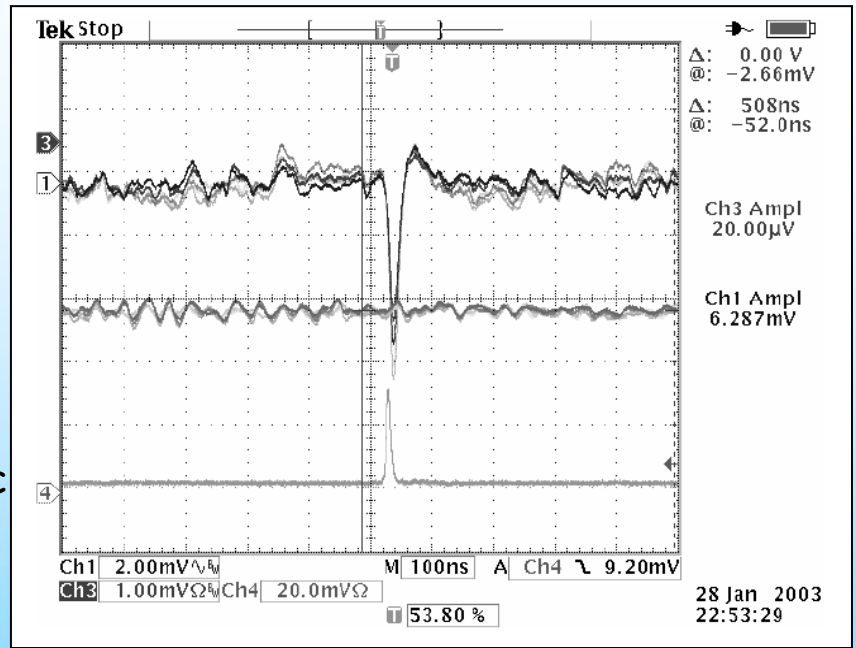
Feasibility Study of Monitoring the Population of the  
CERN-LHC Abort Gap with Diamond Based Particle  
Detectors, Oliver Stein, IPAC2015

# Beam in Gap

Using laser wire at SNS:



----->  
In Gap  
Delay + 20 dB gain  
=> dynamic range  $10^4$



Beam in Gap Measurements at the SNS Front-End;  
PAC 2003, Aleksandrov, A; et al,